SHRP-S-665

Concrete Bridge Protection and Rehabilitation: Chemical and Physical Techniques

Feasibility Studies of New Rehabilitation Techniques

John G. Dillard, James O. Glanville, William D. Collins,
Richard E. Weyers and Imad L. Al-Qadi

Virginia Polytechnic Institute and State University

Strategic Highway Research Program
National Research Council
Washington, DC 1993

SHRP–S-665
Contract C-103

Program Manager: *Don M. Harriott*
Project Manager: *Joseph F. Lamond*
Production Editor: *Marsha Barrett*
Program Area Secretary: *Carina S. Hreib*

July 1993
Reprint February 1994

key words:
concrete bridges
corrosion inhibitors
reinforcement corrosion

Strategic Highway Research Program
National Academy of Sciences
2101 Constitution Avenue N.W.
Washington, DC 20418

(202) 334-3774

75/NAP/294

Acknowledgments

The research described herein was supported by the Strategic Highway Research Program (SHRP). SHRP is a unit of the National Research Council that was authorized by section 128 of the Surface Transportation and Uniform Relocation Assistance Act of 1987.

We wish to acknowledge the help of the SHRP coordinators, and maintenance and material engineers at the state transportation departments who graciously assisted us in the field installations of the experimental corrosion abatement techniques which make up the basis for this study, especially Washington, Minnesota, New York and Pennsylvania.

Contents

List of Figures

List of Tables

Abstract

The objective of this study was to examine and develop feasible chemical methods for the corrosion protection of reinforcing steel in concrete bridges. A broad spectrum of chemicals were evaluated, corrosion inhibitors, chloride scavengers, and polyaphrons.

Screening tests were developed to evaluate inhibitor effectiveness and their ability to penetrate concrete. The evaluation of the inhibitors led to the recommendation of various types of inhibitors with potential application in reinforced concrete as well as 3 different treatment techniques.

Reinforced concrete specimens were cast and subjected to repeated exposure to NaCl solution and evaluated to investigate the inhibitors effectiveness after removing contaminated concrete. Corrosion progress was monitored by measuring half-cell potential, corrosion rate, and chloride concentration. When active corrosion was indicated, chloride contaminated concrete was removed to the rebar level through a grooving process. The grooves were chemically treated through solution ponding and backfilling with treated mortar. Seventeen treatments were evaluated. Mortar cubes were cast containing various treatment concentration and tested for compressive strength and resistivity. DCI, Alox 901, Cortec 1337, Cortec 1609, sodium tetraborate, and zinc borate were found effective in abating corrosion after concrete removal. However, both borate compounds cause set retardation.

Polyaphrons were investigated as a possible corrosion preventor/reducer inhibitor. Carbon steel coupons were immersed in different polyaphron solutions. The cationic surfactant aphrons were found to be the most stable in the salt/pore solution environment. To study the diffusion rate of aphrons in concrete mixtures, concrete, mortar and cement paste specimens were cast. The results indicated that the diffusion rate of polyaphrons through various mixtures is very slow and therefore was not recommended as a practical concrete bridge treatment.

Executive Summary

The objective of this study was to identify and develop new chemical treatment techniques for inhibiting the corrosion of reinforcing steel in concrete. In accomplishing the objective, three independent but interrelated studies were performed and are reported in Part I, II, and III.

The objective of Part I was to assess the corrosion inhibiting effectiveness of a large number of chemicals which had the potential of abating the corrosion of steel in chloride-contaminated concrete. A reinforcing steel cleaning and sample preparation method which would not affect the corrosion mechanism was first developed. A rapid screening test method was next developed to assess the efficiency of the large number of corrosion inhibitors which have the potential of abating corrosion of steel in concrete. Electrochemical potential measurements were used to determine the effectiveness of the corrosion inhibitors. Finally, migration characteristics of promising inhibitors through concrete was evaluated in order to assess the feasibility of developing a treatment process without removing the sound but chloride-contaminated concrete. In addition, the surface chemistry of select inhibitors were studied in order to identify the corrosion inhibiting mechanism and thus better understand the limitations of application.

Of the 26 corrosion inhibitors that were evaluated, 5 were identified as having the potential of stopping the corrosion of steel in concrete, sodium nitrite, sodium tetraborate, Alox 901, VCI 1337, and VCI 1609. These inhibitors and similar chemical species were further evaluated in Part II, the feasibility development phase.

In addition to the 5 inhibitors identified in Part I, Part II evaluated the corrosion abatement performance of 2 other corrosion inhibitors (zinc borate and TCI), 2 sealers (silicone and styrene-acrylic), and a chloride scavenger (hydroxylapatite). A total of 17 treatment combinations were evaluated. Specimens 8.5 x 16 x 3.25 in (22.6 x 40.6 x 8.3 cm) containing 2 0.5 in (1.27 cm) diameter reinforcing bars were cast with 0.75 in (1.91 cm) of cover. Specimens were air cured (1 and 3 days), dried in an oven for 24 hours at 150°F (65.5°C) and subsequently ponded with a sodium chloride solution until corrosion initiated. A 2 in wide strip of the cover concrete was removed andthe corrosion abatement treatment applied. For some treatments, the corrosion abatement treatment included the addition of the chemical to the backfill mortar. Specimens were again ponded with a sodium chloride

solution after the groove backfilled mortar was moist cured for 7 days. Corrosion abatement effectiveness was assessed by monitoring the corrosion potential and the corrosion current density. Five corrosion inhibitors were identified as being effective in chloride contaminated concrete. Field treatment processes using the 5 inhibitors were further developed and corrosion abatement performance further evaluated in Task 5 of this study, Concrete Bridge Protection and Rehabilitation: Chemical and Physical Techniques, Corrosion Protection Systems.

Part III of this report addresses the use of polyaphrons as a corrosion inhibitor carrier to stop the corrosion of steel in chloride-contaminated concrete. Migration studies using electrical potential as the driving force demonstrated that the migration rate was too slow for practical use.

1

Background

According to conservative estimates, one-half of all highway bridges in the United States (1,2) are deteriorating from chloride induced corrosion of the reinforcing steel. A similar situation prevails in the United Kingdom (3). Reinforcing steel corrosion in bridges is an outcome of the repeated wintertime application of deicing salts such as sodium chloride and calcium chloride (4,5). Chloride destroys the reinforcing steel passive layer and forms corrosion products, which occupy a greater physical volume. The resulting internal expansion causes cracking and spalling of the concrete cover. Once cracking has occurred conditions deteriorate rapidly. The principal factors that must be controlled to inhibit corrosion include oxygen, chloride ions, water, and the pH of the concrete. Approaches to control these factors have used inhibitors, electrochemical protection procedures, scavengers, buffers, and coatings (6-10).

The use of corrosion-inhibitors is one approach to prevent or reduce the corrosion of steel. Most corrosion inhibitors for steel are used in acidic or neutral conditions where uninhibited attack may be very rapid; by comparison, corrosion of steel under the alkaline conditions in concrete is very slow. However, because even slow corrosion can cause significant damage during the long life required of reinforced concrete bridges, concrete inhibitors do have a role to play (11). At least one corrosion inhibitor is currently commercially available. Calcium nitrite as a concrete admixture has been widely used during the past decade. Concrete containing calcium nitrite has considerable resistance to chloride induced corrosion (12,13).

The work reported here involved 3 tasks: 1) to search for substances (i) that could be applied to existing, chloride-contaminated bridge components, (ii) that would penetrate the concrete, and (iii) that, on arrival at the reinforcing steel, would stop or inhibit corrosion; 2) to employ screening tests under laboratory conditions to test (i) inhibitor effectiveness and (ii) inhibitor penetration through concrete; and 3) to study the surface chemistry of reinforcing steel following interaction with inhibitors. Such an inhibitor substance would permit a relatively inexpensive treatment of reinforcing steel corrosion in existing

components without removing concrete.

Corrosion of Steel Reinforcement in Concrete

Corrosion of steel in concrete occurs by an electrochemical reaction in which 2 of the anodic and cathodic reactions are:

Anodic reaction: $Fe \Rightarrow Fe^{2+} + 2e^-$

Cathodic reaction: $H_2O + 1/2O_2 + 2e^- \Rightarrow 2OH^-$ (1)

The development of anodes and cathodes is due to the presence of heterogeneities in the corrosion cell. Heterogeneities can exist at the surface of reinforcing steel due to metallurgical segregation, varying grain orientations, and local differences in the electrolyte, such as concentration gradients [14].

The spontaneous anodic steel corrosion reaction quickly stops in a highly alkaline medium such as portland cement concrete, unless sufficient levels of chloride or other aggressive agents are present. The steel is passivated by the high pH of the pore water solution. This passivation is due to the formation of a thin layer of gamma ion oxide (Fe_2O_3) that serves as a stable barrier to further metal dissolution. In the absence of chloride ions in solution, the gamma iron oxide film on steel is reported to be stable at pH levels as low as 11.5 [16].

The two major causes of the destruction of the passive layer on steel reinforcing steel are the presence of chloride ions in combination with oxygen and the decrease in the pH value of the pore solution caused by carbonation reactions which consume both calcium and sodium hydroxides within the pore water solution. Carbonation, however, is not a major problem for bridges because the penetration depth of carbonation is, in most cases, less than the reinforcement cover depth on decks. Concrete of a normal water/cement ratio is unlikely to show carbonation beyond a depth of approximately 1/2 in. (1.27 cm) even after prolonged weathering [16]. Reinforcement corrosion causes a decrease in bar diameter, cracking and spalling due to the expansive iron oxide products.

While the structure of the passive film formed in high pH environments and the mechanism of its deterioration by chloride ions is not fully understood, it is generally accepted that the chloride ions become incorporated in the passive film, displacing some of the oxygen present and increasing both the passive film's solubility and conductivity.

Because there are imperfections in the passive film and an inhomogeneous distribution of chloride ions along the reinforcing steel surface, the passive film layer breaks down on a local scale, creating microgalvanic cells. The local areas of high chloride concentration and film imperfections act as anodic sites where the iron dissolution takes place, while the remaining passive areas serve as cathodes at which oxygen reduction occurs. In addition to chloride and oxygen availability, the rate of corrosion will also depend on the cathode/anode

ratio and the electrical resistivity of the concrete between the cells.

In the concrete surrounding the anode area, the concentration of positive iron ions increases and the pH decreases; consequently the formation of the negative hydroxyl ions occurs at the cathodic sites. The decrease in pH at the local anodic sites allows for the formation of a soluble complex of iron chloride [14]. The iron-chloride complex forms by the reactions:

$$Fe^{++} + 2Cl^- \rightarrow Fe^{2+} + C1^- + 2e^-$$

$$Fe^{2+}C1_2 + 2H_2O \rightarrow Fe(OH)_2 + 2H^+ + 2C1^-$$

The soluble $FeCl_2$ complex can diffuse away from the anode, promoting further corrosion. When the complex diffuses away from the anode where both the pH and concentration of dissolved oxygen are higher than the immediate anode area, the complex breaks down and iron hydroxide precipitates. This frees chloride ions which again react with ferrous ions at the anodic sites. As long as there is sufficient oxygen and moisture, the corrosion process is autocatalytic in nature and it continues without depleting the chloride. Should the soluble iron-chloride complex diffuse away from the steel-concrete interface and the iron oxidize in a void, then no expansive forces are created. Only when the iron oxidizes at the concrete-steel interface are expansive forces created and subsequent spalling occur.

Chlorides may be present in concrete from several different sources. They may be introduced through unbound chloride-containing aggregate or by the addition of calcium chloride as a set accelerator. The predominant source of chlorides, however, is from the environment, including deicing salts and sea water. The transport of chlorides through concrete has both a primary and secondary mode. The primary mode of transport is chloride diffusion through the pore water solution in concrete. The secondary mode of transport is chloride penetration through cracks. Cracks may develop as a result of externally applied loads, drying shrinkage, subsidence, or expansive stresses placed on the concrete from the volume of corrosion products formed on embedded reinforcing steel.

Through diffusion and transport through cracks, a critical chloride threshold level is reached at the concrete/steel interface at which corrosion begins. For reinforced concrete, a limiting or maximum allowable value of 0.4% Cl^- /cement wt [17] and 1.2 lbs Cl^- /yd^3 (0.71 kg/m^3) of concrete [18] have been determined. It has also been determined that a chloride ion to hydroxyl ion ratio greater than 0.6 Cl/OH^- is needed to initiate corrosion [19].

Factors Affecting Corrosion in Reinforced Concrete

A number of factors play a role in the initiation and propagation of corrosion in reinforced concrete. The water/cement ratio and consolidation of the concrete, reinforcing steel cover depth, and curing conditions can all be optimized to decrease the diffusion rate and increase the time it takes for the chlorides to initiate corrosion.

The chloride ion can affect the corrosion reaction differently depending upon the cation associated with it. The rate of corrosion in concrete mixed with calcium chloride has been found to be greater than the rate in concrete mixed with sodium chloride. Although the mechanism for this effect is not well understood, the difference in corrosion rates is partially due to calcium chloride's diffusivity which is 3 to 4 times that of sodium chloride [20].

An essential factor required for corrosion of steel in concrete is the presence of oxygen. The rate of oxygen diffusion through concrete is significantly affected by the extent to which the concrete is saturated with water. Investigations have shown that conditions will be conducive to corrosion in those parts of a concrete structure that are exposed to periods of intermittent wetting and drying, and the rate of steel corrosion will be slow if the concrete is continuously water-saturated [21]. In saturated concrete, dissolved oxygen will primarily diffuse through the pore water, while in dry concrete, the diffusion of gaseous oxygen is more rapid. However, in order to react at the cathode, the oxygen must be in a dissolved form, therefore, corrosion is more active in reinforced structures that are partially dry or undergo intermittent wetting and drying.

Another factor of importance is the effect of concrete resistivity or electrical resistance on the corrosion reaction. Resistivity is mainly controlled by water content, with oven-dry concrete having a resistivity of 4×10^8 Ω-in (1×10^9 Ω-cm) and water saturated concrete on the order of 4×10^3 Ω-in (1×10^4 Ω-cm) [20]. When concrete is dry, the corrosion cell no longer has the electrolyte provided by the ion containing pore solution; therefore, lower moisture contents reduce the ionic conduction in the concrete which reduces the corrosion rate. Admixtures can also affect the resistivity of concrete by contributing or binding ions, or filling pores which reduces amount of electrolyte.

Inhibitor Use in Reinforced Concrete

There is no general theory of corrosion inhibition that applies to all situations because the mechanism of inhibition varies depending upon the factors causing corrosion and the nature of the inhibitor. The fundamental concept of inhibition is the development of a stable compound with the metal surface and the formation of an adsorption complex with the metal oxide.

Inhibitors are of three basic types: anodic, cathodic, and mixed. Anodic inhibitors function by arresting the reaction at the anode. In ideal situations, they react with existing corrosion products to form a highly insoluble film that adheres tightly to the metal surface [22]. This film can act as a barrier to metal dissolution by preventing the metal surface from contacting the corrosive electrolyte. Cathodic inhibitors function to reduce the cathodic reaction. However, cathodic inhibitors are less effective than anodic inhibitors because their reactive products do not bond as well to the metal surface. A mixed inhibitor may be desired in many cases because microcell corrosion is common in reinforcing steel. The microscopic distances separating the anodic and cathodic areas that characterize microcell corrosion may

warrant the use of a mixed inhibitor since the anodic and cathodic sites cannot be isolated. The mixed inhibitor would affect both the anodic and cathodic reactions simultaneously.

Numerous chemical admixtures, both organic and inorganic, have been recommended as specific inhibitors of steel corrosion. However, many of the admixtures have deleterious effects on concrete, such as set retardation. Some inorganic compounds which have been suggested as inhibitors are stannous chloride, zinc and lead chromates, potassium dichromate, calcium hypophosphite, sodium nitrite, and calcium nitrite [23]. Organic inhibitors that have been recommended are sodium benzoate, ethyl aniline, and mercaptobenzothiazole [23]. Calcium nitrite has been the most promising inhibitor used in the United States [24]. Sodium nitrite, which is still used extensively in Europe, was used prior to the development of calcium nitrite, but it caused a number of deleterious effects, including low strength, erratic setting times, efflorescence, and the increased probability of alkali-aggregate reaction [25].

One form of inhibitor that has received little attention for use in concrete is the scavenger. Scavengers are substances that remove corrosive reagents from solution through binding reactions. Most of the scavengers used in corrosive environments act as scavengers of dissolved oxygen and aqueous solutions. Substances such as sodium sulfite and hydrazine react with dissolved oxygen to form reaction products that do not contribute to the corrosion process. Unfortunately, these scavengers show little promise for concrete due to the normally unlimited supply of oxygen. Added to concrete, these substances would be quickly depleted of their scavenging ability. Although scavengers are not currently used in reinforced concrete, interest exists in finding or developing substances to bind chloride ions in reinforced concrete.

Inhibitors were originally used as admixtures in fresh concrete to prevent future corrosion. However, inhibitors may be applied through impregnation and diffusion through the surface of the concrete in existing chloride-contaminated structures.

2

PART I: Evaluation of Feasible Corrosion Inhibitor Treatments

Introduction

The principal objectives of this work were 1) to develop a rapid, inexpensive screening test to evaluate potential corrosion-inhibiting agents for reinforcing steel in concrete, 2) to examine chemical surface changes of reinforcing steel following treatment with inhibitors with the intent of developing a rapid, surface-sensitive qualification scheme for potential inhibitors, 3) to assess the relative mobility of inhibitors through concrete in the effort to predict the rate at which an inhibitor could be delivered to reinforcing steel in concrete, and 4) to evaluate electrochemical potential changes during the process of corrosion and its inhibition. It was envisioned that the most promising candidate inhibitors, as identified in these tests and characterization studies, would be brought forward into a program of larger-scale testing in concrete presented in part two of this report.

Research Approach

As part of the investigation, companies that offer corrosion inhibitors were contacted and sample materials were obtained for evaluation and testing. Among the materials investigated were common and well-known corrosion inhibitors. These materials served as reference standards against which the performance of new materials could be compared. Thus, the selection of candidate materials was based on the industrial state-of-the-art and included a group of inhibitors which offered a range of inhabitation modes. Some materials were film-formers while others altered the reinforcing steel surface chemically.

In this section of the report, the experimental approach for each aspect of the research is first outlined, then results and discussion for the respective investigations are presented, and

finally a detailed summary of the specific recommendations is presented. The organization of research activities in this part of the report is as follows:

A. rebar source, surface preparation and test solutions;
B. rapid screening test development;
C. surface characterization of reinforcing steel and the interaction of reinforcing steel with inhibitors;
D. migration of corrosion inhibitors through concrete;
E. electrochemical studies of the effect of inhibitors on reinforcing steel corrosion;
F. potential long-term testing methods;
G. impregnation of concrete disks with polymeric materials.

Experimental Program

Rebar Source, Surface Preparation, and Test Solutions

Reinforcing steel reinforcing steel produced from a single heat were obtained from Roanoke Electric Steel Co., Roanoke, VA. Bulk analysis of the reinforcing steel material (wt. %) was provided by the vendor and is summarized in Table 2.

The #5 reinforcing steel, conforming to ASTM 615, test specimens were prepared by first cutting bar sections in half longitudinally; 1" specimens were then cut from the split bar. Test specimens were cleaned in an organic solvent to remove dirt and grease. Cleaning solvents selected for tests included hexane, isopropanol and acetone. Specimens were also cleaned in a 50% (w/w) sulfuric acid, distilled water solution for one minute at room temperature, rinsed three times with distilled water, and dried at 230° F (110° C).

Corrosion of reinforcing steel in chloride-contaminated concrete occurs where aqueous solutions within the pores of the concrete contact the reinforcing steel. The existence of such pore solutions is necessary to provide a conduit by which chloride ions may diffuse from the surface of the concrete to the reinforcing steels. In the work reported here, a synthetic pore solution, which contained a high concentration (3.5 w/w %) of NaCl, was used (26).

Synthetic pore solution was prepared with reagent grade laboratory chemicals. The composition of the synthetic pore solution was 0.300 M sodium hydroxide, 0.600 M potassium hydroxide, and saturated calcium hydroxide in distilled water (26). Prior to use, all solutions were air saturated.

Rapid Screening Test Development

Rebar test specimens were prepared in replicate (usually 5 or 10 replicates per test) by

placing approximately 0.34 oz. (10 mL) of the aerated test solution in a small plastic vial and completely submerging a single reinforcing steel test specimen into the solution. The vials were loosely capped and placed in a laboratory oven and maintained at 140° F (60° C). Solutions were replenished periodically and replaced every two weeks.

Each test specimen was carefully examined with a 5x hand magnifying lens and graded periodically on the basis of estimate percent surface corrosion. The corrosion observations were made on the original (curved) surface of the reinforcing steel only (not the freshly cut surface).

Accurately weighted quantities of the inhibitors were added to the chloride-doped simulated pore solution to test the comparative effectiveness of the inhibitors. Control solutions were chloride-doped pore solution without added corrosion inhibitor. Corrosion inhibitors were obtained as reagent grade chemicals from laboratory supply houses. Commercial products were obtained as manufacturer's samples. Their chemical nature and manufacturer are presented in Table 1.

To calculate molarities of commercial samples (Table 1 inhibitors) of proprietary composition and, hence, of unknown molecular weight, a molecular weight of 250 g/mol was assumed.

Surface Characterization of Reinforcing Steel and Its Interaction With Inhibitors

To facilitate the preparation of samples for surface analysis, a notch was cut in the 1 in. (2.54 cm) specimens at approximately 3/4 in. (1.91 cm) from one end of the specimen. After immersion in the inhibitor test solution, the 3/4 in. (1.91 cm) portion of the treated bar was separated from the 1 in. (2.54 cm) specimen and analyzed. By using this procedure the integrity of the treated reinforcing steel surface could be maintained, and no cutting of the samples was required following treatment. The curved, outer portion of the reinforcing steel specimen was analyzed.

The test solutions were simulated pore solution (0.600M KOH, 0.300M NaOH, saturated with $Ca(OH)_2$), pore solution containing 3.5% (w/w) NaCl; and pore solution containing 3.5% (w/w) NaCl and 0.3 M inhibitor. The inhibitors studied included sodium nitrite ($NaNO_2$), sodium molybdate (Na_2MoO_4), sodium dihydrogenphosphate (NaH_2PO_4), sodium monofluorophosphate (Na_2PO_3F), sodium tetraborate $Na_2B_4O_7$), and three commercial reagents: Dequest 2000, 50% active aqueous solution; Dequest 2010, 60% active aqueous solution; and Dequest 2054, 35% active aqueous solution.

The test solutions were aerated for at least one hour before reinforcing steel samples were introduced into the solutions. Exposure times were varied from 1 - 8 days. Samples were maintained at 140° F (60° C). Five replicate specimens of each exposure were used to provide data for statistical analysis of the results.

Table 1. Commercial Corrosion Inhibitors

INHIBITOR	CHEMICAL NATURE
Monsanto Chemical Co.	
Dequest 2000	amino tris (methylene phosphonic acid), 50% active aqueous solution
Dequest 2010	hydroxy-ethylidene diphosphonic acid, 60% active aqueous solution
Dequest 2054	hexapotassium hexamethylene diamine (methylene tetraphosphonate), 35% active aqueous solution
Alox Chemical Company	
Alox 901 Alox 502 A Alox 2291 Alox 319 F Alox 350 Alox 2162 Aqualox 2268	proprietary organic compounds
Angus Chemical Company	
Alkaterge T-IV	oxazoline compound
Amine CS-1135	oxazoladine blend
Miranol Incorporated	
Miramine TOC	substituted imidazoline of tall oil fatty acid
Monocor BE	borate ester
Mona Industries Ltd	
Monacor 39	imido ester carboxylic acid derivative
Witco Corporation	
Witcamine PA 78-B	salt of fatty imidazoline
Witcamine PA 60-B	salt of fatty imidazoline

Two kinds of experiments were carried out with respect to reinforcing steel immersion in pore solutions: initial and delayed. In experiments termed "initial" inhibition, hexane cleaned reinforcing steel was immersed for 8 days in pore solution at 140°F (60°C) containing 0.300 M inhibitor and 3.5% NaCl. At the end of the exposure period, reinforcing steel specimens were removed, rinsed with distilled water and characterized by XPS (X-ray photoelectron spectroscopy). For experiments indicated as "delayed" inhibition, hexane cleaned reinforcing steel was immersed for 8 days in pore solution at 140°F (60°C) containing 3.5% NaCl. At the end of this period, the specimens were then immersed for 8 days in pore solution at 140°F (60°C) containing 3.5% NaCl plus 0.300 M inhibitor. At the end of the exposure time, the reinforcing steel samples were removed from solution, washed

with distilled water, and the surface chemistry evaluated via XPS.

Surface analysis measurements (27) were carried out using a PHI Perkin-Elmer 5300 photoelectron spectrometer (28). Photoelectrons were generated using Mg K_α radiation (hv = 1253.6 eV). Ejected photoelectrons were analyzed using a hemispherical analyzer and the electrons were detected using a position sensitive detector. In the presentation of elemental analysis results, photoelectron spectral peak areas were measured and subsequently scaled to account for ionization probability and an instrumental sensitivity factor to yield results which are indicative of surface concentration in atomic percent. The precision for the concentration evaluations was determined from measurements on 5 different reinforcing steel specimens. The binding energy scale was calibrated by setting the C1s hydrocarbon peak binding energy at 285.0 eV (29). At least two different measurements on 2 different reinforcing steel samples were made and the average results are considered.

Migration of Corrosion Inhibitors Through Mortar

Mortar cylinders, 1.18 in (3.0 cm) in diameter and approximately 3.94 in (10 cm) long, were cast with a water to cement ratio of 0.47. To better simulate the penetration of solute through concrete, the sand content of the mortar mixture was equivalent to that of the total aggregate content of a typical bridge deck concrete. The cylinders were cured in a humidity chamber for 7 days.

The cured mortar cylinders were sliced to form disks approximately 0.25 $\pm$ 0.04 in. (0.6 $\pm$0.1 cm) thick. The edges of these disks were sealed with an epoxy resin, leaving an effective penetration diameter of 0.60 in (1.5 cm). Rubber "O"-rings were placed on the epoxy surfaces while the epoxy was still tacky to assure good adhesion between the "O"-ring and the concrete surface. A schematic representation of the mortar disk specimen is shown in Fig. 1. The disks were then placed between 2 glass flanges and connected to a vacuum source.

The specimen and holder were attached to a vacuum line to detect leaks in the epoxy seal or in the concrete disks themselves. This evacuation process also dried the specimens. The specimen holder was then attached to a vacuum flask and evacuated using a water aspirator. In this arrangement, one side of the disk was exposed to the vacuum and the other side was exposed to air at atmospheric pressure as shown in Fig. 1. A measured quantity of solution was placed on the air side of the system and a rubber stopper was placed on the open tube to eliminate any solvent loss due to evaporation. Vacuum was maintained on the specimens for various periods of time, and the fluid remaining in the reservoir was measured. When surface analyses were to be carried out, the disk was carefully removed from the apparatus, dried at 140°F (60°C) for 15-20 min.

Solutions studied for penetration of inhibitors through mortar were: 0.300M RbCl; chloride-containing simulated pore solution containing 3.5% NaCl by weight; and chloride-containing simulated pore solutions with inhibitor at a concentration of 0.300M. In the preparation of

the inhibitor solutions, sufficient inhibitor was added to pore solution to achieve a concentration of 0.300M. The inhibitors of interest in this study were sodium metaborate, $Na_2B_4O_710H_2O$, and sodium monofluorophosphate, Na_2PO_3F (MFP).

XPS analyses were performed on selected portions of the specimens using a PHI Perkin-Elmer 5300 electron spectrometer which has been modified for small-spot measurements (28). Due to the porous nature of the concrete and the amount of water retained in the specimens (even after heating), the specimens were maintained at liquid nitrogen temperature (-150°C) for the XPS analysis. The XPS analysis allows identification of elements that originate from the inhibitor and to determine their surface concentrations and thus, the penetration time of solute through the disk. The analysis of the specimens was carried out for upper and lower (vacuum side) portions of fractured disk specimens. The spot size for the analysis was 0.04 by 0.12 in. (1 by 3 mm). The binding energy data were used to determine the chemical nature of inhibitor elements.

Electrochemical Studies of the Effect of Inhibitors on Reinforcing Steel Corrosion

Electrochemical measurements were made to determine the corrosion potential of steel reinforcement reinforcing steel immersed in test solutions. For all experiments, a standard calomel electrode was used as the reference electrode. The potentials were measured using a Fisher Accumet Model 910 pH/voltmeter. ASTM Standard C876 (30) relates potential ranges to the probability of corrosion was adopted. These values were converted from a copper sulfate electrode (CSE) scale to a saturated calomel electrode (SCE) scale. In order to obtain satisfactory results, several protocols were assessed.

Protocol 1

Test specimens were prepared by cutting 3 1/2-inch (8.9 cm) rods from the standard reinforcing steel. Bulk and surface analyses of the rods are summarized in Table 2, page 18. One end of each specimen was drilled and tapped to permit electrical connections. The specimens were cleaned in hexane and allowed to dry. The cut end and wire connection were coated with epoxy (Tru-Bond TB-700).

The test solutions were simulated pore solution containing 3.5% NaCl by weight, and simulated pore solution containing 3.5% NaCl by weight and the following concentrations of inhibitor: 0.002M, 0.01M, 0.05M, and 0.1M. The inhibitors studied were sodium nitrite ($NaNO_2$), sodium monofluorophosphate (Na_2PO_3F), and sodium tetraborate ($Na_2B_4O_7$). The test solutions were aerated for 2 hours prior to reinforcing steel immersion. Duplicate samples of reinforcing steel, each contained in 8.45 oz. (250 mL) of solution, were

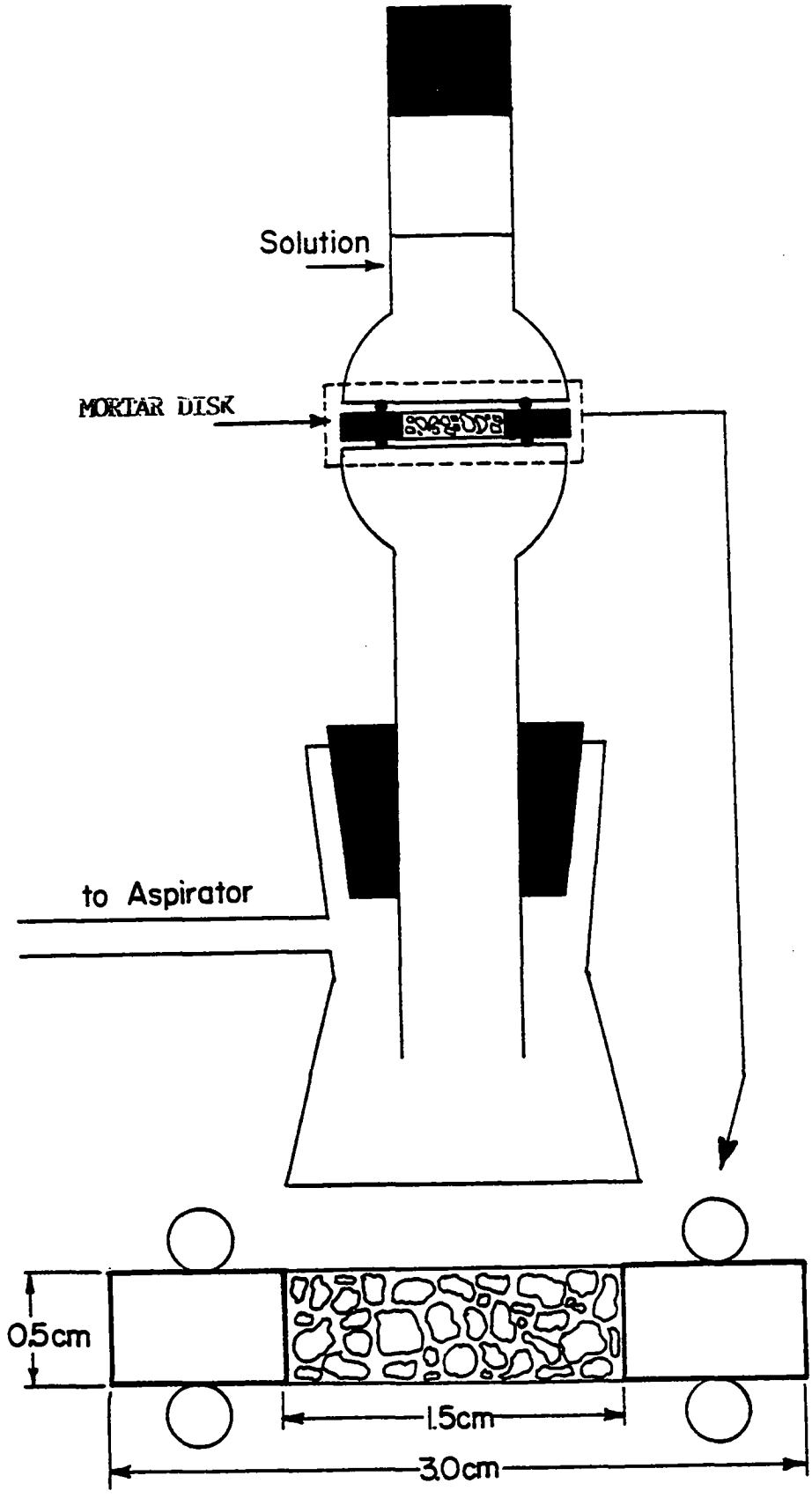

Fig. 1 Schematic diagram of the solution penetration-aspirator apparatus and mortar disk.

maintained at 140°F (60°C) for 18 weeks. To minimize evaporation of solution, the bottles were covered with plastic. The test solutions were replaced every 2-3 weeks to maintain proper aeration, volume, concentration, and pH. Potential measurements were taken every 2 weeks.

Protocol 2

In these experiments, 3 in x 1 in x 1/4 in (7.62 x 2.54 x 0.64 cm) segments of A36 flat stock steel were tested. The bars were drilled and tapped in one end to permit electrical connections. Bars were cleaned in hexane and allowed to dry. Additional bars were cleaned in a 1:1 solution of sulfuric acid and deionized water. The latter bars were also scrubbed with a Scotchbrite pad, rinsed with deionized water, allowed to dry, cleaned with hexane, and allowed to dry. Two coats of Nybco epoxy paint were applied to each end of the reinforcing steel and allowed to cure according to the manufacturer's specifications.

The test solutions were simulated pore solution; pore solution containing 3.5% NaCl (by weight); pore solution containing 3.5% NaCl (by weight) and 0.300M $NaNO_2$; and pore solution containing 3.5% NaCl and 0.670M $NaNO_2$. The test solutions were aerated for 2 hours before use. The solution volume was maintained at 6.76 oz. (200 mL). Specimens were maintained in solution for 28 weeks at 140°F (60°C). Duplicate specimens were prepared and the bottles were covered with plastic. The test solutions were replaced every 2 weeks. Potential measurements were taken every 2 weeks.

Protocols 3 and 4

The third and fourth protocols also utilized A36 flat stock steel. Electrical contact was made with an alligator clip attached to an insulated copper wire/BNC connector. The bar segments in these experiments were washed in hexane and allowed to dry. When the potential measurements were to be taken, the bar was removed from the test solution, the end of the bar was dried, and electrical connection was made with the alligator clip.

For the third experiment, each specimen was placed in a 4.22 oz. (125 mL) solution of deionized water containing 10% NaCl (by weight). These specimens were placed in an oven at 140°F (60°C) for one hour in order to produce an active corrosion potential. Each bar was then placed in 4.22 oz. (125 mL) of the test solution and the bottle loosely capped. The test solutions were pore solution; pore solution containing 3.5% NaCl (by weight); and pore solutions containing 3.5% NaCl (by weight) and sodium tetraborate inhibitor at the concentrations; 0.002M, 0.01M, 0.5M, and 0.1M. Another bar specimen was immersed in the original "precorrosion" solution; this specimen served as a control or reference specimen. The solutions were aerated for 2 hours prior to reinforcing steel immersion. The test samples were prepared in duplicate and maintained at 140°F (60°C) for 56 days. The test solutions were replaced every 2 weeks. Potential measurements were taken several times weekly and then at selected intervals.

In the last protocol (fourth protocol), bars were cleaned in hexane and dried. The bars were "precorroded" in aerated deionized water containing 10% NaCl (by weight) at pH 8.5 - 8.6 for 1 week at 140°F (60°C). Measurements of the corrosion potentials were taken after 1 week. The bars were subsequently placed in 3 duplicate test solutions. The pH of each duplicate solution was adjusted to 8, 10 and 12, respectively. These adjustments were made with HCl, NaOH and $NaHCO_3$. The solutions consisted of deionized water containing 10% NaCl (by weight) and deionized water containing 10% NaCl (by weight) and 0.100M inhibitor. The inhibitors were sodium nitrite, sodium tetraborate, sodium monofluorophosphate and tetrabutylphosphonium bromide ($[CH_3(CH_2)_3]_4PBr$). The volume was maintained at 4.22 oz. (125 mL) and the temperature at 140°F (60°C) for 9 days. Potential and pH measurements were taken after 1, 3, 6, 9 and 18 days. The solutions were replaced after 18 days. At this time, the NaCl concentration was decreased to 1.75% (by weight) and the inhibitor concentration was increased to 0.600M, except for the concentration of tetrabutylphosphonium bromide, which was maintained at 0.100M. Additional duplicate test solutions and reinforcing steel specimens were prepared to include pH 12.5 and pH 13.0. Potential and pH measurements were taken after 3 and 6 days at the new conditions. The pH of each solution was readjusted after the third day.

Results, Discussion and Conclusions

Rebar Cleaning and Sample Preparation

Initial reinforcing steel cleaning experiments were carried out so that throughout the study a common pretreatment designed to remove grease and dirt would be used, and thus a kind of "standard" surface would be studied. To this end, the organic solvents alcohol, and hexane, and an aqueous acid solution were investigated to discover which treatment least altered the as-received reinforcing steel surface. The surface analysis results obtained in these experiments are summarized in Table 2. Hexane cleaning was selected for the following reasons:

1) the chemical content and the chemical nature of the surface elements on the reinforcing steel surface were not altered significantly;
2) residual solvent on the treated surface was minimal and less than that found following treatment with alcohol, acetone, or other organic solvents.

Following alcohol cleaning, a greater concentration of oxygen and lower concentrations of copper and zinc are at the surface. In addition the chemical nature of carbon was altered to about 25 at.% whereas the concentration of this group on as-received reinforcing steel was about 10 at.%. For sulfuric-acid-treated reinforcing steel, significant surface concentration changes are noted among the metals: the iron and copper concentrations are greater than the as-received specimens, whereas the surface contents for calcium and zinc are below the detection level, <0.1 at.%. Thus, cleaning the reinforcing steel surface with sulfuric acid caused significant change in surface chemical content. The present experiments are to

simulate, as closely as possible, long-term reinforcing steel exposure to the corrosive conditions found in the construction and/or repair of bridges; the severe alterations caused by sulfuric acid cleaning were not accurate simulations of normal exposure. Thus, it was concluded that cleaning with a hydrocarbon solvent (hexane) was the preparation method most likely to yield good results in accelerated laboratory corrosion tests.

Rapid Screening Test

At the beginning of this study, all basic test parameters were open to investigation. Preliminary experiments led to the conclusion that testing would have to be conducted at an elevated temperature if results were to be achieved after a reasonably short time. The final choice of 140°F (60°C) is sufficiently high for rapid testing, yet sufficiently low that the needs for solution replenishment and replacement are kept within manageable limits.

The baseline data by which the extent of corrosion in chloride-doped pore solution at 140°F (60°C) was judged and is presented in Table 3. Under the conditions finally selected for the screening tests, the controls suffer surface corrosion to the extent of about 1% per day. The results in Table 3 are based on 10 replicate specimens and presents the standard deviations of the average percent corrosion. Despite the fact that this test is based solely on visual estimates of the extent of corrosion, the estimated standard deviations show that with a sufficient number of replicate specimens, a good estimate of corrosion can be reliably obtained.

Experiments using the known corrosion inhibitors sodium nitrite and sodium monofluorophosphate provided data concerning how long to conduct the tests, at what temperature to maintain the oven, and when to either replenish or change solutions.

Also during the preliminary phase of the investigation a number of studies were made on the effect of specific inhibitor concentration on the extent of corrosion. The effect of varying sodium nitrite concentration on the percent corrosion is presented in Table 4. The effect of varying sodium molybdate concentration is presented in Table 5. As shown, sodium nitrite is a more effective corrosion inhibitor than sodium molybdate.

Sodium nitrite is one of the best available inhibitors under the test conditions, and the results presented in Table 4 demonstrate that it is effective even at concentrations as low as 0.00200 molar. Conversely; sodium molybdate is one of the worst inhibitors under the test conditions. Corrosion in 0.002 molar sodium molybdate environment is indistinguishable

Table 2. Bulk (wt%) and XPS Surface Analysis (atomic %) of reinforcing steel Material.

	BULK ANALYSIS			REINFORCING STEEL TREATMENT			
Element	wt%		calc. at.%	as received	alcohol	hexane	sulfuric acid
C	0.22		1.10	58.4	53.7	56.4	51.9
O		not analyzed		28.7	36.7	31.6	30.2
N		not analyzed		1.41	1.10	1.09	0.96
Fe	97.2		96.5	3.68	3.97	4.64	7.54
P	0.018		0.32	<0.1	<0.1	<0.1	<0.1
S	0.036		0.062	0.85	0.81	0.62	0.58
Si	0.59		1.16	3.26	3.27	2.56	2.04
Na		not analyzed		0.97	<0.1	0.68	0.78
Ca		not analyzed		0.45	0.43	0.59	<0.1
Mn	1.00		1.00	<0.1	<0.1	<0.1	<0.1
Al	0.006		0.01	<0.1	<0.1	<0.1	<0.1
Cu	0.26		0.23	2.06	1.02	1.70	6.01
Zn		not analyzed		0.18	<0.1	0.10	<0.1
Cd		not analyzed		<0.1	<0.1	<0.1	<0.1

Table 3. Results of Control Tests Corrosion

Tests of control samples in chloride doped pore solution without inhibitor (controls) at 140° F (60° C).

Time (days)	Percent Corrosion*
35	26 ± 8
56	52 ± 22

*Reported values are the average of ten replicate samples.

Table 4. Corrosion Inhibition of Sodium Nitrite

Corrosion of reinforcing steel samples in chloride-doped pore solution at 140° F (60° C), exposure time, 28 days.

Sodium Nitrite Concentration mol/L	Percent Corrosion	Number of Replicates
0.002	5.4 ± 2	10
0.01	6.2 ± 2	10
0.05	4.8 ± 2	10
0.1	3.8 ± 1	10
0.5	3.4 ± 1	10
Control	21 ± 1	10

Table 5. Corrosion Inhibition of Sodium Molybdate

Corrosion of reinforcing steel samples in chloride-doped pore solution at 140° F (60° C), exposure time 33 days.

Sodium Molybdate Concentration* mol/L	Percent Corrosion	Number of Replicates
0.00200	25 ±14	10
0.0100	23 ± 9	10
0.0500	13 ± 9	10
0.100	11 ± 3	10
0.500	8 ± 2	10
Control	25 ± 1	10

from that in the control solutions, see Table 5. However, at high concentration sodium molybdate has a modest inhibiting effect.

Based on the results of the concentration studies, it was determined that an inhibitor concentration of 0.002 molar would be used in the screening test. The final test parameters used in the screening test are summarized:

- Test Solution: 0.3 M sodium hydroxide, 0.6 M potassium hydroxide, saturated with calcium hydroxide, 3.5% by mass sodium chloride, aerated for a minimum of 90 minutes.
- Test Specimen: 1 in (1.27 cm) long, half cylinder of reinforcing steel. reinforcing steel prepared by hexane cleaning.
- Test Conditions: 140°F (60°C) for 30 days with bi-weekly replacement of test solution. One reinforcing steel test specimen submerged in 3.38 oz. (10 mL) of test solution in a small vial.
- Specimens: Minimum of 5 replicates.
- Evaluation: Visual estimation per ASTM G46-76.

Selection and Performance of the Corrosion Inhibitors

The known corrosion inhibitors for bare steel reinforcing steel were among those first tested. As presented in Table 6, both sodium nitrite and sodium monofluorophosphate rank high, based on the results obtained. These results demonstrate that the rapid screening test has practical value. While by themselves they do not validate the test, had these inhibitors performed badly, the test itself would be suspect.

A number of criteria were used in selecting materials to be tested. Known inhibitors in alkaline systems, such as sodium metasilicate, were natural candidates. The phosphonic acid salts (Dequests) were selected because of their high solubility in alkaline systems and potential ability to form surface films. A standard listing of commercially available inhibitors (32) provided many sources of up-to-date information, and, wherever possible, industry experts were asked for their recommendations. Eventually, a wide range of potential inhibitors was tested. Details of the chemical composition (where known) and the sources of the inhibitors are described in the experimental section. The results of these studies are shown in Table 6. Because the test is relatively inexpensive to conduct, many commercial materials could be investigated in a relatively short period of time.

Near the end of the investigation, highly promising agents and recently discovered corrosion-inhibiting agents were studied. As a result of these tests, some agents exhibited improved performance, for reasons unknown, compared to earlier tests (see Table 6) while some new

materials demonstrated good performance in the screening test. The materials demonstrating improved/good performance and the performance of the new compounds are summarized (the % surface corrosion is given in parenthesis): Improved performance - Witcamine PA-78B (2.2); Witcamine PA-60B (5.8); sodium silicate (3.6); calcium borate (6.6); Alox 2291 (6.2); new materials - Alox 901 (5.0); Alkaterge T-IV (6.2); zinc borate (3.3); and boric acid (5.6).

Summary and Observations

A useful, rapid screening technique has been developed to test the effectiveness of corrosion inhibitors for reinforcing steel corrosion. Known corrosion inhibitors recommended for this use, such as sodium nitrite and sodium monofluorophosphate, perform well in the test. These results tend to confirm the utility and validity of the test. Under the conditions chosen, it is concluded that a visually estimated corrosion of greater than 9% is sufficient to exclude a particular inhibitor from further testing. Highly promising corrosion inhibitors are those that exhibit less than 7% corrosion under the test conditions.

Many organic, commercial inhibitors also perform well, as do certain borate salts. Reported are the averages of 5 replicate samples exposed to chloride-doped pore solution at 140°F (60°C) for the number of days stated. The inhibitor concentration was 0.002 M. Tests of the practical efficiency of borate salts in the treatment of chloride-contaminated concrete that remains in place are warranted because borate salts are inexpensive. Certain of the organic corrosion inhibitors may find use in treating the reinforcing steel in situations where bridge deck rehabilitation involves concrete removal and exposure of the reinforcing steel.

Surface Characterization of Reinforcing Steel and Its Interaction with Inhibitors

Surface-sensitive analytical techniques, especially Electron Spectroscopy for Chemical Analysis (ESCA)/X-ray and Photoelectron Spectroscopy (XPS) (27-29) have been used extensively to study the surface changes in reinforcing steel after its exposure to simulated pore solution , simulated pore solution with chloride doping, and simulated pore solution with chloride doping and added inhibitors. The surface analyses were carried out to determine the chemical nature of inhibitor constituents on the reinforcing steel surface, to evaluate the surface concentration of inhibitor elements, and to correlate the results with corrosion test experiments. It was reasoned that surface analysis measurements could not only aid in understanding the role and mechanism of corrosion inhibitor action, but that such measurements would also be valuable for determining the effectiveness of inhibitors in short-term screening tests.

The surface analysis results (atomic % composition) following the immersion of reinforcing steel in pore solution containing NaCl were compared with the corresponding data for hexane-cleaned reinforcing steel in Table 7. The principal alterations in surface chemistry as a result of the immersion of hexane-cleaned reinforcing steel in pore solution containing

NaCl are increases in oxygen, iron, silicon, sodium, potassium, and chlorine; and decreases in carbon, nitrogen, and copper. It is reasonable to conclude that the changes are related to the formation of iron oxide on the reinforcing steel surface. The presence of calcium, potassium, and chlorine on the treated reinforcing steel may arise from adsorption of these elements on the oxide surface. Associated with the alteration in the oxygen atomic concentration is a change in the shape of the oxygen 1s photopeak. The photopeak presented in Fig. 2A exhibit features attributed to oxide oxygen (BE = 529 eV), as the dominant peak for hexane-cleaned reinforcing steel. The spectrum for reinforcing steel immersed in pore solution shows that contributions by hydroxide dominate (BE = 530 eV), although the

Table 6. Summary Results of Inhibitor Screening Test Values*

Inhibitor	Exposure (days)	Percent Corrosion (%)
Alox 901	34	4.8
Sodium nitrite	28	5.4
Sodium monofluorophosphate	28	5.4
Aqualox 2268	28	5.6
Sodium tetroborate	28	5.6
Alox 350	34	6.4
Alox 2162	34	6.4
Miramine TOC	34	6.4
Alox 600	34	6.8
Monacor 39	34	7.2
Sodium Nitrate	34	8.0
Sodium silicate (1:3.22, $Na_2O:SiO_2$)	34	9.8
Sodium metasilicate	34	10.0
Sodium carbonate	34	10.0
Alox 502 A	34	10.2
Witco PA 78B	34	10.4
Alox 2291	34	10.6
Witco PA 60B	34	10.8
Sodium dihydrogen phosphate	28	12.6
Amine CS-1135	34	12.8
Alox 319F	34	12.8
Potassium dichromate	34	14.0
Dequest 2010	21	15.0
Potassium nitrate	34	15.0
Dequest 2000	28	15.0
Monocor BE	34	15.4
Calcium borate	34	19.0
Dequest 2054	21	20.8
Calcium sulfate	34	22.4
Sodium molybdate	33	25.0
Control (no inhibitor)	35	26.0

* Reported are the averages of five replicate samples exposed to chloride-doped pore solution at 140°F (60°C) for the number of days stated. The inhibitor concentration was 0.002 M.

concentration of oxide oxygen remains at a significant level (see Fig. 2C). Additional although the concentration of oxide oxygen remains at a significant level (see Fig. 2C). Additional oxygen photopeaks in the curve-resolved spectrum are attributed to oxygen in silicon-containing species and adsorbed water. In the discussion of the analysis for reinforcing steel treated in the inhibitor solutions, the first comparison will be made with results obtained for reinforcing steel cleaned in hexane and immersed in chloride-containing pore solution. Following that, the results for the materials from "initial" and "delayed" inhibition experiments will be compared.

Sodium Nitrite

The surface analysis results following the treatment of reinforcing steel with sodium nitrite in pore solution containing chloride are given in Table 7. The findings for the initial inhibition experiments indicate an increased surface content only for carbon. The concentrations for oxygen and calcium decrease while the surface contents for nitrogen, iron, silicon, and sodium remain essentially unchanged. The results for nitrogen are of particular interest. The percent nitrogen and the N 1s binding energy (399.0 eV) for sodium nitrite-treated reinforcing steel are similar (within experimental error) to the results found for reinforcing steel treated only in pore solution containing chloride. A nitrogen-containing species with a binding energy not characteristic of nitrite (N 1s BE in sodium nitrite = 404.1 eV) is detected, which indicates that nitrite is not chemisorbed on the reinforcing steel surface. Alterations in the oxygen photopeak indicate that a chemical change has taken place on the reinforcing steel surface as a result of immersion in nitrite-containing pore solution. Thus, any nitrogen-containing reaction product must be released into solution or the adsorbed nitrogen will exhibit a binding energy at 399.0 eV. The decrease in the oxygen concentration may at first appear surprising in view of the fact that nitrite appears to alter the surface chemistry of reinforcing steel. Nevertheless, the change that occurs is an alteration in the distribution of oxygen surface groups. The oxygen 1s photopeak was curve-resolved into contributions from oxide oxygen bonded to transition metals (BE = 529 - 530 eV); hydroxide oxygen associated with metals (BE = 530 - 531 eV); oxide oxygen for alkali and alkaline earth metal compounds and silicon oxide species (BE = 531 - 532 eV); and adsorbed water (BE = 532 - 533 eV). The OH^- oxygen (BE = 530 eV) decreases while the relative percent for the transition metal oxide oxygen (BE = 529 eV) increases for the nitrite-treated sample (see Table 8 and Fig. 2B). Oxygen associated with other functionalities remains unchanged. These findings can be interpreted to suggest that the probable role of nitrite in the inhibition process is to decrease surface hydroxide functionality while increasing that for oxide species. Considering that sodium nitrite is an effective corrosion inhibitor (33, 34), the surface analysis results suggest that one of the characteristics of useful inhibitors would be those that increase the surface concentration of metal-oxide functionality, especially iron oxide content.

The results for delayed inhibition specimens indicate little or no change (within the error limits) in elemental composition compared to the results for initial inhibition materials. The principal alteration is the increase in the concentration of metal-oxide oxygen from 23.6% to

Table 7. Surface Analysis Results for reinforcing steel Specimens Following Interaction with Inhibitors*.

Treatment	Element	C	O	N	Fe	Si	Na	Ca	Cl	Inhibition element
Hexane Cleaned		60.3	28.3	1.83	4.07	1.33	1.67	0.21	--	--
		(5.3)	(3.5)	(0.67)	(1.04)	(0.78)	(0.9)	(0.2)		
8 days chloride-contg. pore sol. 60° C		37.4	43.0	0.57	6.43	2.69	3.72	4.24	1.33	--
		(2.6)	(3.2)	(0.23)	(0.89)	(0.15)	(0.46)	(0.28)	(0.08)	
0.300M $NaNO_2$	Initial	49.8	33.2	1.11	5.23	2.08	3.90	1.78	1.10	--
	Inhibition	(8.3)	(4.9)	(0.96)	(2.27)	(0.38)	(1.03)	(1.01)	(0.22)	
	Delayed	57.3	30.7	0.47	5.02	2.39	1.92	1.27	0.44	--
	Inhibition	(3.7)	(2.8)	(0.12)	(0.58)	(1.02)	(1.11)	(0.22)	(0.13)	
0.300M Na_2MoO_4	Initial	41.6	39.6	1.13	7.29	3.31	4.07	0.81	1.01	Mo 0.46
	Inhibition	(3.7)	(2.2)	(0.21)	(1.08)	(0.56)	(0.83)	(0.27)	(0.09)	(0.15)
	Delayed	30.6	45.4	1.92	9.13	5.07	3.83	1.67	1.06	Mo 0.52
	Inhibition	(0.74)	(2.7)	(0.43)	(1.92)	(1.98)	(0.39)	(0.83)	(0.51)	(0.07)
0.300M NaH_2PO_4	Initial	35.1	42.3	0.32	5.94	1.67	10.2	0.14	1.81	P 1.54
	Inhibition	(3.84)	(0.41)	(0.40)	(1.42)	(0.36)	(2.6)	(0.03)	(0.55)	(0.44)
	Delayed	20.1	48.8	0.22	12.0	2.5	11.5	1.21	1.85	P 2.27
	Inhibition	(7.4)	(4.4)	(0.17)	(1.3)	(0.31)	(3.3)	(1.637)	(0.49)	(0.55)
0.300M Na_2PO_3F	Initial	48.5	32.6	0.38	5.82	2.04	6.60	0.06	1.54	F 0.27
	Inhibition	(9.9)	(5.7)	(0.87)	(3.2)	(0.55)	(2.80)	(0.09)	(1.05)	(0.27)
										P 0.71
										(0.29)
0.300M Na_2PO_3F	Delayed	35.5	40.3	0.32	8.39	3.01	6.15	0.50	1.55	F 0.77
	Inhibition	(4.6)	(3.9)	(0.23)	(0.86)	(0.78)	(1.83)	(0.23)	(0.05)	(0.18)
										P 1.20
										(1.0)

* The Results are given in atomic percent and the standard deviations are given in parenthesis.

Table 7. (Cont'd)

Treatment	Element	C	O	N	Fe	Si	Na	Ca	Cl	Inhibition element
0.300M $Na_2B_4O_7$	Initial	61.1	29.4	0.19	<0.1	1.03	3.23	3.15	1.20	B 5.03
	Inhibition	(4.9)	(4.1)	(0.27)		(0.76)	(1.58)	(1.16)	(0.51)	(3.81)
	Delayed	39.7	38.8	1.30	0.29	0.73	7.13	1.95	4.77	B 6.14
	Inhibition	(2.3)	(4.8)	(1.13)	(0.51)	(0.35)	(1.82)	(0.30)	(2.12)	(1.50)
0.300M Dequest 2000	Initial	18.9	48.9	4.44	5.73	0.55	5.97	0.5	0.08	P 13.2
	Inhibition	(3.9)8.	(2.8)	(0.33)	(1.97)	(0.35)	(0.68)	(0.33)	(0.12)	(0.9)
	Delayed	7	45.6	4.39	6.60	0.78	5.75	0.10	0.64	P 13.6
	Inhibition	(1.4)	(1.9)	(0.17)	(0.42)	(0.23)	(1.82)	(0.18)	(0.3)	
0.300M Dequest 2010	Initial	17.9	50.5	<0.1	14.6	4.56	4.12	0.34	2.20	P 2.72
	Inhibition	(1.4)	(0.7)		(1.5)	(1.21)	(1.35)	(0.11)	(0.81)	(0.45)
	Delayed	21.3	48.6	0.27	6.20	2.53	5.70	0.10	1.40	P 2.59
	Inhibition	(9.9)	(4.9)	(0.38)	(1.51)	(0.73)	(1.69)	(0.10)	(0.34)	(0.78)
0.300M Dequest 2054	Initial	47.4	33.7	1.50	4.06	1.56	2.28	2.74	0.66	P 3.06
	Inhibition	(2.8)	(3.0)	(0.37)	(1.50)	(0.30)	(0.49)	(1.02)	(0.36)	(0.58)
	Delayed	44.3	36.9	1.08	3.80	1.69	2.07	2.07	0.63	P 2.69
	Inhibition	(8.7)	(5.0)	(0.16)	(0.88)	(0.88)	(0.90)	(0.90)	(0.22)	(1.08)

35.5%. It is likely that the increase is associated with the formation of additional passive iron oxide at the surface. This interpretation is similar to that suggested by others who undertook characterization studies (33, 34). In screening tests it was demonstrated that sodium nitrite is an effective corrosion inhibitor.

Sodium Molybdate

The interaction of sodium molybdate with reinforcing steel either via initial or delayed inhibition experiments (see Table 8) produced an increased surface concentration of iron and associated iron oxide. Molybdenum was detected on the reinforcing steel surface at a concentration of about 0.5 atomic % and a corresponding increase in the oxygen associated with Mo(VI) at BE = 531.0 eV was noted. A comparison of the Mo $3d_{5/2}$ binding energy for Na_2MoO_4 (BE = 232.4 eV) with that for molybdenum from the two reinforcing steel exposure experiments (BE = 232.2 and 232.3 eV, respectively, for initial and delayed inhibition experiments) shows that molybdenum as molybdate, Mo(VI), is adsorbed on the reinforcing steel surface. A decrease in calcium and an increase in silicon concentrations were found compared to the data obtained for reinforcing steel exposed only to chloride-containing pore solution. Within experimental error, the concentration of other elements did not change. The increase in iron and oxide oxygen and the detection of molybdenum as Mo(VI) indicate that molybdenum affects the reinforcing steel surface through an adsorption process such that oxide constituent contributions are increased at the surface. If molybdate acts as an oxidizing agent, the surface analysis results provide no indication of what the reduced molybdenum product would be. The molybdenum photopeak was characteristic only of molybdenum (VI), i.e., no reduced molybdenum species were detected at the surface. Lack of detection of reduced molybdenum could occur if the reduced product is not adsorbed on the reinforcing steel surface or if the concentration of reduced molybdenum is too small to contribute significantly to the Mo 3d photoelectron signal. However, screening corrosion tests performed in this study show that molybdate is a relatively poor inhibitor. Oxygen spectra were not curve-resolved, only interpreted in a qualitative manner.

Sodium Dihydrogenphosphate (DHP)

The interaction of sodium dihydrogenphosphate (DHP) with reinforcing steel surfaces results in little or insignificant change in oxygen, nitrogen, silicon, or iron concentrations, while the concentrations for sodium and phosphorus increase dramatically for the initial inhibition experiments. In these experiments, the calcium content is reduced significantly compared to that found for reinforcing steel treated only in chloride-containing pore solution. A comparison of the initial and delayed inhibition results indicates a significant increase in iron content.

An alteration in the distribution of oxygen species on the surface accompanies the change in surface concentrations for oxygen in both initial and delayed exposures. The O 1s photopeak was resolved into 3 components which are characteristic of metal oxide (BE = 529 - 530 eV); metal hydroxide and phosphate oxygen (BE = 531 - 532 eV); adsorbed oxygen, and

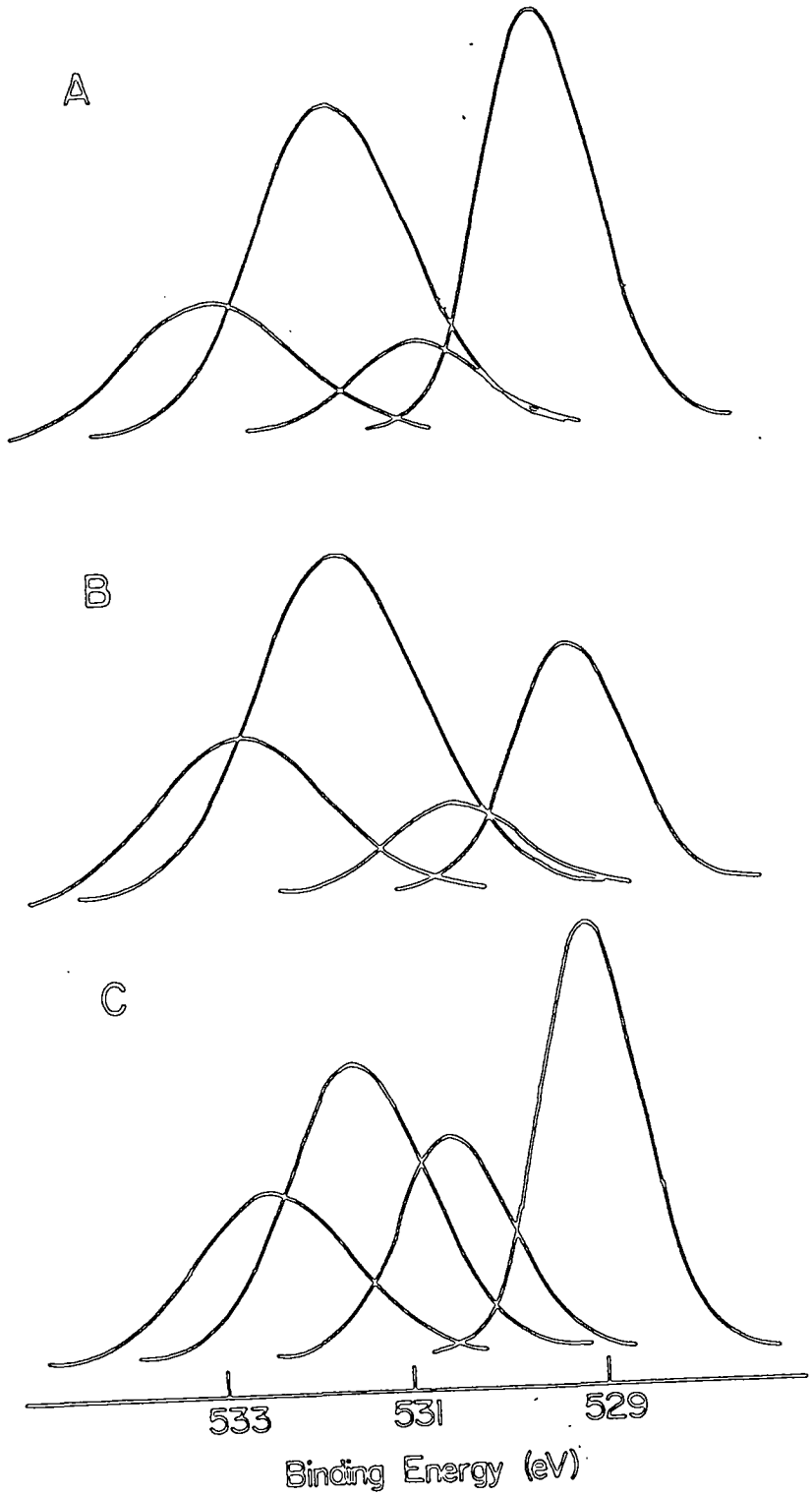

Fig. 2. Oxygen 1s Photoelectron Spectra

probably water (BE = 532 - 533 eV). Compared to reinforcing steel treated in only chloride-containing pore solution, the concentration of oxygen surface species for metal oxide is greater following phosphate treatment. The concentration of oxygen attributable to OH^- is less following phosphate treatment. The dominant contribution to the O 1s photopeak in the range of 531 to 532 eV is oxygen bound to phosphorus. The detection of phosphate phosphorus on the treated surface combined with the decrease in OH^- group content may indicate a surface acid/base reaction as the process promoting reinforcing steel surface changes that relate to inhibition. The adsorption of phosphate may also aid in corrosion inhibition by passivating potentially active corrosion sites on the reinforcing steel surface. Screening tests as a part of this work show that dihydrogenphosphate is only a modest corrosion inhibitor.

Sodium Monofluorophosphate (MFP)

Inhibition experiments were carried out with monofluorophosphate to compare the results with those found for dihydrogenphosphate (DHP). The results are presented in Table 8. The principal differences, compared to DHP, are that the oxygen, iron, sodium, and phosphorus concentrations are lower on MFP-treated reinforcing steel. The results indicate that MFP interacts with reinforcing steel to a lesser extent than DHP. The oxygen functionality distribution is also consistent with this finding in that metal oxide content and phosphate-oxygen concentration are both lower for the reinforcing steel surface treated with MFP. Interestingly the expected 1:1 phosphorus to fluorine atomic ratio for PO_3F^{2-} is not found on the reinforcing steel surface. The P/F ratio for the initial inhibition specimens is 2.6, and that for the delayed inhibition samples is 1.6. This non-unity ratio suggests the loss of fluorine for adsorbed phosphate inhibitor. A process that may account for this observation is hydrolysis of MFP (either partial or complete) at the reinforcing steel surface or in solution. Either process would liberate fluoride and phosphate into solution and might result in subsequent adsorption of fluoride and/or phosphate. The phosphorus 2p binding energy for phosphorus adsorbed on reinforcing steel from MFP is equivalent to that for phosphate (PO_4^{3-}) in phosphate salts. The equivalence of binding energies is consistent with the proposed hydrolysis process. Corrosion screening tests (see Table 6) demonstrate that MFP is a good corrosion inhibitor.

Sodium Tetraborate

The reaction of sodium tetraborate with reinforcing steel produced a unique result, as shown in Table 8. The oxygen photopeak is characteristic of oxide oxygen from borate and the boron 1s binding energy is equivalent to that for pure sodium borate. Boron is detected at 5% and 6%, on initial and delayed inhibition reinforcing steel specimens, respectively. No iron was detected ($<0.1\%$) in the measurement of the Fe 2p photoelectron spectra for borate-treated reinforcing steel. The fact that iron is not detected at the surface while oxygen and boron photopeaks characteristic of borate are detected suggests that borate reacts, under the chosen experimental conditions, to produce a coating on the reinforcing steel. The behavior of forming a coating on reinforcing steel is unlike the modes of interaction found

for other investigated inhibitors.

Upon comparison of initial versus delayed inhibition, the atomic concentrations vary as noted; sodium and chlorine increase while calcium decreases. The increase in sodium is consistent with the increase in borate concentration and may indicate adsorption of sodium on the borate coating.

Table 8. Curve Resolved O 1s Results for reinforcing steel and reinforcing steel Immersed in Pore Solutions with and without Inhibitor

Specimen Treatment	Metal Oxide BE=529-530	Metal Hydroxide BE = 530-531	Silicon-oxygen oxy anion-oxygen BE = 531-532	adsorbed oxygen water BE = 532-533
hexane cleaned	31.5	15.2	27.7	25.6
pore solution (8 days)	21.7	7.1	50.2	21.0
pore solution + 3.5% NaCl (8 days)	16.0	3.5	61.7	18.9
pore solution + 3.5% NaCl (8 weeks)	15.0	4.3	56.9	23.8
$NaNO_2$ (*ii*)*	23.6	3.6	45.6	27.2
$NaNO_2$ (*di*)+	23.6	3.6	45.6	27.2
Na_2MoO_4 (*ii*)*	32.9	<2.	37.4	29.8
Na_2MoO_4 (*di*)+	35.9	<2.	43.6	20.6
NaH_2PO_4 (*ii*)*	38.8	<2.	42.8	18.4
NaH_2PO_4 (*di*)+	42.1	<2.	41.6	16.3
Na_2PO_3F (*ii*)*	34.5	<2.	46.7	18.8
Na_2PO_3F (*di*)+	31.2	<2.	48.8	20.0
$Na_2B_4O_7$ (*ii*)*	3.1	8.7	59.2	29.0
$Na_2B_4O_7$ (*di*)+	2.2	2.1	72.7	23.0

* (*ii*): initial inhibitation
+ (*di*): delayed inhibitation

The findings for borate treatment suggest that such a coating could function as a barrier layer on the reinforcing steel to inhibit chloride-induced corrosion. Sodium tetraborate exhibits excellent corrosion inhibition in screening tests (See Table 6).

Dequests

Dequests (phosphorus-containing compounds having various structures) are widely used for corrosion prevention in alkaline aqueous environments. Dequest 2000 is a trialkylphosphate amine. There are significant differences in atomic composition upon comparing initial and delayed inhibition results. The important surface composition changes for Dequest-treated reinforcing steel compared to reinforcing steel treated in chloride-containing pore solution are increases in nitrogen, phosphorus, and sodium, and a decrease in calcium. The P/N surface ratio of these samples is 3:1, a result indicative of the presence of adsorbed Dequest active component, trialkylphosphate amine. The oxygen spectra indicate contributions from iron oxide, but the principal contribution is from the phosphate functional group. The phosphorus atomic composition (13 at %) indicates significant adsorption on reinforcing steel specimens.

The adsorption of Dequest 2010 on reinforcing steel is noted by the appearance of phosphorus in the spectra for initial and delayed inhibition specimens. The concentration of the respective individual elements is equivalent when comparing initial and delayed treatments, except for iron and silicon. For the latter elements the concentration is greater following the initial inhibition treatment. The oxygen photopeak could be resolved to indicate contributions from metal oxide and adsorbed oxygen (probably water), (see Table 8). However, the principal contribution is from the phosphate-oxygen species. The phosphorus 2p binding energy data are indicative of the adsorption of the phosphorus component without change in chemical nature, i.e., no measurable or detectable change in the oxidation state of phosphorus occurs. Based on the percent surface phosphorus, the adsorption of Dequest 2010 is less favorable by at least a factor of 4 (in a mole percent basis) compared to the adsorption of Dequest 2000 on reinforcing steel specimens.

The interaction of Dequest 2054, (an ethylenediaminete trialkylphosphate) with reinforcing steel does not produce any significant differences in the surface composition when comparing initial and delayed tests. Based on the amount of phosphorus present, the quantity of this material present on reinforcing steel is a least a factor of two less than that for the active component in Dequest 2010. The oxygen functionality includes contributions principally from iron oxide and phosphate from the inhibitor. In general, the corrosion inhibition performance of Dequest materials is not superior to the simple metal salts discussed earlier.

Summary and Observation

The mode of inhibitor interaction with reinforcing steel samples can be grouped into 3 classes based on the surface analysis results:

- nitrite: interactions lead to the formation of an iron oxide surface but the inhibitor itself is not adsorbed as nitrite;
- borate: Interacts to form a coating on the reinforcing steel surface rendering substrate iron undetectable by surface-sensitive analytical measurements;

- other inhibitors: interact via adsorption on reinforcing steel and lead to enhancement of oxide oxygen surface functionalities. In some instances, the oxide functionality could be associated with iron oxide.

On the basis of surface analysis measurements alone, it is impossible to conclude that any one inhibitor is better or worse than another, either in initial or delayed inhibition processes. However, the present findings are fully consistent with the known corrosion inhibition abilities of materials in current use. Furthermore, because the promotion of a characteristic surface iron oxide layer is typical of known inhibitors, it is concluded that any new substance that produces a similar layer is itself likely to be a good candidate inhibitor. In addition, another potentially beneficial corrosion-inhibition process has been revealed in studies of sodium metaborate solutions where a coating is produced on the reinforcing steel surface.

Migration of Corrosion Inhibitors Through Concrete

The effectiveness of an inhibitor is influenced or even controlled by its deliverability to the concrete-rebar interface. The study of a related phenomenon, diffusion of chloride in concrete, has attracted attention as a part of the effort to understand the corrosion of steel reinforcing bars in concrete structures. However, the diffusion of corrosion inhibitor has not been investigated. In this part of the study, the migration of inhibitors in aqueous solutions, using sample test specimens designed to permit accelerated migration of inhibitor solution, has been examined. The principal objectives of this phase of the work were to evaluate the rate of inhibitor migration, to determine whether any change in the chemical nature of the inhibitor had occurred as a result of interaction with concrete, and to inquire whether the anion to cation concentration ratio was affected by migration through the mortar disks. The use of mortar disks permitted acquiring information regarding the migration of inhibitors in a short time frame. The combination of short experiment times and sensitive surface analysis methods enabled rapid evaluation of inhibitor migration and a determination of the chemical nature of the migrating solutes.

The study of the migration of inhibitor solute species through concrete disks was investigated by determining the volume of solution passing through the disks and by analyzing the upper and lower disk surfaces after exposing the disks to the solution for designated periods of time. In the presentation of the results, the volume of solution migrating through the disks is normalized by dividing the volume transported by the thickness of the disk. The data points presented in Fig. 3 represent the migration of solutions for rubidium chloride, sodium chloride in pore solution, and sodium tetraborate in chloride-containing pore solution. The data points are not distinguished, in the figure, since the volume change measured for each solution followed the same behavior. The volume change is a linear function of the square root of time. This finding is in agreement with the prediction of the Washburn equation (35). The significant advantage of the present sample configuration is that the chemical nature of the diffusing species can be determined by subsequent surface analysis of fractured or whole concrete disks.

In the surface characterization measurements, the composition of a mortar (cement + sand) disk was determined in order to evaluate what elements, at what concentration, were present on the disk surface and thus what species could be studied without interference in the migration process. The average elemental composition from measurements on a representative group of disks is presented in Table 9. The surface chemistry is characterized by silicon, calcium, sodium, potassium, oxygen, sulfur, and carbon. Chlorine was detected at the detection level (<0.2%) in some specimens. (The chemical nature of the metals, as inferred from binding energy measurements, corresponds to that expected for alkali (+1) and alkaline earth (+2) metals.) Silicon is present as silicon-oxygen species and sulfur exists as sulfate in these specimens. In the concrete specimens, concentrations of inhibitor elements that are of interest are low or below the detection limits. Thus only the detection of inhibitor that had migrated through the disk was possible.

The results for the migration experiments involving aqueous solutions of RbCl are summarized in Table 10. Rubidium chloride was chosen because rubidium is readily amenable to XPS analysis and is not present in concrete and thus provides an unambiguous result. Solutions of RbCl were ponded on one surface and evacuated on the other side of two disks of different thickness, 0.16 and 0.20 in. (4.1 and 5.1 mm), for 48 and 120 hours, respectively.

The concentrations of rubidium on the top and bottom portions of the disks were approximately equal, indicating that after each time period, the salt had migrated through the disk. Within the experimental error the chlorine content was the same for top and bottom parts of the disks. However, the chlorine content was significantly less than the rubidium concentration. If equivalent migration had taken place, equal atomic concentrations of rubidium and chlorine should have been detected. The migration of rubidium appears, from the presented results, to occur more rapidly. To maintain electroneutrality, the migration of rubidium with another anion, as a cation-anion pair, could have taken place, leading to a lower chloride concentration. The identity of another potential anion is not revealed from the present XPS results.

Since the migration experiments involving inhibitors was conducted using chloride-containing pore solution, the migration of pore solution containing 3.5% NaCl (by weight) was also investigated. The surface analysis data are given in Table 11. The analytical results for sodium and chlorine reveal that the cation migrated through the disk within 8 or 24 hours, for the specimens studied. The respective sodium concentrations on the top and bottom portions of the two disks are equal. The chloride concentration, on either the top or bottom part of the specimen, is less than that for sodium. It appears that an anion exchange process must be taking place with species in the concrete specimen. Elements that could be associated with the cation, including halide ions, were not detected in the XPS measurements. Although sulfate sulfur was detected in the spectra, the concentration of sulfur does not change sufficiently or in a consistent manner such that it could be associated with cation migration. Migration of hydroxide ions along with the cation could take place and provide an explanation for the observed results. An examination of the O 1s

photoelectron spectra do not reveal any significant increase in hydroxide oxygen. However, an increase associated with hydroxide migration would be difficult to distinguish since the concentration of oxygen from other chemical species in the concrete is high, especially silicon-oxygen and calcium-oxygen-containing entities.

The results for penetration into concrete by sodium borate in chloride-containing pore solution are presented in Table 12. Surface analysis results are presented as a function of time for the upper and lower surfaces of the disks following penetration of the solute. Penetration of borate to the bottom of the disk occurs at about 24 hours as evidenced by the large boron percent (6.1%) for that specimen. This percentage is to be compared with the value of 0.8% boron for the bottom surface of the specimen examined after 1.5 hours. It is also noted that the chlorine and sodium concentrations are greater for the 24 hour specimen than for the 1.5 hour specimen. This finding is related to the migration of sodium chloride from the pore solution. In addition, the silicon and calcium contents are smaller for those surfaces where inhibitor is present. This result is attributed to the fact that small crystalline particles of inhibitor material were visible on the disk surface, thus masking the silicon and calcium presence in the concrete. Since the inhibitor solution was in contact with the upper surface of the disks for the duration of these experiments, it is surprising that the boron content for the upper surfaces was not constant. The values range from 5.4% (48 hours) to 1.5% (25 hours). The variation in the percent may be a result of the heterogeneity of concrete and the relatively small spots (1X3 mm^2) that were analyzed on the disks. The binding energies for the B 1s level in the salt that appeared on the upper, BE = 192.2 eV, and lower, BE = 192.3 eV, disk surfaces were equivalent to the value, BE = 192.2 eV, measured for 0.300M sodium borate-pore solution frozen on the XPS sample probe. Thus, it is concluded that interaction of aqueous borate with concrete does not result in degradation or decomposition of the inhibitor. These results indicate also that introduction of borate inhibitor to the reinforcing steel-concrete interface as a result of borate migration should be possible in a reasonable time period.

The experiments with MFP (sodium monofluorophosphate) yielded the surface analysis results given in Table 13. Before considering the results, it is informative to recall the elements that exist in the inhibitor solution. The solution, composed of NaOH, NaCl, and Na_2PO_3F, (plus KOH and Ca(OH)2) yield respective total concentrations of Na = 1.500M; Cl = 0.600M; P = 0.300M; and F = 0.300M, or the atomic ratio Na:Cl:F:P = 5:2:1:1. Analysis of the top surface of the disk in contact with MFP-pore solution for 8 hours exhibits a ratio Na:Cl:F:P = 5:0.75:1.1:1.2. This result is in agreement with the expected ratio except that the chlorine content is significantly lower than expected. Examination of the results for longer exposures reveals that the chlorine percent remains at about 0.3%, a level which is near the detection limit for chlorine. It is reasonable to suggest that chlorine as chloride is adsorbed below the surface of the disk. Following 24 hours of exposure and up to 114 hours, the concentration of sodium at the upper disk surface remains at a concentration of 5-6%, while the concentration on the lower surface is in the range of 1-3%. If it is recognized that sodium from NaCl and NaOH represent 60% of the total sodium present, and if the initial sodium content for the 8 hour top surface is taken as representative

Table 9. XPS Analysis of As-Prepared Mortar

Element	Composition*
C	20.6
O	56.1
Si	13.9
Ca	6.11
S	1.24
K	1.07
Na	0.82
Cl	<0.2

*Results in Atomic Percent.

Table 10. XPS Analysis for RbCl Penetration Through Concrete Disks: Solution penetration Results - 0.300M RbC1

Disk Thickness Surface (mm)	Time (hr)	Atomic Concentration C	O	Si	Ca	Cl	Rb
1 (top) 4.1	48	45.5	40.0	7.1	5.0	0.3	2.1
1 (Bottom)	48	32.7	48.4	9.4	6.7	0.5	2.2
2 (Top) 5.1	120	30.3	49.3	12.1	5.0	0.4	2.1
2 (Bottom)	120	46.1	37.5	7.2	2.9	0.2	3.8

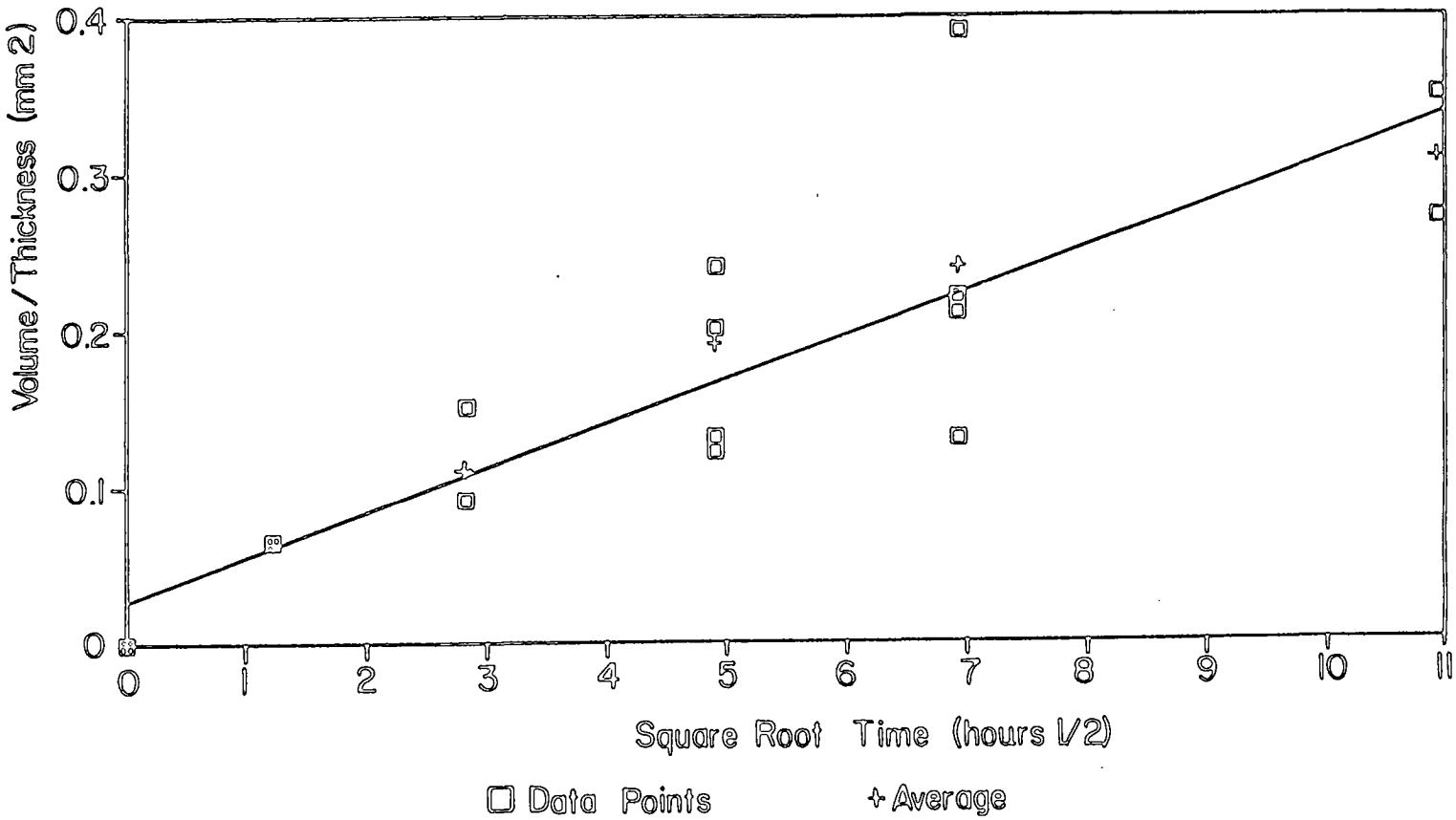

Fig. 3. Washburgn Plot of Pore Solution Migration Versus Square Root of Time

Table 11. XPS Analysis of Chloride-Containing Pore Solution Migration Through Concrete. (Solution: Pore Solution + 3.5% NaCl)

Disk Thickness (in)	Time Surface (hr)	Atomic Concentration C	O	Si	Ca	Cl	Rb
7 - Top (0.22)	8	49.7	34.1	6.1	2.7	1.9	5.5
7 - Bottom	8	43.2	41.4	5.8	5.1	0.4	4.1
8 - Top (0.26)	24	46.3	35.0	7.2	4.6	2.1	4.8
8 - Bottom	24	52.9	34.0	4.9	4.4	0.4	3.3

1 inch = 25.4 mm

Table 12. XPS Analysis for Sodium Tetraborate Pore Solution Migration Through Concrete (Pore Solution + 3.5% NaCl + 0.3 M $Na_2B_4O_7 \cdot 10H_20$).

Disk Thickness (in.)	Time Surface (hr)	Atomic Concentration (%) C	O	Si	Ca	Cl	B	Na
9 Top (0.24)	0.17	38.4	41.3	4.8	5.7	0.3	3.0	6.5
9 Bottom	0.12	44.7	39.1	7.6	6.5	0.2	0.7	1.2
10 Top (0.22)	0.5	46.7	36.1	7.5	5.4	0.2	1.73	2.4
10 Bottom	0.5	45.9	39.0	8.4	4.7	0.2	0.2	1.5
11 Top (0.22)	1.5	36.5	43.1	6.4	6.1	0.2	3.6	4.2
11 Bottom	0.5	35.6	43.9	9.9	5.8	0.2	0.8	3.7
12 Top (0.25)	25	37.2	42.2	8.3	6.1	0.4	1.5	4.5
12 Bottom	25	33.4	39.3	2.9	2.0	3.1	6.1	13.2
4 Top (0.19)	48	32.7	45.0	6.3	5.3	0.4	5.4	5.0
4 Bottom	48	39.9	37.1	1.0	0.9	3.6	5.8	11.7

1.0 inches = 25.4 mm

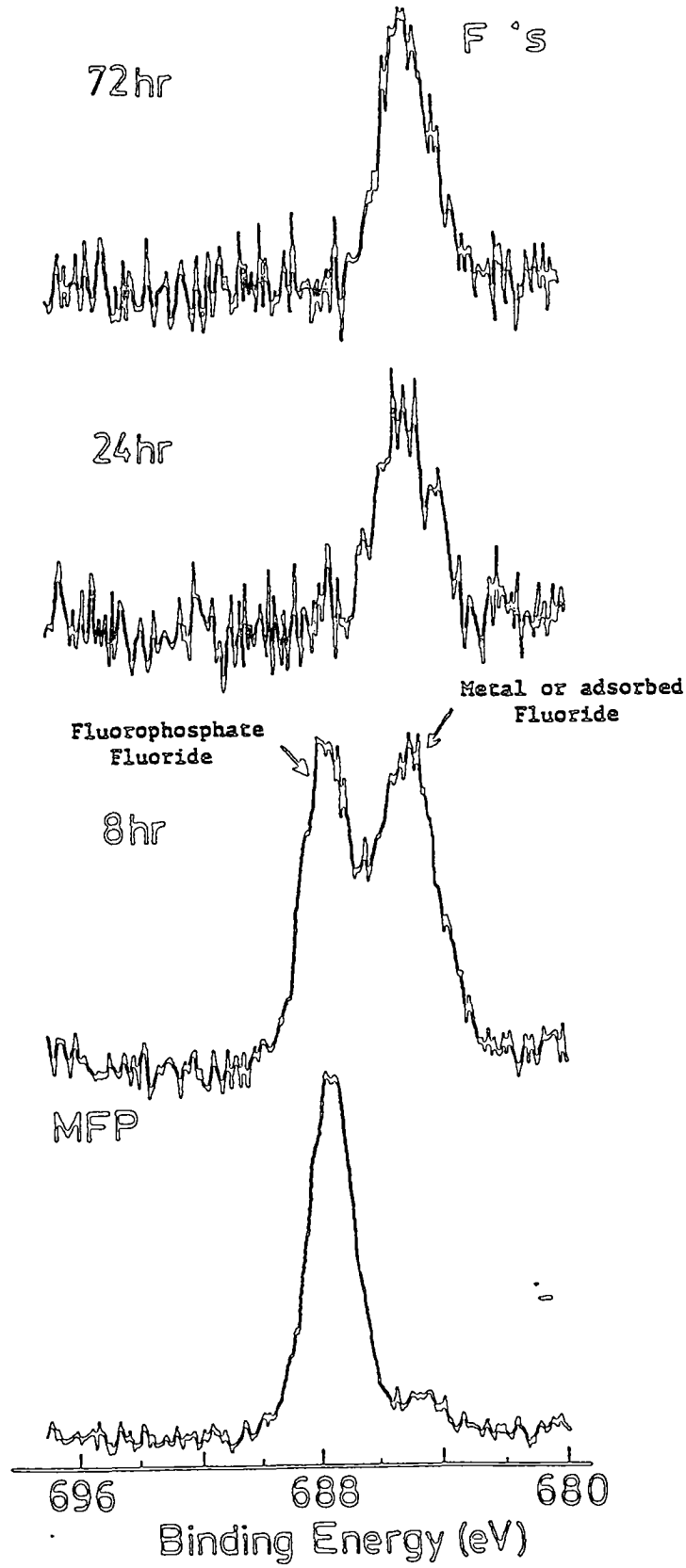

Fig. 3A. The Fluorine 1s Photoelectron Spectra.

Table 13. **XPS Analysis for Sodium Monoflurophosphate Pore Solution Migration Through Concrete (Pore Solution + 3.5% NaCl + 0.300 MFP).**

Disk Thickness (in.)	Time Surface (hr)	Atomic Concentration (%) C	O	Si	Ca	Na	Cl	F	P
17 Top (0.28)	8	45.7	29.5	1.6	0.8	13.9	2.1	3.1	3.3
17 Bottom	8	39.0	41.5	10.8	6.4	1.2	0.3	0.5	0.3
20 Top (0.23)	24	34.4	43.4	6.2	5.4	5.2	0.2	0.9	4.3
20 Bottom	24	34.5	45.6	10.4	5.8	2.9	0.2	0.2	0.4
21 Top (0.30)	48	31.4	44.6	4.3	7.1	5.0	0.3	0.8	6.5
21 Bottom	48	32.8	46.5	10.1	7.2	2.4	0.3	0.3	0.4
22 Top (0.24)	72	27.5	46.9	4.0	7.9	5.0	<0.2	1.3	7.4
22 Bottom	72	41.6	42.7	8.0	5.7	1.1	0.4	0.3	0.2
23 Top (0.28)	114	41.6	35.8	5.1	4.9	6.0	0.3	1.1	5.2
23 Bottom	114	45.2	39.2	7.4	6.1	1.2	0.4	0.2	0.4

1.0 inches = 25.4 mm

of the concentration for sodium for solute that has not migrated sufficiently into the disk, then the expected concentration for sodium, if it had penetrated the disk at longer times, would be greater than 8%. The sodium content on the lower disk surface, 1-3%, indicates that sodium has not penetrated the disks in these experiments.

The concentration of phosphorus on the top disk surfaces remain at about $6\pm1\%$, while that on the lower portion of the disks is $0.3\pm0.1\%$. The concentration of fluorine does not change significantly on the lower disk surfaces. These data indicate that phosphorus and fluorine and thus MFP does not appear to migrate through the concrete disks under the present experimental conditions.

The surface analytical results for MFP elements show that before 8 hours the P:F ratio was the expected 1:1, within experimental error. Beyond 8 hours, the P:F ratio is in the range 8.1 to 4.7, with an average value of 5.8 for 4 specimens. This result indicates that chemical alterations must be occurring for MFP as a result of its interaction in pore solution with concrete. The photoelectron spectra in the F 1s region for a frozen (-150° C) 0.300M MFP pore solution and for the top portions of disks following migration experiments are shown in Fig. 3. For MFP dissolved in pore solution, only one fluorine photopeak is detected; F 1s BE = 687.5 eV. This binding energy is consistent with values measured for fluorine bonded to phosphorus in other fluorophosphates (36). The F 1s photoelectron spectrum is for the top portion of a disk following MFP interaction with concrete for 8 hours reveals 2 fluorine peaks with binding energies at 688.0 and 685.3 eV. The higher binding energy photopeak is

associated with fluorine attached to phosphorus in monofluorophosphate.

The fluorine photopeak at the lower binding energy is assigned to fluoride as metal fluorides or as adsorbed fluoride. In the fluoride spectra for concrete specimens that had been exposed to MFP for longer time periods (24 and 72 hours, see Fig. 3A), only one F 1s peak is noted with a binding energy at approximately 685 eV. These findings support the notion that interaction of MFP with concrete leads to chemical changes in MFP and that these changes occur within 24 hours. The surface analysis results are consistent with the formation of fluoride and phosphate specimens in the hydrolysis reaction. Assuming that fluoride is produced, the surface analytical results, which show a greater concentration of phosphorus on the disk surface, indicate that fluoride is not as strongly adsorbed on the concrete surface as is phosphate or that fluoride diffuses into the concrete disk at a faster rate than phosphate. These findings demonstrate that MFP itself may not be the effective inhibitor, but its hydrolysis products may be the active species delivered at the reinforcing steel-concrete interface.

Summary and Observation

The migration of inhibitor constituents through mortar disks has been studied, and the migration followed a square root of time dependence. The migration time was determined by measuring the change in volume for solutions in contact with concrete disks while one side of the disk was maintained under vacuum. Analysis of the disk surfaces was used also to measure the time required to penetrate the disks. The chemical nature of the emerging solute was evaluated with respect to elemental concentrations and chemical form from binding energy measurements using photoelectron spectroscopy. The transport of sodium tetraborate through the disk resulted in no chemical change in the inhibitor. Migration of sodium monofluorophosphate, however led to hydrolysis of the salt. It is suggested that the hydrolysis of monofluorophosphate produces fluoride ions and phosphate species in solution. The effect of these ions on the integrity and strength of concrete was not investigated.

Electrochemical Studies of the Effect of Inhibitors on Reinforcing Steel Corrosion

The measurement of electrochemical potential has been used to evaluate relative inhibitor effectiveness. Measurements were made as a function of time; both in the presence and absence of inhibitors and at various concentrations. The results are presented and comparisons are made with parallel tests using visual inspection and surface analytical techniques.

Protocol 1

The variation in potential for the 18-week tests is summarized in Figs. 4 through 6, for sodium monofluorophosphate, sodium nitrite, and sodium tetraborate, respectively. The

important result is that these 3 inhibitors were effective in making the corrosion potential more positive. Only in the last 8 weeks did the potential approach a passive condition (i.e., potential of reinforcing steel in pore solution only) for some of the reinforcing steels in inhibitor-containing solutions. There are 2 aspects of this experiment which mitigate against its use as a screening technique. First, there was great variability in the potential measurements taken with cylindrical reinforcing steel. Second, the effect of the inhibitors was revealed only after 12-14 weeks, and over this period complications were introduced by the deterioration of the electrical connections and the epoxy which covered them. To combat these problems, A36 flat bar was used in all subsequent experiments measuring the potential of the reinforcing steel-SCE reference electrode couple.

Protocol 2

The objectives of this experiment were the following: to determine whether flat stock A36 steel gives less variability in potential measurements than cylindrical reinforcing steel, to determine the influence of sodium nitrite concentration on electrochemical potential, and to determine whether the method of cleaning (acid-washing plus cleaning in hexane compared to cleaning only in hexane) influences the potential measurements using flat stock mild steel.

The results of these studies showed that flat mild steel showed less variability in potential measurement, and the effects of the inhibitor were revealed after approximately four weeks. The results are presented in Figs. 7 through 10. Fig. 11 shows the variation in potential for acid-washed/hexane-cleaned flat reinforcing steel in pore solution containing no chloride or inhibitor. The results demonstrate that the measured potential was relatively constant during the test. The results in Figs. 12 and 13 show the dramatic change in potential for flat stock immersed in pore solution containing 3.5% NaCl (by weight). In these tests the potential was more negative, indicating that severe corrosion occurred within two weeks of initiating the test. The effect of added $NaNO_2$ at two different concentrations is shown in Figs. 7 through 10. It is apparent in these figures that more positive potentials were obtained in a shorter time for the more concentrated inhibitor solution.

The significant conclusions after 12 weeks are the following:

- Flat mild steel stock gave less variability in potential measurements than cylindrical rebar.
- The method of cleaning did not seem to influence the differences in potential measurements.
- The higher concentration (0.670M) of sodium nitrite did not give a more positive potential than the highest concentration previously used (0.300M).
- The time to recovery of an "inhibited" reinforcing steel surface was more rapid for more concentrated solutions.

The only corrosion observed on the reinforcing steel specimens was located at the reinforcing steel-epoxy interface. Upon removing the epoxy, the ends of the bars immersed in 0.670M

$NaNO_2$ were comparable to the ends of the bars in pore solution only; they appeared only slightly corroded. However, the corrosion on the ends of the bars exposed to the salt/no inhibitor solution was severe. The bars immersed in pore solution containing chloride and 0.300M sodium nitrite were somewhat corroded. The potentials were monitored for 10 weeks following the removal of the epoxy, and a substantial increase was noted in the control (salt/no inhibitor). It seems that the ends of the reinforcing steel became repassivated when exposed to the highly alkaline conditions of the pore solution (pH 13.5).

Protocol 3

Protocol 3 was devised to investigate the effect of sodium tetraborate on precorroded A36 flat bar stock. After 1 day of being immersed in pore solution containing 3.5% NaCl (by weight, and the pore solution, sodium chloride and sodium tetraborate, the potentials of the precorroded reinforcing steel increased dramatically. The results are presented in Fig. 14. This occurred for all specimens, even the control. The potentials increased even further over the next several days, and remained in the low-probability of corrosion state for the length of the experiment. An interpretation of this result is that in the highly alkaline conditions of the simulated pore solution prevented the ongoing activity of the corrosion cell. Also, with the lack of stress points and areas in which the pH could be more acidic than the pore solution (13.5), the initiation of corrosion could not take place.

Protocol 4

This protocol was designed to produce a control condition of continuously active corrosion, thus enabling one to screen inhibitors without immediate repassivation. There was not a substantial difference in potential between the control and inhibitor solutions during the first 18 days. However, with the decreased salt concentration and/or increased inhibitor concentration, differences in inhibitor performance were revealed as presented in Tables 14 and 15. In general, sodium nitrite, a known corrosion inhibitor, performed the best over the wide range of pH values. It produced the highest increase in potential for pH values, 8, 10, 12 and 12.5. Sodium monofluorophosphate, another known corrosion inhibitor, performed second best, except at pH 13.0 where it ranked relatively poorly. Sodium tetraborate exhibited excellent behavior in this experiment and ranked as the best inhibitor at pH 13.0. Tetrabutylphosphonium bromide was ineffective at 0.100M concentration except at pH 13.0. There were also noticeable changes in pH. For the sodium nitrite solutions, there was a general increase in pH at initial pH values of 8 and 10. This may be attributed to the formation of OH^- anions in solution from hydrolysis involving NO_2^- with H_2O. For sodium monofluorophosphate solutions, there was a decrease in pH for initial pH values of 10 and 12. A process which may account for this observation is the hydrolysis of MFP in solutions to produce HF.

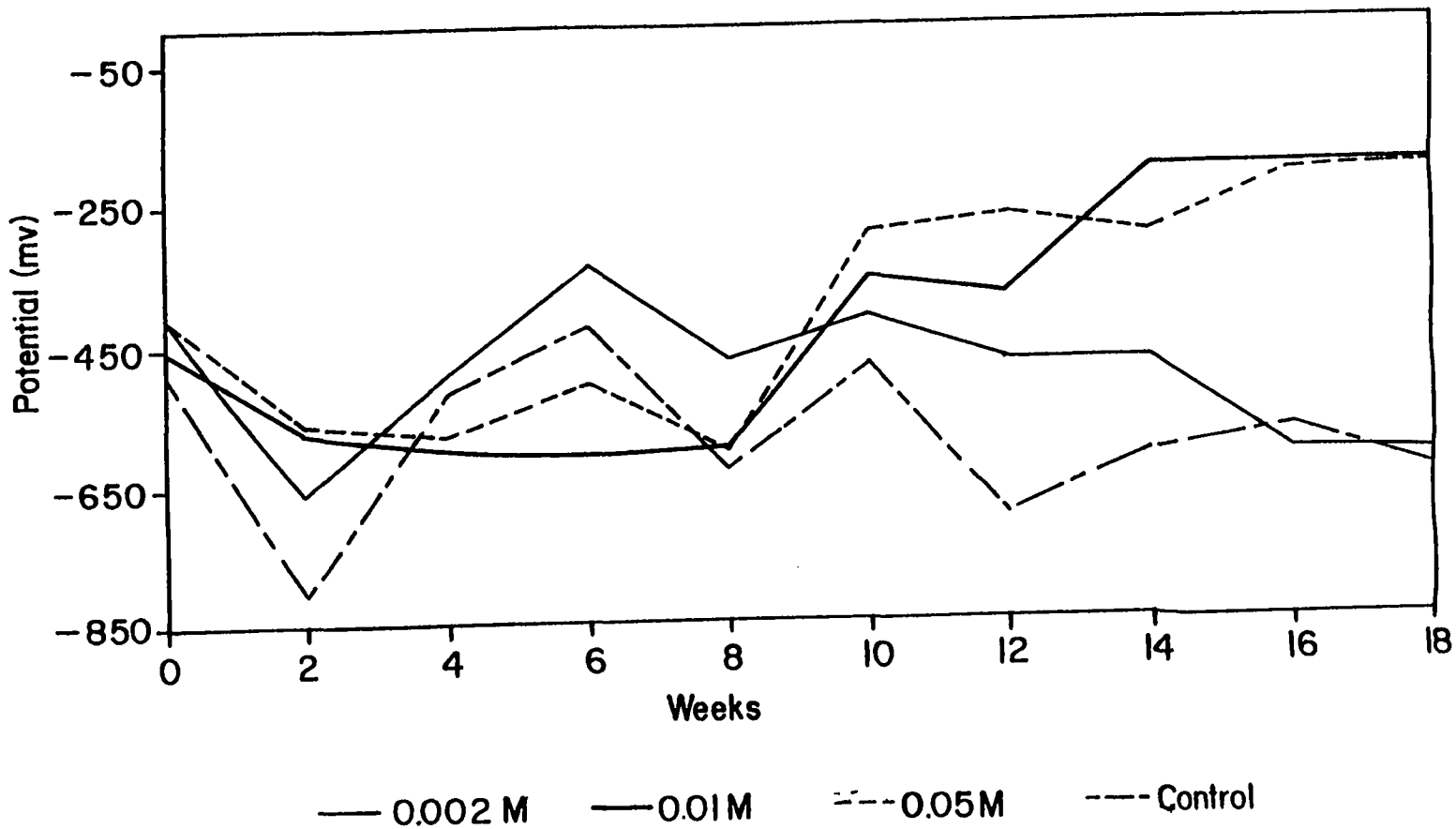

Fig. 4. Variation of Potential (SCE) as a Function of Time for reinforcing steel Rod Treated for 18 Weeks at 140°F (60°C) in 3.5% (by weight) Chloride-containing Pore Solution and Selected Concentrations of Sodium Monofluorophosphate.

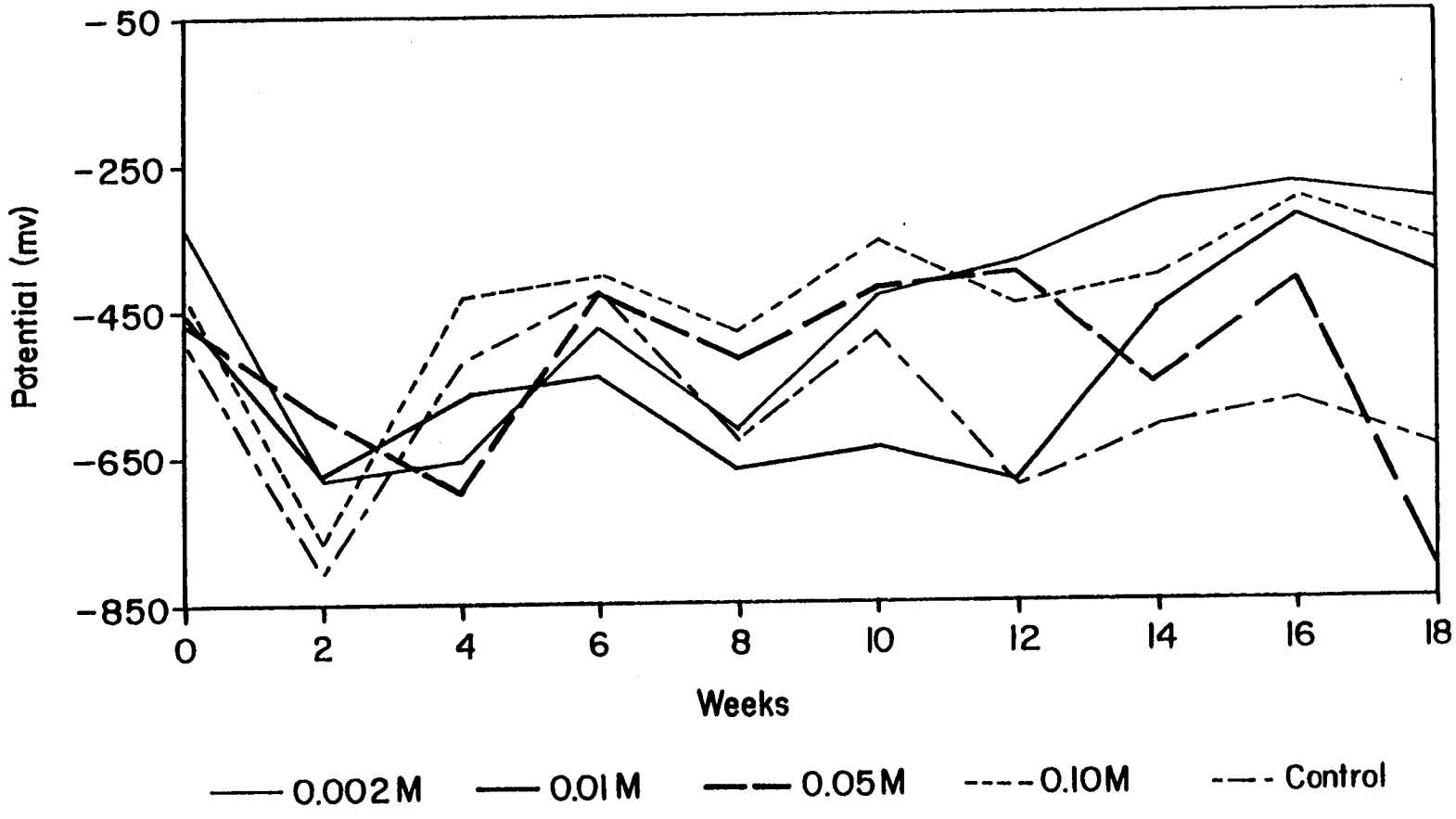

Fig. 5. Variation of Potential (SCE) as a Function of Time for reinforcing steel Rod Treated for 18 Weeks at 140°F (60°C) in 3.5% (by weight) Chloride-containing Pore Solution and Selected Concentrations of Sodium Nitrite.

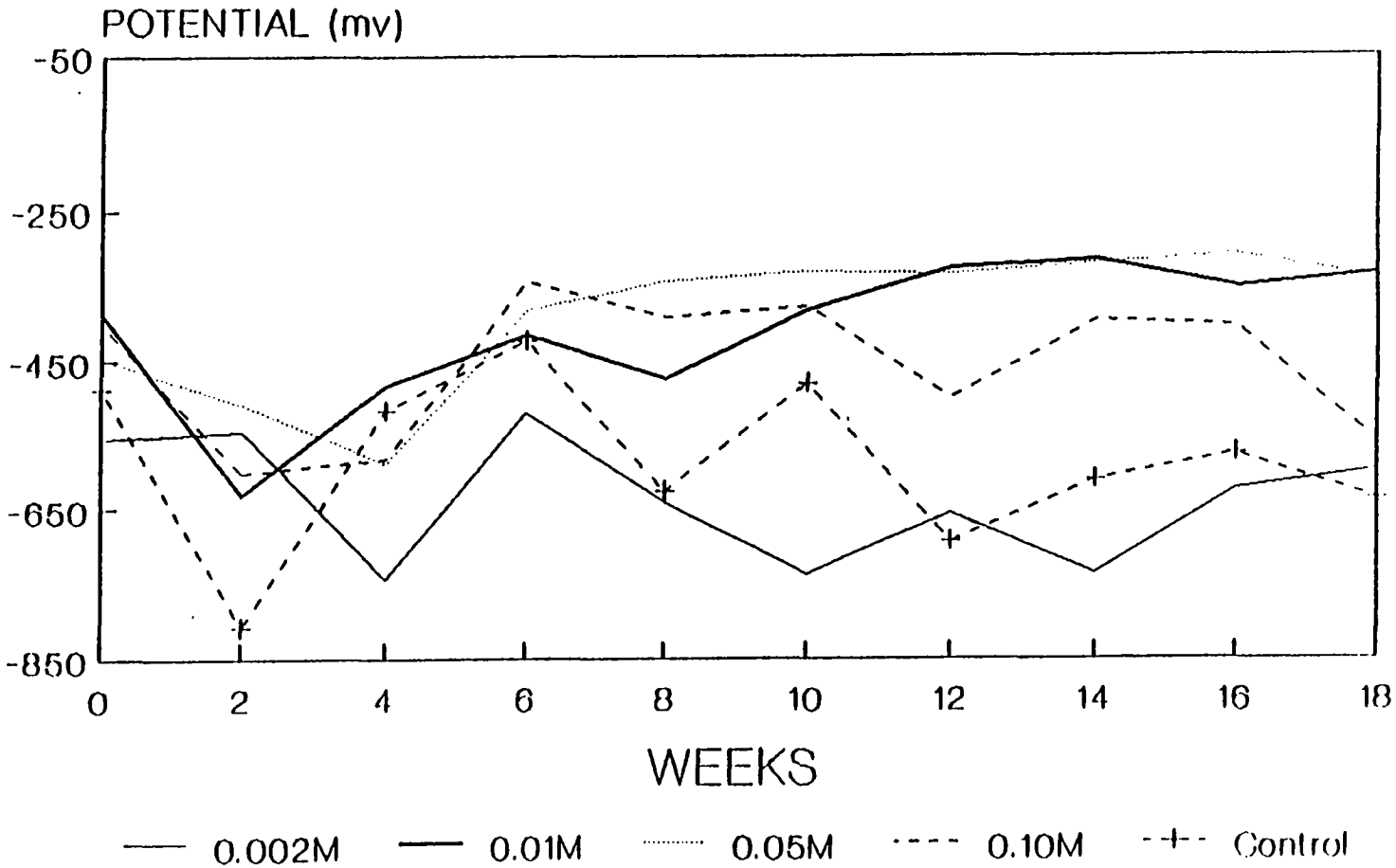

Fig. 6. **Variation of Potential (SCE) as a Function of Time for reinforcing steel Rod Treated for 18 Weeks at 140°F (60°C) in 3.5% (by weight) Chloride-containing Pore Solution and Selected Concentrations of Sodium Tetraborate.**

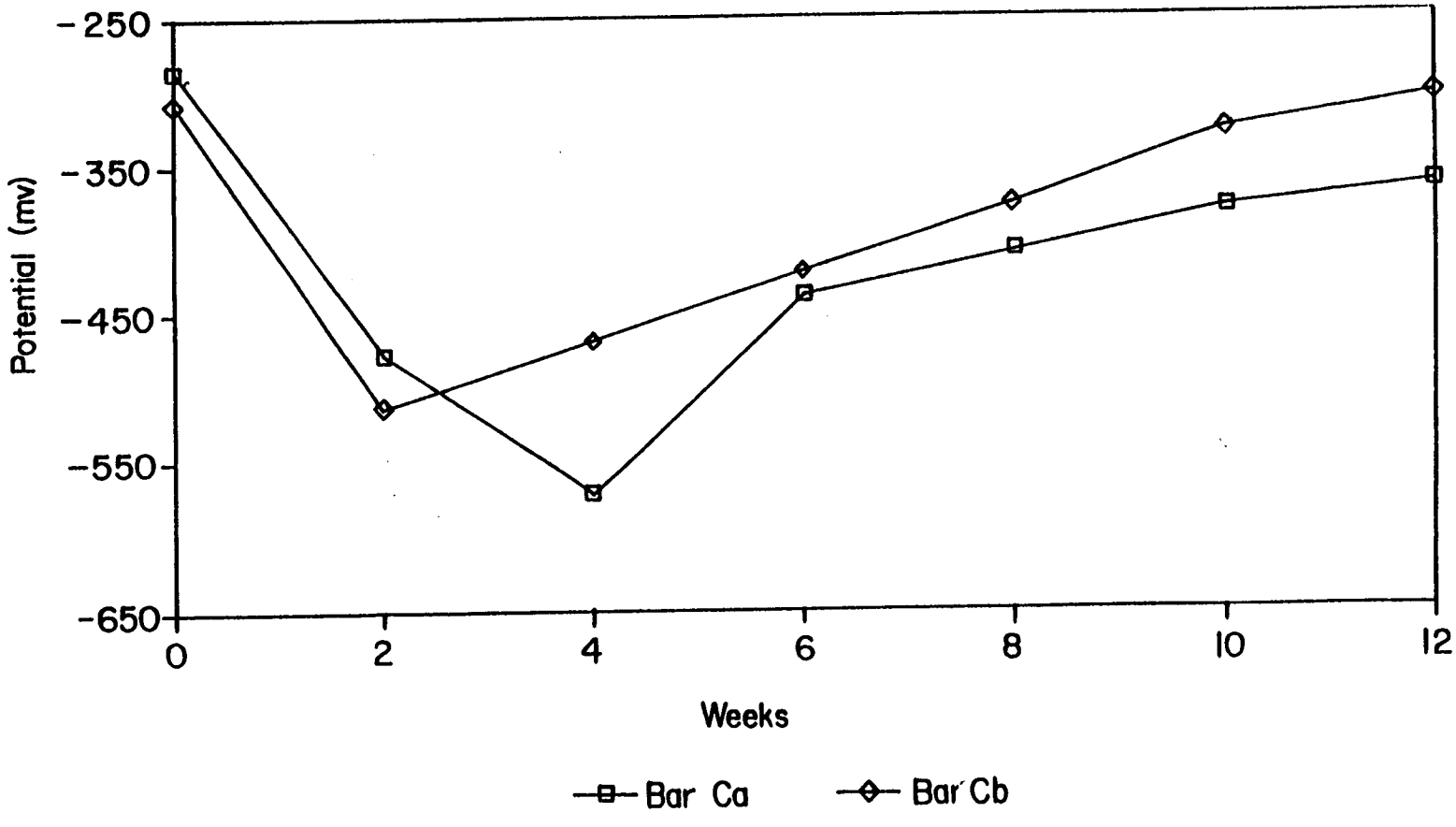

Fig. 7. Variation in Potential (SCE) for Acid-washed, Hexane-Cleaned Flat Steel Bar Treated for 12 Weeks at 140°F (60°C) in 3.5% (by weight) Chloride-containing Pore Solution and 0.300M Sodium Nitrite.

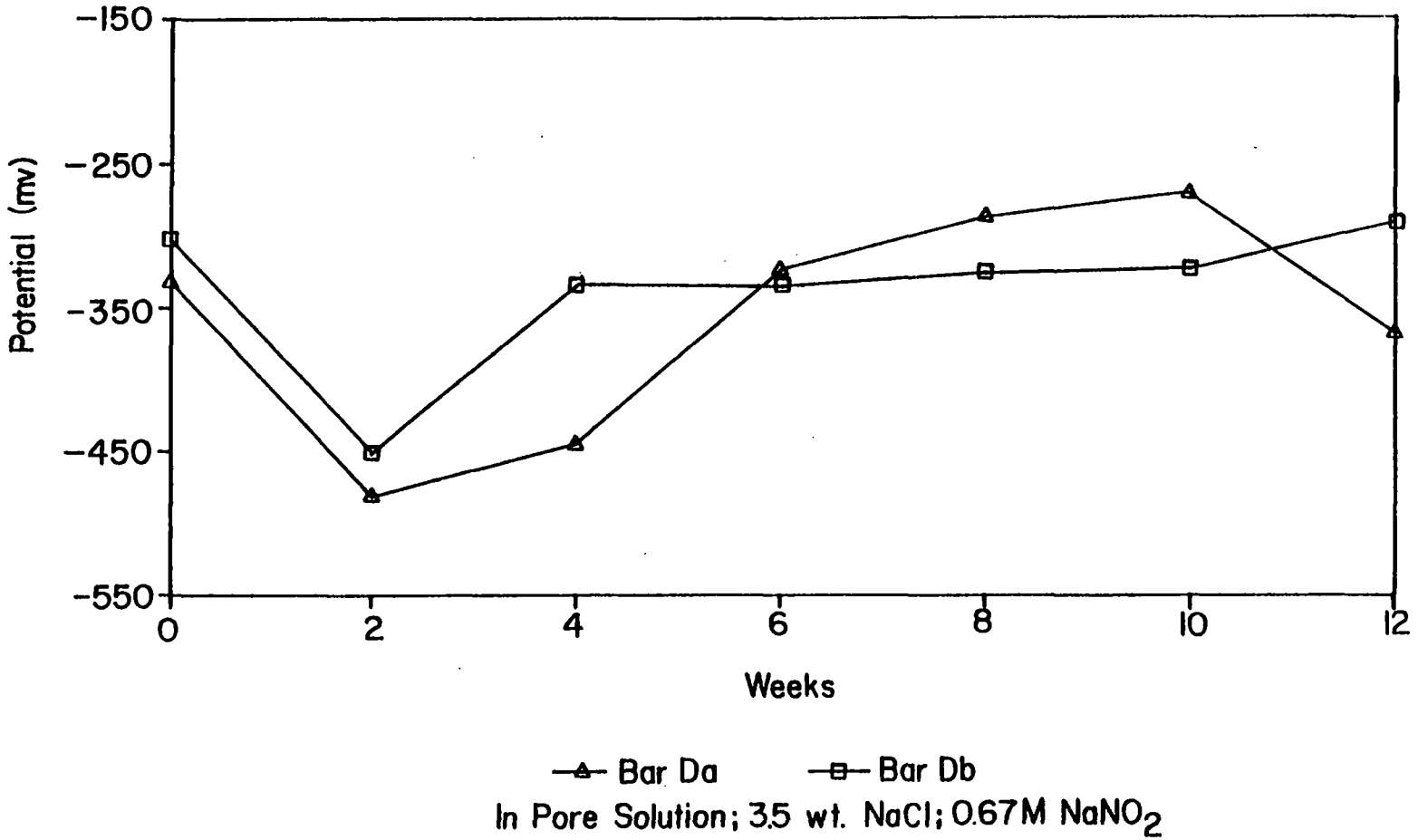

Fig. 8. Variation in Potential (SCE) for Acid-washed, Hexane-Cleaned Flat Steel Bar Treated for 12 Weeks at 140°F (60°C) in 3.5% (by weight) Chloride-containing Pore Solution and 0.670M Sodium Nitrite.

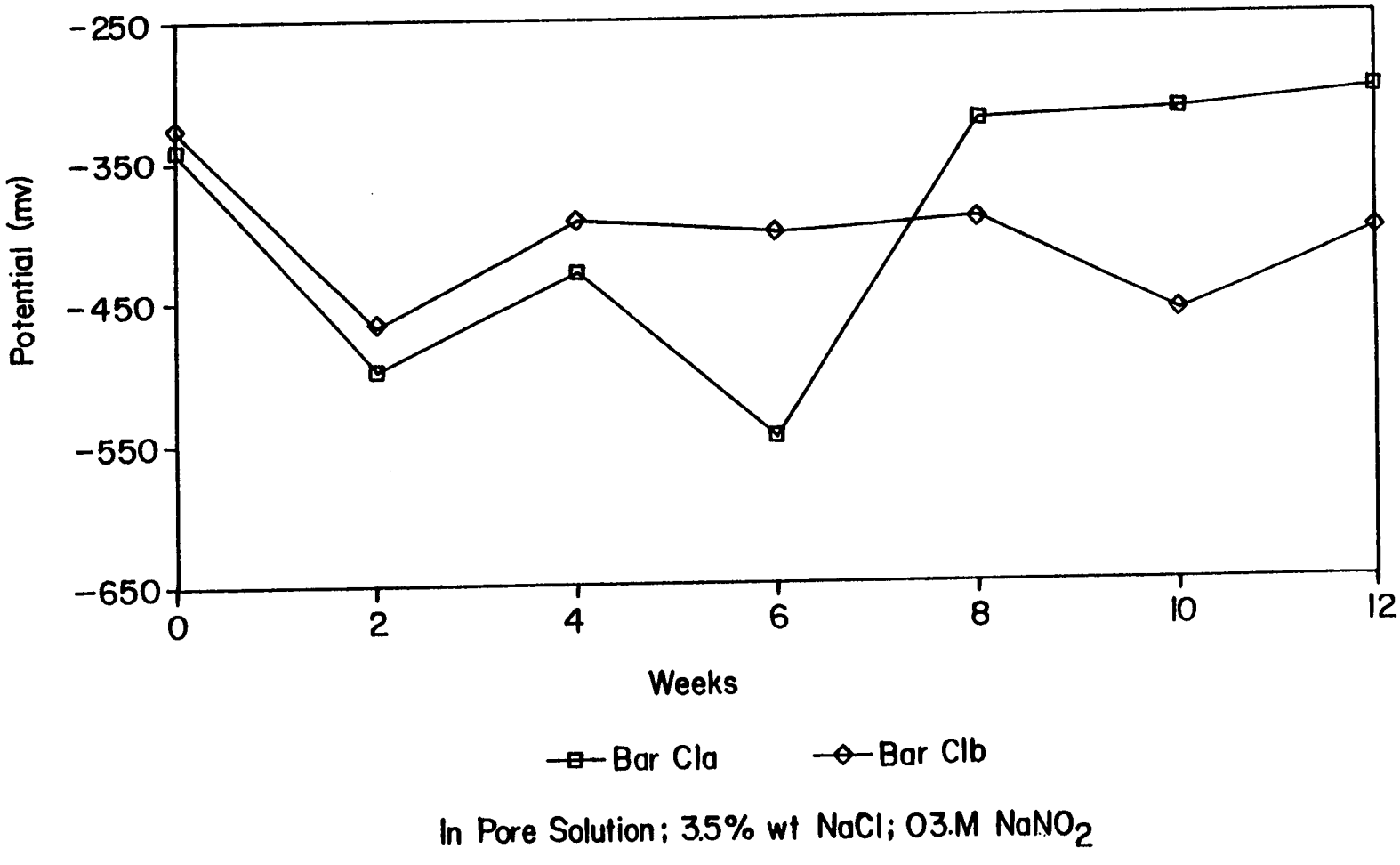

Fig. 9. Variation in Potential (SCE) for Hexane-Cleaned Flat Steel Bar Treated for 12 Weeks at 140°F (60°C) in 3.5% (by weight) Chloride-containing Pore Solution and 0.3M Sodium Nitrite.

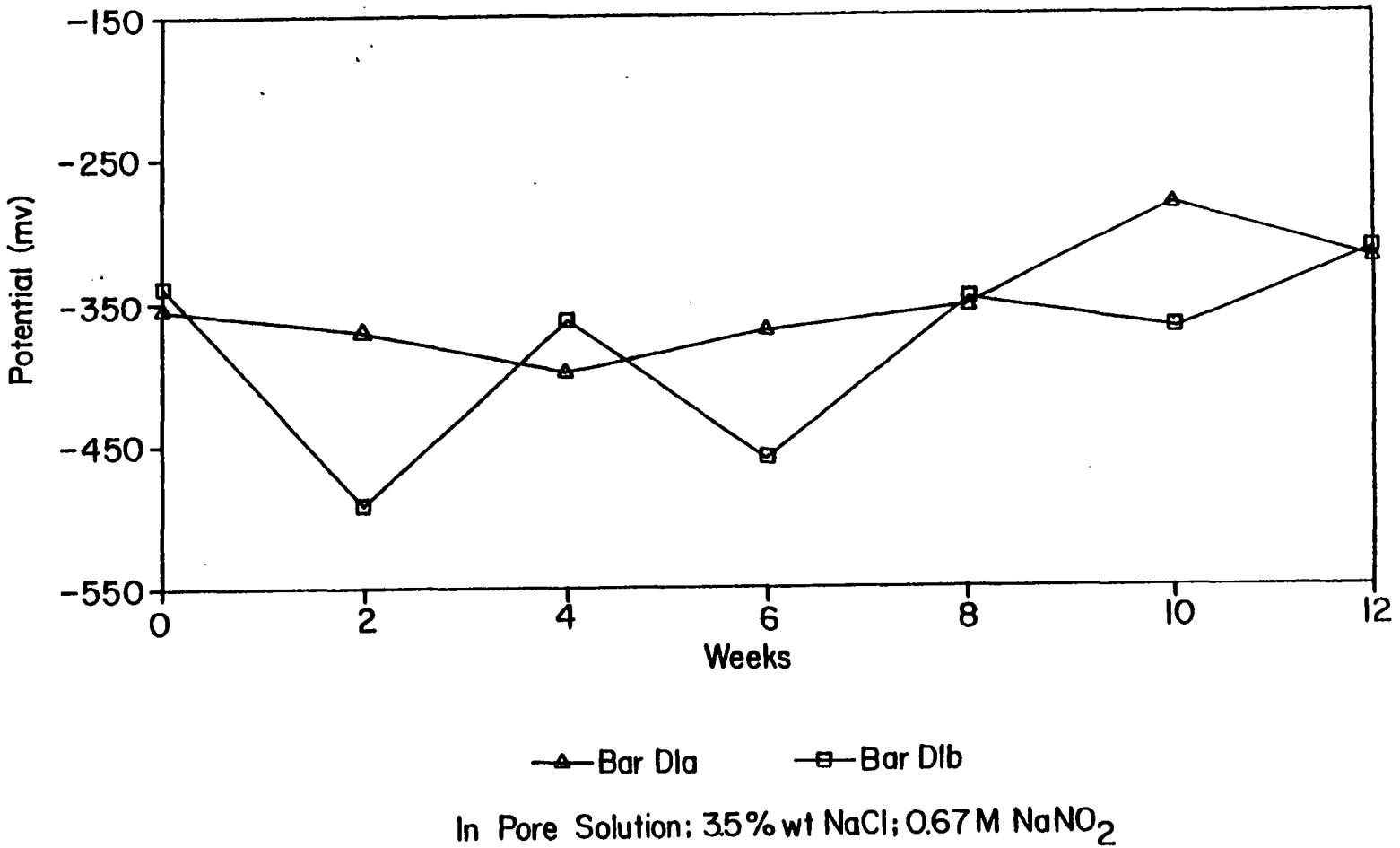

Fig. 10. Variation in Potential (SCE) for Hexane-Cleaned Flat Steel Bar Treated for 12 Weeks at 140°F (60°C) in 3.5% (by weight) Chloride-containing Pore Solution and 0.67 M Sodium Nitrite.

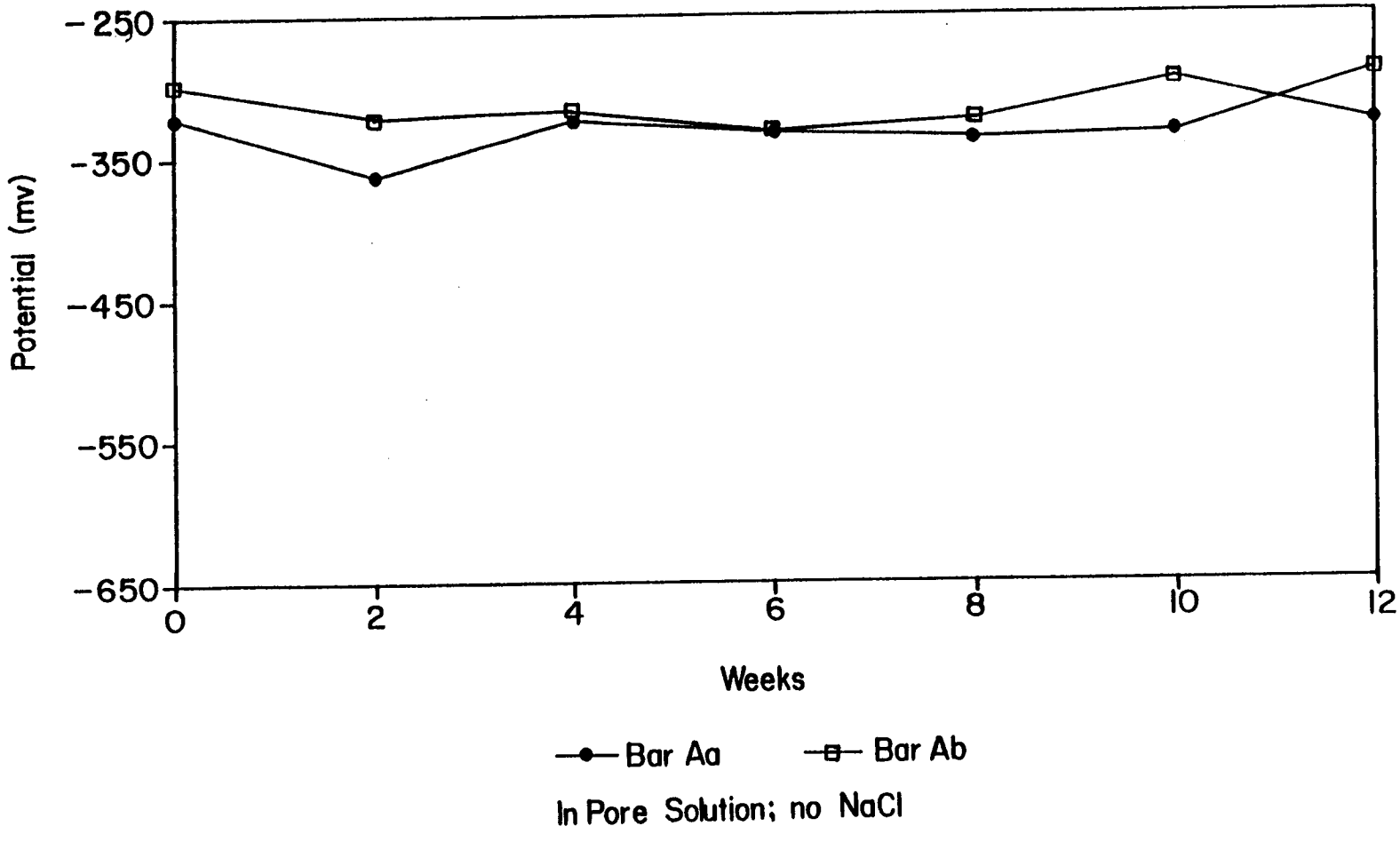

Fig. 11. Variation in Potential (SCE) for Acid-washed, Hexane-Cleaned Flat Steel Bar Treated for 12 Weeks at 140°F (60°C) in Pore Solution Containing No Chloride.

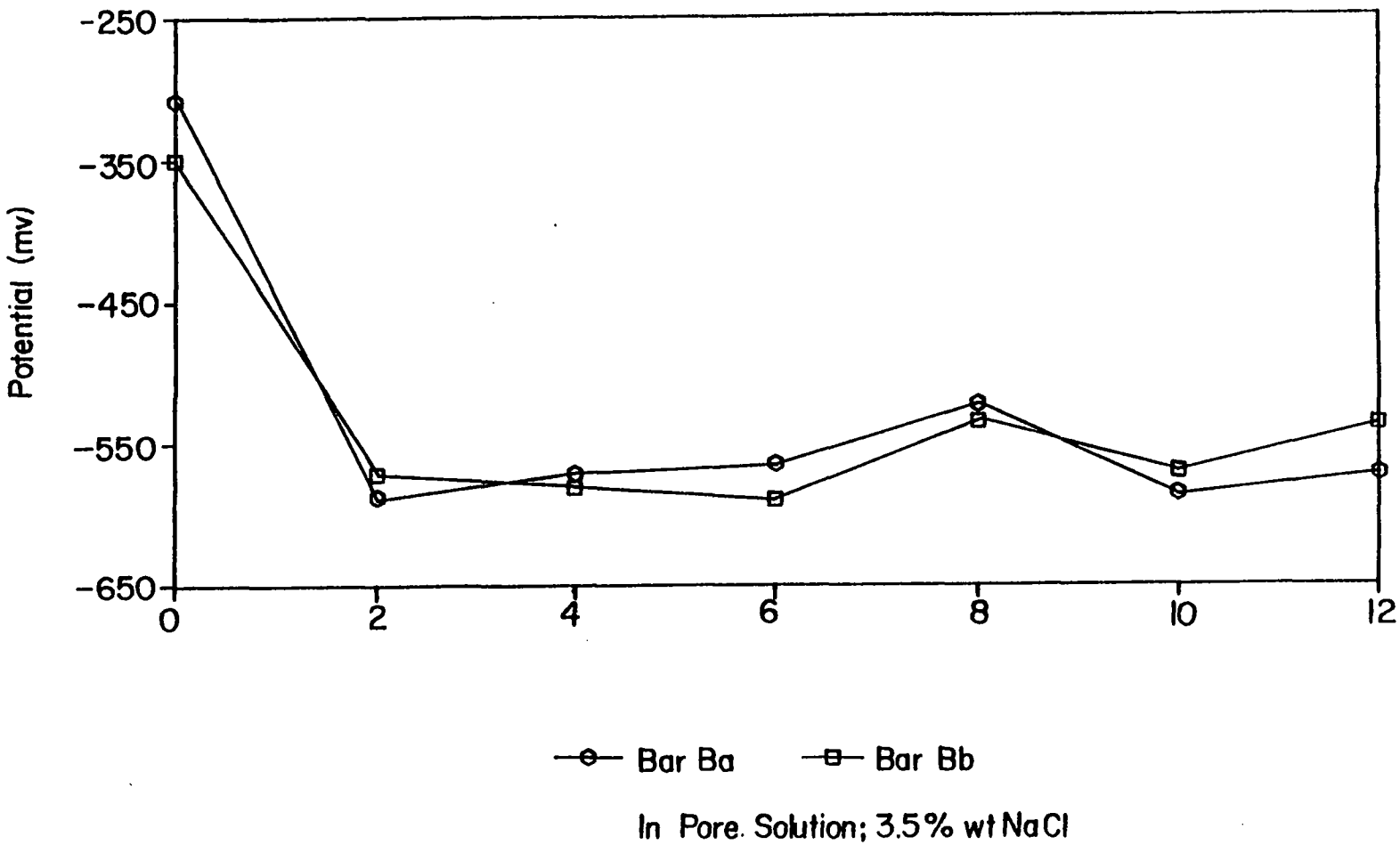

Fig. 12. Variation in Potential (SCE) for Acid-washed, Hexane-Cleaned Flat Steel Bar Treated for 12 Weeks at 140°F (60°C) in 3.5% (by weight) Chloride-containing Pore Solution.

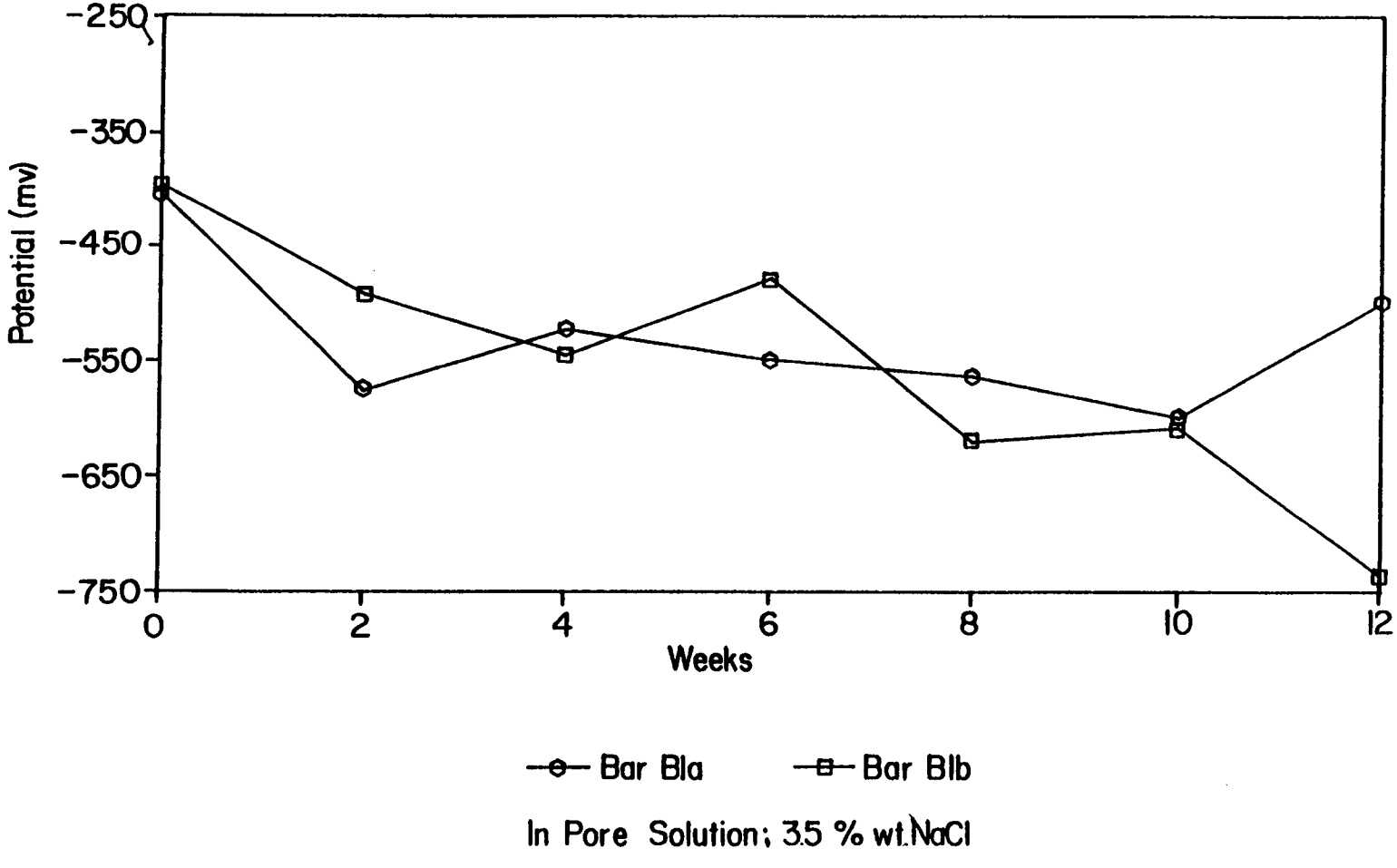

Fig. 13. **Variation in Potential (SCE) for Hexane-Cleaned Flat Steel Bar Treated for 12 Weeks at 140°F (60°C) in 3.5% (by weight) Chloride-containing Pore Solution.**

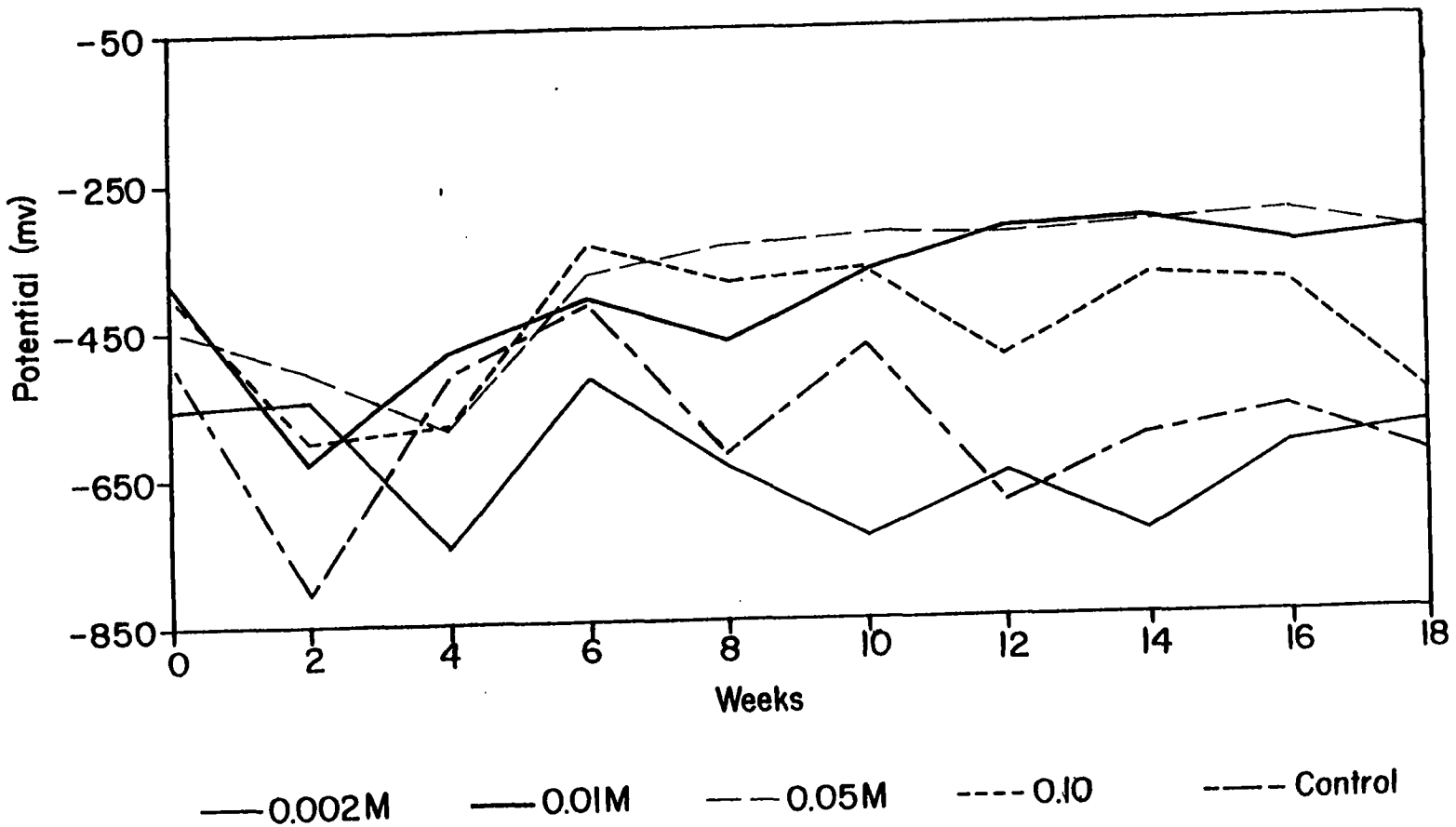

Fig. 14. **Corrosion Potentials (SCE) for Precorroded Flat Bar Treated for 18 Weeks at 140°F (60°C) in 3.5% (by weight) Chloride-containing Pore Solution and Sodium Tetraborate.**

Comparison of Visual Inspection and Surface Analysis

Corrosion screening tests demonstrate that sodium nitrite, sodium monofluorophosphate and sodium tetraborate are all good corrosion inhibitors. Results from Protocols 1, 2 and 4 support these findings. Surface analysis measurements suggest that sodium tetraborate reacts to form a coating on the reinforcing steel surface. This coating could function as a barrier layer to inhibit chloride-induced corrosion, thereby increasing the electrochemical potential values as noted in Protocols 1 and 4. Furthermore, surface analysis of MFP-treated reinforcing steel suggests hydrolysis of MFP as a likely cause of the resultant non-unity phosphorus-to-fluorine atomic ratio on the reinforcing steel surface. This idea is supported by the decrease in pH noted for initial pH values 10 and 12 in Protocol 4.

Summary and Observation

Known corrosion inhibitors, sodium nitrite and sodium monofluorophosphate, are effective at making the corrosion potential of reinforcing steel in chloride-doped pore solutions more positive, as is sodium tetraborate. Sodium tetraborate is especially effective at pH 13.0, the pH that most closely simulates the concrete environment.

Pore solution produces an environment that is too alkaline for rapid screening of inhibitors. This highly basic solution results in rapid repassivation of corroded reinforcing steel. It does not accurately simulate the reinforcing steel in concrete conditions because the high alkalinity is continually maintained.

Long-term monitoring of corrosion potentials is a useful method to study the behavior of corroding reinforcing steels in a bridge deck or laboratory test pad. However, the procedure is too slow for screening inhibitors at reasonable concentrations.

Recommendations

The following are the recommendations for part one of this investigation.

Treatment Method I:

> This technology is well known as a liquid/solution treatment for existing structures with or without preliminary drying or any concrete removal. After preliminary drying, a concrete structure will readily imbibe a solution during subsequent cooling and reabsorption of moisture. The technique is the most direct available for delivering inhibitor to the reinforcing steel surface without any physical concrete removal.
>
> Known materials for this application include calcium nitrite solutions. Materials recommended for further evaluation: solutions of alkaline and alkaline earth metal borates, calcium borate, zinc borate, and alkali silicates.

Treatment Method II:

Partial removal of concrete by milling, grooving, or drilling to displace heavily contaminated concrete and provide more efficient access of inhibiting agents to the reinforcing steel.

Recommendations from C-103-2B, "Removal of Chloride-Contaminated Concrete", for materials for further evaluation: alkaline and alkaline earth metal borates, boric acid, zinc borate. Treatment may be with solutions (with or without preliminary drying); in situ treatment with the recommended inhibitors in solid form deserves engineering evaluation.

Table 14. Protocol 4 Inhibitor Screening Test Values.*

Test Series	Corrosion Potentials (SCE) Before Inhibitor	1 day	3 days	6 days	9 days
Control					
pH 8	-634	-547	-492	-487	-497
pH 10	-649	-560	-527	-527	-556
pH 12	-642	-508	-483	-469	-504
0.100 M Sodium tetraborate					
pH 8	-628	-528	-492	-501	-498
pH 10	-649	-490	-463	-463	-507
pH 12	-647	-648	-389	-432	-489
0.100 M Sodium nitrite					
pH 8	-645	-495	-455	-469	-473
pH 10	-630	-497	-457	-461	-470
pH 12	-646	-463	-448	-434	-465
0.100 M Sodium monofluorophosphate					
pH 8	-635	-487	-472	-486	-495
pH 10	-645	-497	-471	-476	-483
pH 12	-636	-509	-503	-473	-522
0.100 M Tetrabutylphosphonium bromide					
pH 8	-635	-554	-480	-475	-511
pH 10	-632	-554	-504	-528	-547
pH 12	-636	-531	-498	-490	-529

*(Average-duplicates exposed to 10% NaCl (by weight) in DI water at 140°F (60°C). The inhibitor concentration was 0.1 M.

Table 15. Results of Protocol 4 Inhibitor Screening Test Values.*

Test Series	Before Inhibitor	After 18 days previous exposure 10% NaCl in (by weight) DI water, 60°C 0.1 M inhibitor	After 3 days at New Cond.	After 6 days at New Cond.
		Corrosion Potentials (SCE)		
Control				
pH 8		-486	-458	-431
pH 10		-520	-491	-508
pH 12		-500	-516	-428
pH 12.5	-627		-416	-341
pH 13.0	-651		-554	-652
0.600 M Sodium tetraborate				
pH 8		-473	-433	-442
pH 10		-462	-411	-409
pH 12		-424	-367	-334
pH 12.5	-651		-372	-246
pH 13.0	-639		-137	-211
0.600 M Sodium nitrite				
pH 8		-481	- 49	- 27
pH 10		-445	-125	- 61
pH 12		-406	-158	- 79
pH 12.5	-648		-167	-114
pH 13.0	-621		-252	-266
0.600 M Sodium monofluorophosphate				
pH 8		-467	-396	-344
pH 10		-452	-358	-308
pH 12		-459	-425	-290
pH 12.5	-635		-172	-161
pH 13.0	-647		-563	-619
0.100 M Tetrabutylphosphonium bromide				
pH 8		-482	-468	-443
pH 10		-549	-513	-502
pH 12		-517	-498	-505
pH 12.5	-623		-403	-367
pH 13.0	-631		-539	-317

* Averages of duplicate samples exposed to 1.75% NaCl (by weight) in deionized water. The inhibitor concentration was 0.600 M for all inhibitors except tetrabutylphosphonium bromide which was 0.100 M.

3

Part II: Development of Feasible Corrosion Inhibitor and Chloride Scavaging Treatments

Introduction

The non-electrical techniques which are employed in reinforced concrete construction to protect steel against corrosion can be categorized into three basic types of protection schemes:

1. modifications to the concrete to either decrease the diffusion of chlorides,
2. increase the threshold level of chlorides needed to initiate corrosion, and
3. modifications to the reinforcing steel.

Most of the protection techniques currently used are grouped into the first category in which the concrete environment is directly altered. This can be accomplished in the concrete design stage by utilizing the lowest water/cement ratio and by complete consolidation to reduce the permeability of the concrete, and by design and construction of required cover depths. However, in severely aggressive environments, additional measures may be necessary to increase the impermeability of the concrete.

One widely-used technique to increase concrete impermeability is the placing of overlay systems on bridge decks, which includes the use of latex-modified concrete, polymer concrete, and low-slump dense concrete.

Polymers are also extensively used as both concrete surface coatings and for impregnation. Epoxy surface coatings reduce the rate of penetration of chloride-containing moisture and somewhat limit the ingress of oxygen necessary to fuel the corrosion process. Polymer impregnation involves the penetration of a liquid monomer into the voids of hardened

concrete and subsequent in situ polymerization. Current impregnation measures have centered around the use of methyl methacrylate.

Common corrosion prevention practice also incorporates the use of corrosion inhibiting admixtures, both organic and inorganic. The mechanism of inhibition varies, depending upon the chemical nature of the inhibitor and the factors causing the corrosion, but fundamentally, they act to form a stable film on the reinforcing bar surface which in turn requires higher levels of Cl^- or longer time periods in order to penetrate to the bare metal surface. Inhibitors are currently being used as admixtures in new concrete structures as a preventative measure.

Besides modification of the concrete environment, the reinforcing steel surface may also be treated prior to concrete placement. However, this technology has little application in this investigation because the scope of the project is limited to treating existing chloride-contaminated concrete built with bare reinforcing steel.

Research Objective and Approach

The primary objective of Part II is to evaluate the effectiveness and feasibility of removing chloride-contaminated concrete in conjunction with the application of chemical treatments as a possible method for mitigating corrosion in chloride-contaminated bridge components.

The objective was fulfilled through the completion of two phases of testing. The first phase consisted of the accelerated exposure of small scale reinforced concrete specimens to a simulated deicing salt environment until the initiation of corrosion. The chloride-contaminated concrete above the reinforcing steels in each specimen was removed and the remaining groove was treated chemically through a ponding of treatment solution and/or backfilling with a chemically treated mortar. Several corrosion inhibitors, polymer sealers, and a chloride scavenger were tested individually and in combination to ascertain the most effective treatment. Seventeen different treatment combinations were applied to specimens and an untreated control specimen was included. The corrosion behavior of the specimens was monitored after treatment. From this phase of the study, the relative effectiveness of the treatments could be compared over a prolonged exposure period.

The second phase of the study addressed the effects of the treatment chemicals on the strength and resistivity of mortar when admixed. The treatments were evaluated through the testing of mortar cubes cast with varying concentrations of the chemicals. The testing involved the measurement of compressive strength and electrical resistivity during several points in the curing stage of the mortar cubes. These tests would assess the acceleration or retardation of the hydration process and identify changes in resistivity that may increase or decrease the corrosion rate.

Experimental Program

Introduction

The state of reinforced concrete bridges subjected to chloride-laden environments was simulated in the laboratory using scaled-down reinforced concrete specimens. Thirty two specimens were cast containing two lengths of reinforcing steel in each specimen. After an initial period of curing, the specimens were exposed to alternate wetting with sodium chloride solution and drying at an elevated temperature.

The corrosion activity of the specimens was monitored using both a saturated calomel half-cell (SCE) to measure corrosion potentials and a linear polarization device (3LP) to measure corrosion rates. When corrosion activity in the reinforced concrete was confirmed through both electrochemical measurements and measurements of the chloride ion concentration at the reinforcing steel level, seventeen specimens were deemed suitable for the application of anticorrosion treatments.

The treatment substances consisted of commercial and experimental inhibitors, two polymer sealants, and an experimental chloride scavenging mineral. The application of the treatments involved removal of chloride-contaminated concrete above the corroding reinforcing steels in each specimen and the subsequent treatment through ponding and/or backfilling with a treated mortar. Comparison of the treated specimens to an untreated control specimen and evaluation of the pre- and post-treatment corrosion behavior allowed for the determination of each treatment's effectiveness in reducing corrosion activity. From this study, the most effective treatment could be selected for large-scale study and possible field application.

In addition to the electrochemical testing, tests were also conducted to determine the effect of using the treatment admixtures on mortar strength and resistivity. Mortar cubes were cast containing various concentrations of treatment substances. During the first twenty days of curing, cubes were periodically tested for both compressive strength and mortar resistivity. These measurements served as an indicator of any deleterious effects caused by admixing the treatment substances. The suitability of each treatment is dependent not only on its corrosion-arresting ability but also on any potentially detrimental effect on the properties of concrete.

Apatite, a mineral, was incorporated into the scope of this study as a possible chloride-ion-scavenging mineral. Unlike the other treatments used, apatite has had no formal investigation of its ability to aid in the reduction of corrosion in reinforced concrete. As a result, tests were conducted to determine its effectiveness in consuming chloride ions in both an aqueous medium and in concrete.

Materials

Coarse and Fine Aggregates

The coarse aggregate used in this study was crushed limestone quarried near Blacksburg, Virginia. The fine aggregate used was natural sand, primarily containing mica, quartz and sandstone, and was processed near Wytheville, Virginia. The gradations and other physical characteristics of both aggregates are given in Appendix A, Tables A-1 and A-2.

Cement

For all concrete and mortar mixes in this investigation, Type I Portland cement was used.

Chemical Admixtures

In order to attain the desired concrete and mortar characteristics, an air-entraining admixture, water-reducing agent, and initial set retarder were used.

Corrosion Abatement Treatments

The study included inhibitors, polymer sealants, and a suspected chloride-ion-scavenging mineral.

Based on the results of Part I of this investigation involving aqueous corrosion tests in simulated pore solution and a search of newly introduced commercial products, the following inhibitors and sealants were selected as treatments after removal of chloride-contaminated concrete:

1. DCI (calcium nitrite, $Ca(NO_2)_2$): An anodic inhibitor developed by the WR Grace Company that currently has widespread use as an admixture in new reinforced concrete structures.

2. TCI (sodium monofluorophosphate, Na_2PO_3F): An inhibitor developed by the Domtar Corporation. TCI was developed to be added to deicing salt and through subsequent applications is said by the manufacturer to diffuse to the reinforcing steel surface.

3. Sodium tetraborate ($Na_2B_4O_7$): experimental inhibitor that interacts to form a coating on a reinforcing steel surface which serves as a barrier to metal dissolution [38]. The hydrated form of sodium tetraborate ($Na_2B_4O_7 \cdot 10H_2O$) was used.

4. Zinc borate ($2ZnO \cdot 3B_2O_3$): experimental inhibitor evaluated in conjunction with sodium tetraborate to determine the effectiveness of varying borate forms. This study evaluated the hydrated form of zinc borate ($2ZnO \cdot 3B_2O_3 \cdot 3.5H_2O$).

5. ALOX 901 (proprietary): An organic inhibitor manufactured by the Alox Chemical Company.

6. CORTEC VCI-1337 (proprietary blend of surfactants and amine salts in a water carrier): an organic corrosion inhibitor that is designed to migrate through concrete and is attracted to the surfaces of steel reinforcing bars. The inhibitive substance supposedly migrates via vapor phase transport and forms a protective molecular monolayer on the reinforcing steel surface. This inhibitor was developed to be applied through surface injection.

7. CORTEC VCI-1609 (Proprietary alkanolamine): The inhibitor works under the same principle as VCI-1337 but has a different formulation and is used as an admixture to concrete.

8. Silicone: a Dow Corning sealer dissolved (10% by weight) in hexane. It serves as polymeric barrier on concrete, reducing any ingress of chlorides, oxygen, and water.

9. Styrene-acrylic: a National Starch copolymer sealer dissolved in (10% by weight) in distilled water and treated with a coalescence agent (ethyl acetate). It serves as a polymeric barrier on concrete, reducing any ingress of chlorides, oxygen, and water.

In addition to the above substance, a synthetic hydroxylapatite ($Ca_{10}(PO_4)_6(OH)_2$) was evaluated as a possible chloride-ion-scavenging mineral. The hydroxyl form of apatite was chosen because it is the most widespread apatite mineral and it could be obtained in the necessary quantities for experimentation. Hydroxylapatite has the general formula $M_{10}(XO_4)_6Z_2$ where M can be various metals or H_3O^+, X= As, Ge, P, Si, or Cr, and Z= OH, F, Cl, Br, or CO_3. Apatite is being studied as a possible chloride ion scavenger because substitutional solid solution is extensive among the apatite series members [37]. Therefore, it has been hypothesized that the possible substitution of Cl^- for OH^- in the hydroxylapatite molecule may serve as a corrosion-limiting reaction.

Specimen Preparation

Specimen Configuration

Molding forms for sixteen specimens were constructed in order to cast specimens of dimensions 16 in. (40.6 cm) L x 8.5 in. (21.6 cm) W x 3.25 in. (8.3 cm) H as shown in Fig. 15.

The reinforcing steel used in the specimens was ASTM standard A615 reinforcing steel with a diameter of 0.5 in. (1.27 cm). For each specimen, two pieces of reinforcing steel were cut to a length of 17.5 in. (44.45 cm) and one end of each reinforcing steel was drilled and tapped to accommodate 1/8 in. (.32 cm) diameter screws. The reinforcing steels were

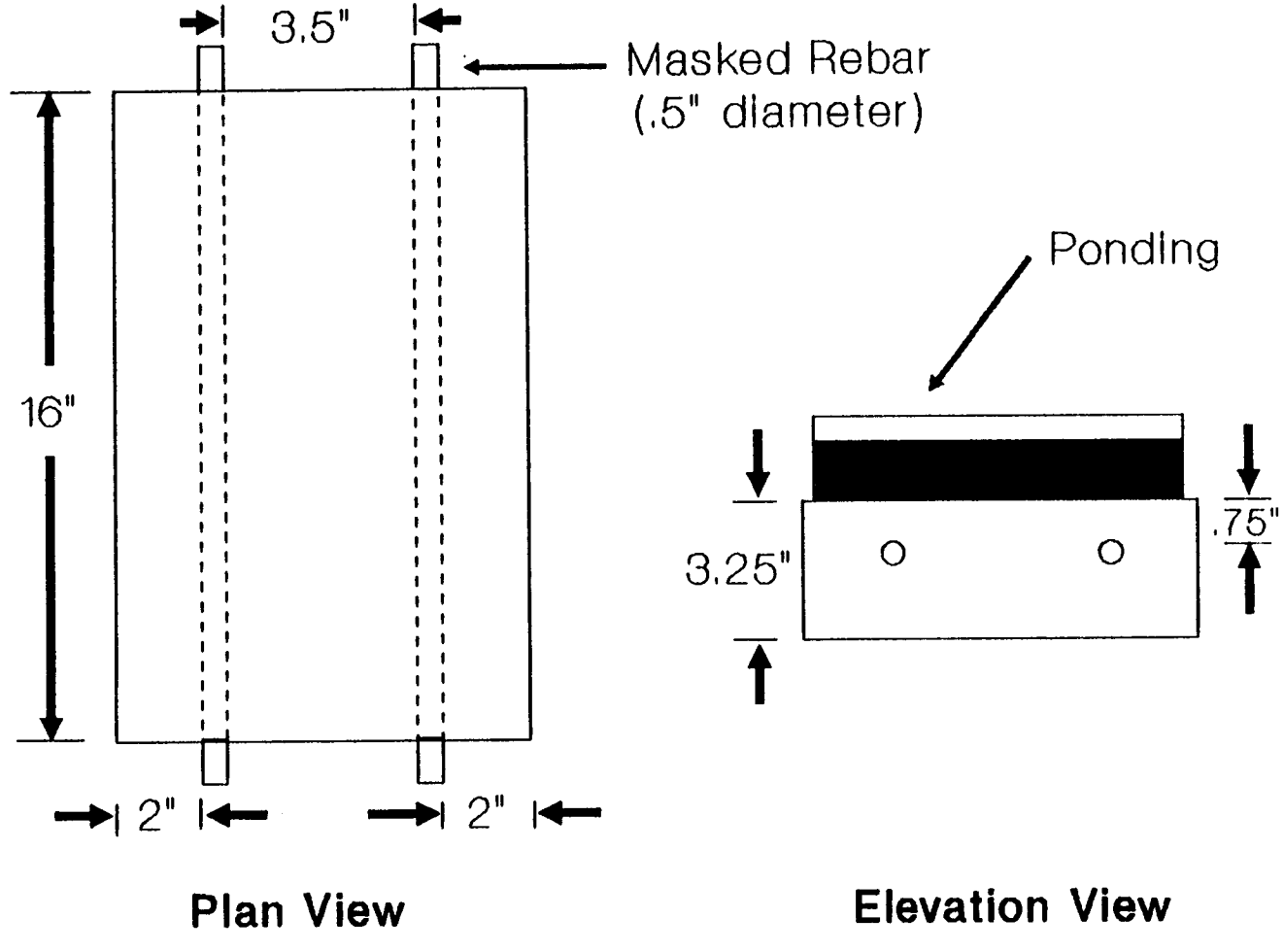

Fig. 15 Specimen Design and Ponding Configuration

cleaned with hexane to remove any residual rust and oil, and 2.5 in. (6.35 cm) of each reinforcing steel end was masked with electroplating tape leaving a bare steel length of 12.5 in. (31.75 cm). Masking the ends of the reinforcing steels eliminated the possibility of the exposed ends corroding after concrete placement and provided a known corroding length of steel.

Specimen Casting

In order to achieve a 3/4 in (1.91 cm) cover depth over the reinforcing steels, the concrete specimens were cast inverted so that the top surface of the final specimen was formed at the bottom surface of the mold. This was done in order to minimize the possibility of subsidence cracking with such a small cover depth.

Several trial concrete batches were mixed to determine the mix composition that yielded the desired concrete properties. The final mix composition and physical properties are detailed in Appendix A, Tables A-3 and A-4. Four batches of this concrete composition were mixed, with each batch providing concrete for four specimens (Set A). The forms were set on a Syntron vibratory table during placement of concrete to insure proper consolidation.

A second set (Set B) of 16 specimens was cast using the same molds and procedure mentioned above. The concrete mix composition and physical properties are presented in Appendix A, Tables A-5 and A-6.

Post-casting Treatment

In order to aid in accelerating the diffusion of chlorides and the eventual initiation of corrosion in the specimens, the cast specimens were only allowed to cure for a short period of time before application of sodium chloride solution. The short cure time allowed for only limited hydration of the concrete, thus leaving the concrete more permeable. Set A specimens cured in air at room temperature for 24 hours at which time they were removed from the formwork and their top surfaces (surface in contact with form bottom) were etched with muriatic acid to remove any residual form oil. Set B specimens were allowed to cure for 72 hours in air before being removed from the formwork and etched.

After the etching process, both sets of specimens were placed in a drying oven at 150°F (65.5°C) for 24 hours. Subjecting the specimens to an elevated temperature served to drive out a portion of the unbound water near the surface of the concrete. Removing water from the pore system would aid in accelerating the diffusion of chlorides through the concrete.

As a means of simulating the single surface diffusion on a bridge deck surface, the sides of each specimen were coated with 2 layers of epoxy. The bottom surfaces of the specimens were left uncoated to allow for oxygen diffusion during the ponding stage. A plexiglass ponding dike was attached to the top of each specimen using a silicon rubber sealant.

Corrosion Initiation

The specimens were subjected to alternating 3 day pondings with 25.4 ozs. (750 ml) of 6% by weight NaCl solution and 4 day dryings in a conditioning chamber. The drying cycle consisted of 24 hours at room temperature and 72 hours at 150 °F (65.5° C). Plexiglass covers were placed over the ponding dikes to minimize moisture loss and solutions were removed after the ponding cycle using a wet/dry shop-vac.

Prior to the first wetting cycle, half-cell potential measurements using a reference half-cell and hand-held multimeter were taken at three positions spanning the area directly above each reinforcing steel. A saturated calomel electrode (SCE) was used as the reference half-cell and measurements were adjusted to the copper sulfate half-cell (CSE) based on the known potential difference. Subsequent potential measurements were taken after the first day of drying following each ponding cycle.

Both sets of specimens were cycled until there was a sustained drop in the half-cell potentials to indicate a high probability of corrosion based on the corrosion probability ranges (30). In order to support the indication of corrosion, a three electrode-linear polarization device (3LP) developed by Kenneth C. Clear, Inc., was used to measure the corrosion current of each reinforcing steel. The 3LP test procedure is based on the Stern-Geary equation (38), with B = 40.76, and simply measures the amount of current change needed to polarize the working electrode (rebar) to a fixed change in potential. Since corrosion current (I_{corr}) is directly proportional to corrosion rate, the I_{corr} values could be used to determine the extent of corrosion activity in the specimens.

The resulting corrosion current values were interpreted based on the following guidelines [39]:

- $I_{corr} < 0.20$ mA/ft^2 -----> no corrosion damage expected
- 0.20 mA/ft^2 $< I_{corr} <$ 1.0 mA/ft^2 -----> corrosion damage possible in the range of 10 to 15 years
- 1.0 mA/ft^2 $< I_{corr} <$ 10 mA/ft^2 -----> corrosion damage expected in 2 to 10 years
- $I_{corr} >$ 10 mA/ft^2 -----> corrosion damage expected in 2 years or less

Corrosion current values greater than 1.0 mA/ft^2 were considered indicative of adequate corrosion activity to start treatments.

Chloride Concentration Measurements

A third means used in characterizing the corrosion activity in the specimens prior to treatment was the measurement of the chloride ion concentration at the reinforcing steel level. Using an impact hammer/drill and vacuum assisted collection device, concrete powder

samples were taken from a depth of 1/2 in. (1.27 cm) to 1 in. (2.54 cm) at a location between the reinforcing steels in each pad. The measurement of the chloride content of such a sample would approximate the chloride ion concentration at the reinforcing steel surface level of 3/4 in. (1.91 cm).

The chloride ion concentration of each sample was measured twice using a specific ion electrode test procedure. The basic procedure involved the extraction of Cl^- from the powder samples via an acidic digestive solution and the use of a Cl^--specific ion probe to measure the concentration in terms of a voltage. This voltage reading is used in a determined calibration equation that yields the ion concentration in terms of lbs/yd^3.

Chloride levels exceeding 1.2 lbs/yd^3 (0.71 kg/m^3) [18] were considered sufficient to initiate corrosion of the reinforcing steel in the specimens.

Treatment of Specimens

Before application of the treatment, the chloride-contaminated concrete above the reinforcing steel in each pad was removed. A groove area 2 in. (5.08 cm) wide and 3/4 in. (1.91 cm) deep was marked off for removal along the length of each pad above each reinforcing steel as shown in Fig. 16. A masonry saw was used to make four 1/8 in. (0.32 cm) wide, 3/4 in. (1.91 cm) deep cuts within the 2 in. (5.08 cm) groove width above each reinforcing steel, being careful not to contact the reinforcing steel. The remaining concrete in the groove area was then removed using a masonry chisel in order to expose the top portion of each reinforcing steel.

Most of the specimens of Set A had developed cracks above the reinforcing steels due to the expansion of corrosion products prior to grooving. During grooving, the first specimen of Set A split in two as the crack above the reinforcing steel propagated under the stress of the masonry saw. The exposed bar was uniformly corroded and had lost about 1/8 in. (0.32 cm) of its diameter, thus, for the most part, specimens from Set A were determined to be too highly corroded for assessing the efficiency of the proposed abatement treatments. However, two of the specimens that exhibited lower corrosion currents and higher potentials were selected to be treated and will be referred to as specimen A-13 and specimen A-15. Specimen A-13 was left ungrooved while A-15 was grooved. No problems were experienced with the grooving of Set B,therefore, eighteen specimens were deemed suitable for treatment.

Application of Treatments

The treatments and combinations of treatments applied to the eighteen specimens are listed in Table 16. The treatment concentrations are expressed in Molar concentrations for ponding application and in terms of % s/s (percent molecular weight of the salt to cement weight) cement for mortar applications. Mortar concentrations were determined as follows:

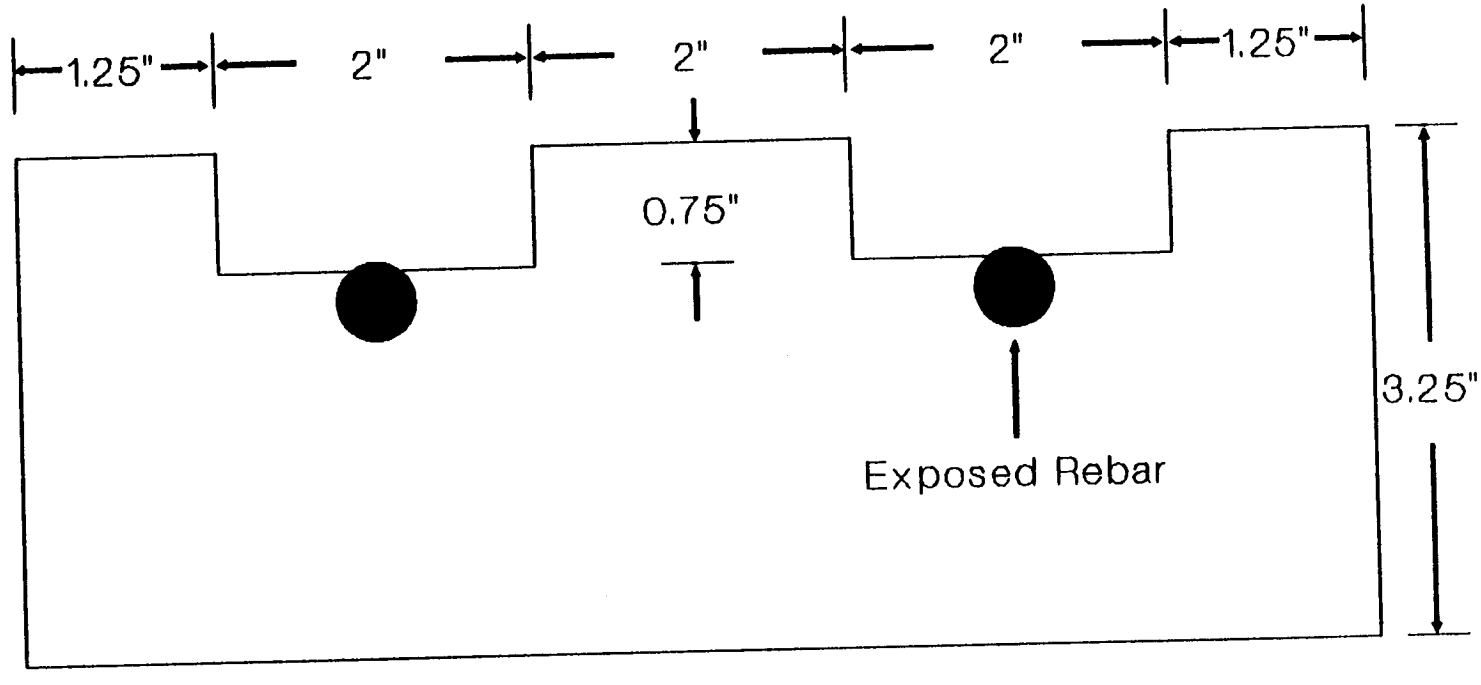

Fig. 16 Specimen Groove Dimensions

Table 16. Corrosion abatement treatments

SPECIMEN	PONDING TREATMENT	MORTAR TREATMENT
B-1 (Control)	None	Untreated
B-2	None	DCI (@ 30% solids) added at 5% s/s cement
B-3	.1M DCI solution	DCI added at 5% s/s cement
B-4	.1M TCI solution	Untreated
B-5	None	Hydroxylapatite added at 24% s/s cement
B-6	None	Sodium tetraborate added at 1% s/s cement
B-7	.1M sodium tetraborate	Sodium tetraborate added at 1% s/s cement
B-8	.1M zinc borate solution	Zinc borate added at 1.7% s/s cement
B-9	.1M ALOX 901 (ethyl alcohol solvent)	Untreated
B-10	.1M TCI solution	Hydroxylapatite added at 24% s/s cement
B-11	None	DCI added at 5% s/s cement and hydroxyl-apatite added at 24% s/s cement
B-12	.1M zinc borate solution	Zinc borate added at 1.7% s/s cement and hydroxylapatite added at 24% s/s cement
B-13	.1M DCI solution and silicone sealer	Untreated
B-14	.1M DCI solution and styrene-acrylic sealant	Untreated
B-15	.1M DCI solution with silicone spray on Bar A, styrene-acrylic spray on Bar B	Untreated
B-16	Direct application of CORTEC 1609	CORTEC 1609 added at .017% s/s cement
A-13	Direct application of CORTEC 1337 to ungrooved surface	No grooves
A-15	Direct application of CORTEC 1337 to grooves	CORTEC 1609 added at .017% s/s cement

Table 17. Mortar Cube Treatment Concentrations

TREATMENT	CONCENTRATION
Control	Untreated mortar
DCI (calcium nitrite @ 30% solids)	2.50%, 5.00%, 10.00% s/s cement
Sodium tetraborate ($Na_2B_4O_7 \cdot 10H_2O$)	0.50%, 1.00%, 2.00% s/s cement based on $Na_2B_4O_7$
Zinc borate ($2ZnO \cdot 3B_2O_3 \cdot 3.5H_2O$)	0.22%, 0.43%, 0.85%, 1.70%, 3.40% s/s cement base on $2ZnO \cdot 3B_2O_3$
Hydroxyl apatite	6.25%, 12.50%, 25.00% s/s cement
CORTEC 1609	0.15%, 0.30%, 0.45% l/s cement

1. DCI: as recommended by the manufacturer.

2. Sodium and Zinc Borates: a concentration equivalent to using .1M solution as mortar mix water was applied based on Part I results.

3. CORTEC 1609: manufacturer's dosage recommendation.

4. Hydroxylapatite: the apatite concentration was based on the theoretical removal of Cl^- by the two hydroxyl groups in each molecule of hydroxylapatite. An apatite concentration was calculated that would theoretically remove 10 lbs Cl^-/yd^3 (5.93 kg/m^3) of concrete.

For both sodium and zinc borate, all concentrations were based on the unhydrated, reactive portions of their molecules, $Na_2B_4O_7$ and $2ZnO \cdot 3B_2O_3$ respectively.

For the ponding treatments, the grooves were filled with the treatment solution, covered with plastic to limit evaporation, and allowed to sit for ten days. For specimens B-13 and B-14, the polymer sealants were ponded in the bottom 1/4 in. (0.64 cm) of the grooves for two hours after which the remaining solvent solution was decanted off. Each bar in specimen B-15 was treated with 10 g of sprayed polymer sealant solution. Specimen A-13 was not grooved in order to evaluate the effectiveness of CORTEC 1337 migratory inhibitor through concrete without exposed reinforcing steel.

Upon completion of the 10-day treatment exposure period, the grooves were backfilled with doped or undoped mortar, depending upon the treatment combination (Table 16). The basic mortar mix for the backfill is detailed in Appendix A, Table A-7. In order to insure adequate bonding between the groove surfaces and the new mortar, the grooves were surface-moistened with water mist and a thick cement slurry was applied to the grooves prior to placement of the mortar. The specimens were placed on a vibratory table during mortar placement to insure proper consolidation.

All the backfilled specimens were placed under moist burlap and a plastic sheet cover and allowed to cure for 7 days. During the curing period, the burlap covers were moistened periodically.

Corrosion of Treated Specimens

At the completion of the 7-day cure, half-cell potential and corrosion current measurements were taken for each bar in the specimens. The ponding dikes were replaced on the specimens and the ponding/drying cycle was resumed, but with 3% by weight NaCl solution.

During the post-treatment corrosion monitoring, careful attention was paid to the formation of any cracks on the specimens, especially around the mortar/groove interface.

Evaluation of Mortar Cube Strength and Resistivity

A corrosion treatment's effect on mortar properties must be considered in addition to its corrosion abatement effectiveness if it is proposed for field use. In order to evaluate the proposed treatments' effects on mortar, 2 in. (4.08 cm) mortar cubes were cast, in accordance to ASTM C-109-80 " Compressive Strength of Hydraulic Cement Mortars," with varying treatment concentrations as shown in Table 17. The mortar cube mixture proportions are presented in Appendix A, Table A-8. Nine cubes were made for each treatment concentration. During the first 20 days of curing, strength and resistivity measurements were taken periodically.

Strength Measurements

Mortar cube compressive strength measurements were conducted after 1, 3, and 20 days of curing in accordance with ASTM C-109, see Table C-6. Mortar cubes that had not hardened sufficiently to be placed in the testing apparatus were considered to have zero strength.

Resistivity Measurements

Mortar cube resistivity measurements were taken after 1, 3, 10, and 20 days of curing. The cubes being used for the 20-day strength tests were utilized for the resistivity measurements. The resistivity of the cubes was obtained through the use of a modified Nilsson Soil Resistance Meter. The procedure for the resistivity measurements is detailed in Appendix B. A resistivity measurement was taken across each of the three opposite faces on three cubes for each treatment concentration. After the completion of each set of measurements, the cubes were returned to baths of saturated lime water for further curing.

Evaluation of the Chloride-Ion Scavenging Ability of Hydroxylapatite

In order to evaluate hydroxylapatite's ability to scavenge chloride ions, three different tests were conducted to determine the possibility and extent of any substitution of Cl^- for OH^- in the hydroxylapatite molecule.

pH Measurements

The substitution of Cl^- for OH^- in an aqueous medium would result in the release of the hydroxyl ion into solution. A simple pH measurement can detect the increased concentration of hydroxyl ions. The pH of the solution that would theoretically result from a 100% Cl^- /OH^- substitution could be determined from the equation:

$$pH = 14.00 - pOH \qquad (1)$$

where,

pOH = -log [moles of OH^-/volume of solution in litres]

A 25 g sample of hydroxylapatite was placed in a beaker of 200 ml of 5% by weight NaCl solution. The solution was agitated using a magnetic stirrer and the pH was measured as a function of time over a span of 24 hours with an electronic pH meter. The pH of the salt solution and of a solution containing 25 g of hydroxylapatite with 200 ml of distilled water was taken for comparison. Another test was run with the apatite/salt solution being heated to a temperature of 150 °F (65.5° C) and pH measurements were taken over a span of 24 hours.

Specific Ion Electrode Measurements

The same technique used in determining the chloride ion concentration in the concrete specimens (see Chloride Concentration Measurements section) was employed to measure the ability of hydroxylapatite to pick up chloride ions. 25 g samples of hydroxylapatite were placed into containers containing 5%, 10%, and 15% by weight NaCl solution. One set of containers was agitated at room temperature for 24 hours while a second set was heated to 150 °F (65.5° C) and agitated for 24 hours using a magnetic stirrer. The hydroxylapatite samples were then filtered from the solutions, rinsed and stirred with distilled water, filtered again, and allowed to dry. Each sample was subjected to 5 cycles of rinsing and drying.

3 g of each sample, including a control sample, were analyzed using the specific ion electrode technique to determine the presence of any chloride ions that may have been scavenged. Since hydroxylapatite is soluble in acidic solutions, any scavenged Cl^- would be released from the crystal structure when subjected to the acidic digestive solution prior to chloride measurement by the specific ion electrode.

Differential Thermal Analysis

Differential thermal analysis (DTA) was conducted on both untreated hydroxylapatite and hydroxylapatite-exposed NaCl solution. Two 25 g samples of hydroxylapatite were exposed to 200 ml of 5% by weight NaCl solution at room temperature and at 150 °F (65.5° C) for 24 hours. The samples were then subjected to the same rinsing/drying process as in the specific ion probe tests. DTA scans were performed on an untreated sample and on both the treated samples to determine the degree of the Cl^-/OH^- substitution. The procedure used for the DTA process is detailed in Appendix B.

Results and Discussion

Throughout the course of Part II, the following topics were subjects of the investigation:

- corrosion abatement effectiveness of chemical treatments applied to corroding reinforced concrete after removal of chloride-contaminated concrete;

- the effects of treatment admixes on the physical properties of cement mortar.

In addition to the above, the chloride-ion-scavenging ability of hydroxylapatite was evaluated.

Pre-Treatment Corrosion Measurements and Observations

Based on half-cell potential measurements taken after the first ponding with NaCl solution, the two sets of specimens exhibited remarkably different corrosion potentials during the first 70 days of exposure. The evolution of the mean corrosion potentials for Set A and Set B is shown in Fig. 17 with the initial value indicating E_{corr} after the first ponding. The mean corrosion potentials for the individual bars in each pad are listed in Appendix C, Table C-1. Half-cell potential measurements were attempted prior to the initial ponding but stable values could not be obtained because of the highly dried concrete.

For ease of understanding and uniformity, the half-cell potential measurements will be referred to in terms of copper-copper sulfate reference electrode (CSE) values.

Since the concrete mix designs for both Set A and B were similar, the difference in curing time seemed to have played a major role in corrosion activity initiation. Set A, cured for one day, exhibited initial corrosion potentials, E_{corr}, values less than -350 mV, indicating more than a 90% probability of corrosion (see Table C-1). Set B , cured for three days, required exposure for more than 20 days before falling below -350 mV. The one-day cure for Set A before ponding left the concrete's pore system extremely open due to the diminished time for cement hydration. This was exhibited during the first ponding in which the Set A specimens absorbed the entire 25 ozs. (750 ml) of 6% by weight NaCl solution in less than 24 hours.

After 100 days of exposure, 14 of the 16 specimens of Set A developed surface cracks caused by expanding corrosion products. These 14 specimens were deemed unsuitable for further evaluation because of the high degree of corrosion.

Verification of corrosion activity in the remaining 18 specimens can be seen in both the average corrosion current of bars A and B, and in the chloride ion concentration measurements taken prior to grooving, as presented in Table 18. I_{corr} values greater than 1.0 mA/ft^2 (1.08 $\mu A/cm^2$) and chloride concentrations values greater than 1.2 lbs/yd^3 (0.71 kg/m^3) were taken as indicators of corrosion initiation.

The values in Table 17 indicate a similarity in corrosion current and chloride ion concentration for each group of specimens made from the same concrete batch (B-1 to B-4, B-5 to B-8, B-9 to B-12, and B-13 to B-16). The decrease in I_{corr} and chloride concentration with succeeding concrete batches indicates improvement in the concrete quality. A possible

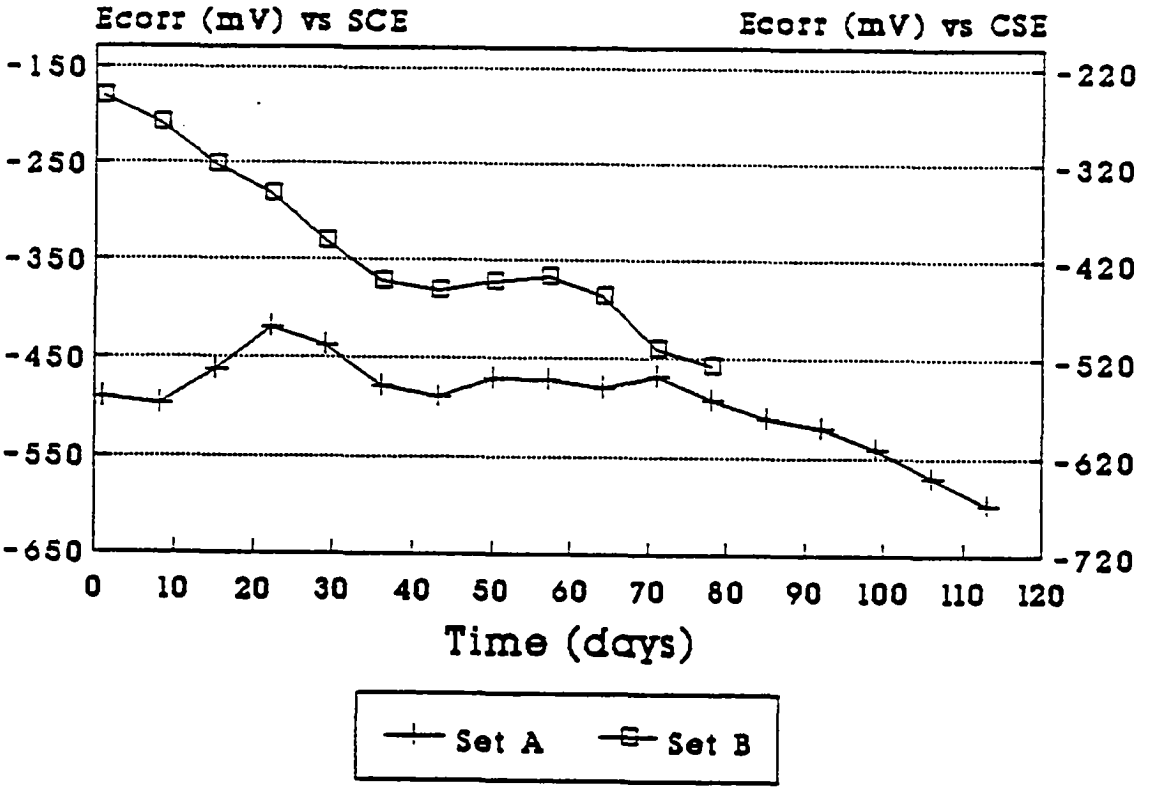

Fig. 17 Mean Pre-Treatment Half-Cell Potentials

Table 18. Average pre-treatment corrosion current of bars A and B combined, and chloride ion concentrations at rebar level for specimens used in treatment study.

Specimen	I_{corr} (mA/ft^2)	Cl^- Concentration at 3/4" depth (lbs/yd^3)		
		Trial 1	Trial 2	Mean
B-1	8.5	11.54	11.13	11.34
B-2	9.2	11.02	11.31	11.17
B-3	11.5	12.84	12.65	12.75
B-4	7.5	11.16	10.84	12.00
B-5	6.7	12.33	12.39	12.36
B-6	6.2	10.66	10.40	10.53
B-7	6.4	11.93	12.22	12.08
B-8	6.0	10.52	10.42	10.47
B-9	3.9	9.85	10.05	9.95
B-10	3.7	11.85	11.69	11.77
B-11	3.9	9.77	9.98	9.88
B-12	3.4	11.24	11.57	11.41
B-13	2.4	9.34	9.01	9.18
B-14	1.5	8.75	8.86	8.81
B-15	1.8	8.14	8.36	8.25
B-16	1.5	7.24	6.80	7.02
A-13	23.5	15.58	16.77	16.18
A-15	22.5	16.33	15.21	15.77

NOTE: 1.0 mA/ft^2 = 1.08 $\mu A/cm^2$
1.0 lbs/yd^3 = 0.59 kg/m^3

explanation may lie in the human factors of increased efficiency and improved casting practices with succeeding batches.

A simple linear regression (SLR) analysis was conducted on both the average pre-treatment corrosion potentials and chloride ion concentrations to determine their degree of correlation with the corrosion current values. A SLR analysis yields the coefficient of determination (r^2) which represents the proportion of the total variability of I_{corr} values that are explained or accounted for by the E_{corr} or chloride concentration values. A high value of r^2 indicates a strong correlation. The r^2 value for the E_{corr} correlation with I_{corr} was 66.0% and the value for the chloride concentration correlation was 81.0%. The chloride concentration showed a greater degree of correlation than E_{corr}, as the chloride sample set was able to account for 15.0% more of the I_{corr} sample set.

I_{corr} is linearly proportional to corrosion rate, but neither E_{corr} nor chloride ion concentration were found to have a high enough correlation (90-95%) to exhibit a linear relationship with I_{corr} and, therefore, they were not used as an accurate measurement of corrosion rate. As a result, in the analysis of the corrosion abatement treatments, I_{corr} measurements will predominantly be presented as an indication of treatment effectiveness.

Evaluation of Corrosion Abatement Treatments

To aid in the treatment effectiveness analysis, the following guidelines are used in data presentation:

- Since corrosion potentials are only an indicator of the probability of corrosion and not the degree or rate of corrosion, E_{corr} data are presented but not focused upon unless pertinent to treatment evaluation in relation to I_{corr}. When displayed, all E_{corr} values are the mean of six measurements taken on Bars A and B in each specimen. All E_{corr} data are tabulated in Appendix C, Table C-2.

- I_{corr} data are presented as the mean of the corrosion current in Bars A and B in each specimen. Since corrosion current is linearly proportional to corrosion rate, corrosion current and corrosion rate will be used synonymously through the analysis of results.

The statistical comparison of Bars A and B using a one-way analysis of I_{corr} variance was performed and their evaluation based on F-ratios and p-values is presented in Table 19. Although some specimens showed significantly different behavior between the bars, it was predominantly due to differences in magnitude while the bars still exhibited similar trends. All the corrosion current data are tabulated in Appendix C, Table C-4.

Due to the high variance in the final half-cell potential and corrosion current measurements prior to treatment, the absolute post-treatment values measured are not an accurate indication or good comparison measure of treatment effectiveness when used alone. Therefore, in

addition to absolute values, the data are also expressed in terms of % change in reference to the last measured E_{corr} or I_{corr} prior to treatment. The % change is computed as follows:

$$\% \text{ change} = [(V_P - V_C)/V_P] \times 100 \qquad (2)$$

where,

V_P = final pre-treatment

V_C = current value

A positive % change indicates a increase in corrosion potential (more noble) or a decrease in corrosion rate (in terms of corrosion current) in reference to the final pre-treatment value. A negative % change indicates a drop in corrosion potential (more active) and an increase in corrosion rate. All % change values for post-treatment E_{corr} and I_{corr} measurements are tabulated in Appendix C, Tables C-3 and C-5, respectively.

For convenience in data display and analysis, the treatments were divided into six treatment groups in addition to the control specimen:

1. DCI (calcium nitrite) and sealers
2. Borates
3. TCI (sodium monofluorphosphate)
4. Alox 901
5. Cortec Inhibitors
6. Hydroxylapatite and hydroxylapatite/inhibitor combinations

Control Specimen

Corrosion potential and corrosion rate evolution for the control specimen (B-1) after removal of contaminated concrete is displayed in Figures 18A and 18B. The control specimen's pre-grooving measurements indicated an extremely low E_{corr} in the > 90% probability of corrosion range and a high corrosion rate. After grooving, the specimen showed minimal improvement between days 1 and 10, most likely due to both the removal of chlorides and the placement of fresh mortar which aids in the pH restoration at the reinforcing steel surface. After day 10, the specimen exhibited increasing corrosion activity resulting in an approximate 70% increase in corrosion rate, indicating little benefit from the removal of the chloride-contaminated concrete.

DCI Treatments and Polymer Sealants

A comparison of the two DCI treated specimens in which one had DCI in the mortar and the

Table 19. One-way analysis of I_{corr} variance between Bars A and B in each specimen at an α=0.05 level.

Specimen	F-Ratio[1]	p-Value[2]	Significantly Different (Yes/No)
B-1	0.09	0.763	No
B-2	3.62	0.067	Yes
B-3	0.12	0.728	No
B-4	10.40	0.003	Yes
B-5	2.14	0.153	No
B-6	0.60	0.445	No
B-7	3.48	0.072	Yes
B-8	6.47	0.016	Yes
B-9	1.12	0.298	No
B-10	2.35	0.136	No
B-11	3.25	0.081	Yes
B-12	2.09	0.158	No
B-13	1.21	0.281	No
B-14	6.08	0.020	Yes
B-15	0.31	0.583	No
B-16	0.00	0.967	No
A-13	0.01	0.932	No
A-15	0.91	0.352	No

[1]Tabulated F-ratio for 16 observation sample sets (B-1 thru B-16) = 2.76. For 12 observation sample sets (A-13) F-ratio = 2.82, and for 11 observation sample sets (A-15) F-ratio = 2.95.

[2]P-values less than 0.10 indicate significant difference [40].

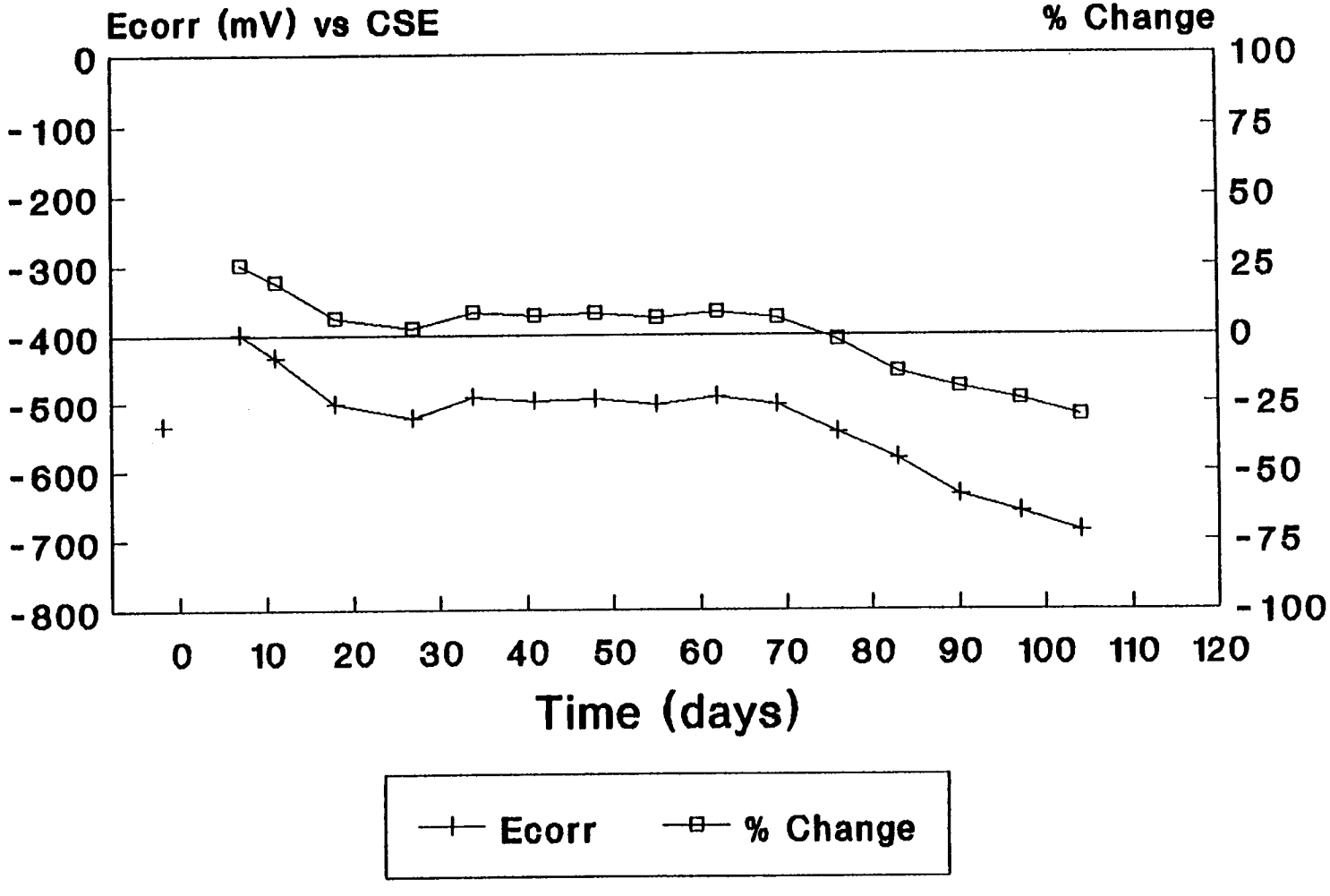

Fig. 18A Control Specimen (B-1) Mean Half-Cell Potentials Post Treatment Percent Change

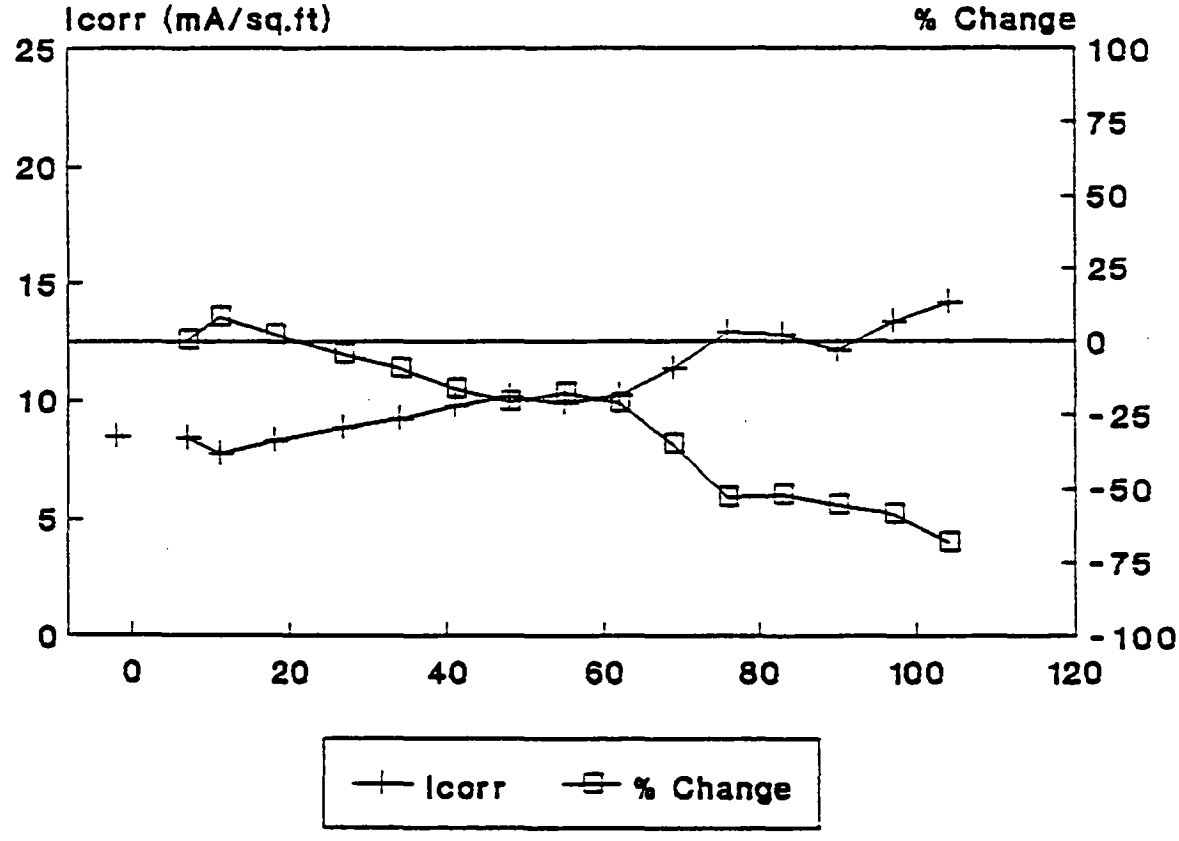

Fig. 18B Control Specimen (B-1) Corrosion Rates and Post-Treatment Percent Change

other was ponded as well as backfilled with DCI mortar showed that the specimen which was ponded exhibited a far better corrosion abatement performance as reflected in Figures 19A thru 19D. I_{corr} values reflect an average 25% reduction in corrosion rate in the mortar treatment specimen (B-2) during the first 40 days and then a 65% increase to more than 15 mA/ft^2 (16.1 mA/cm^2) at day 100. It appears as though the DCI present in the mortar in contact with the reinforcing steel and groove was sufficient to further stabilize the Fe_2O_3 passive layer which resulted in the slight reduction in the corrosion rate for a short period. However, diffusion of DCI was not great enough to sustain a high enough nitrite concentration at the reinforcing steel to compete sufficiently against diffusing chlorides; therefore, the Fe^{2+} ions in solution began complexing with the chlorides to further the corrosion process instead of reacting with the nitrite to eventually enhance the stability of the passive film. The specimen's initial performance was better than the control specimen, but deteriorated rapidly after 40 days.

The DCI specimen treated both through ponding and mortar (B-3) exhibited highly effective corrosion abatement. After day 7, the specimen showed greater than a 50% increase in corrosion potential (more noble) and 60% decrease in corrosion rate for the entire exposure duration through day 104. The ponding appeared to allow the development of a sound passive layer on the reinforcing steels to inhibit the anodic reaction and promoted the diffusion of DCI into the concrete surrounding the reinforcing steels. This passive layer in combination with the high nitrite concentration provided by the ponding and subsequent mortar backfill was effective enough to provide a higher and longer corrosion abatement than just the mortar-treated specimen.

The effectiveness of DCI ponding can also be seen in the three specimens (B-13, B-14, B-15); these grooves were ponded with DCI and a polymer sealer was applied before backfilling with untreated mortar. The post-treatment E_{corr} and I_{corr} values for each polymer sealer applied (see Table C-2) are shown in Figures 19E thru 19H. The corrosion measurements for the styrene-acrylic specimen (B-14) are expressed in terms of Bar A only, due to the development of a crack at the groove interface above Bar B which allowed the rapid diffusion of chlorides and the acceleration of corrosion.

Without distinguishing between the sealers, both the E_{corr} and I_{corr} show an approximate 50% average improvement during the entire 104 days of exposure. However, this is somewhat misleading, because the pre-treatment corrosion rate for each of the specimens was low, falling between 1.5 and 2.5 mA/ft^2. The initial level of corrosion rate can conceivably play a factor in the magnitude of the % change in corrosion potential and rate after treatment. Any treatment method applied to specimens of low corrosion activity would reasonably be expected to cause a greater % change in magnitude than if applied to specimens of higher corrosion activity. Although the absolute change in magnitude would be smaller, the % change in magnitude would most likely be greater. This problem can only be overcome by using specimens of relatively identical corrosion rates or evaluating specimens of varying corrosion rates over a longer duration.

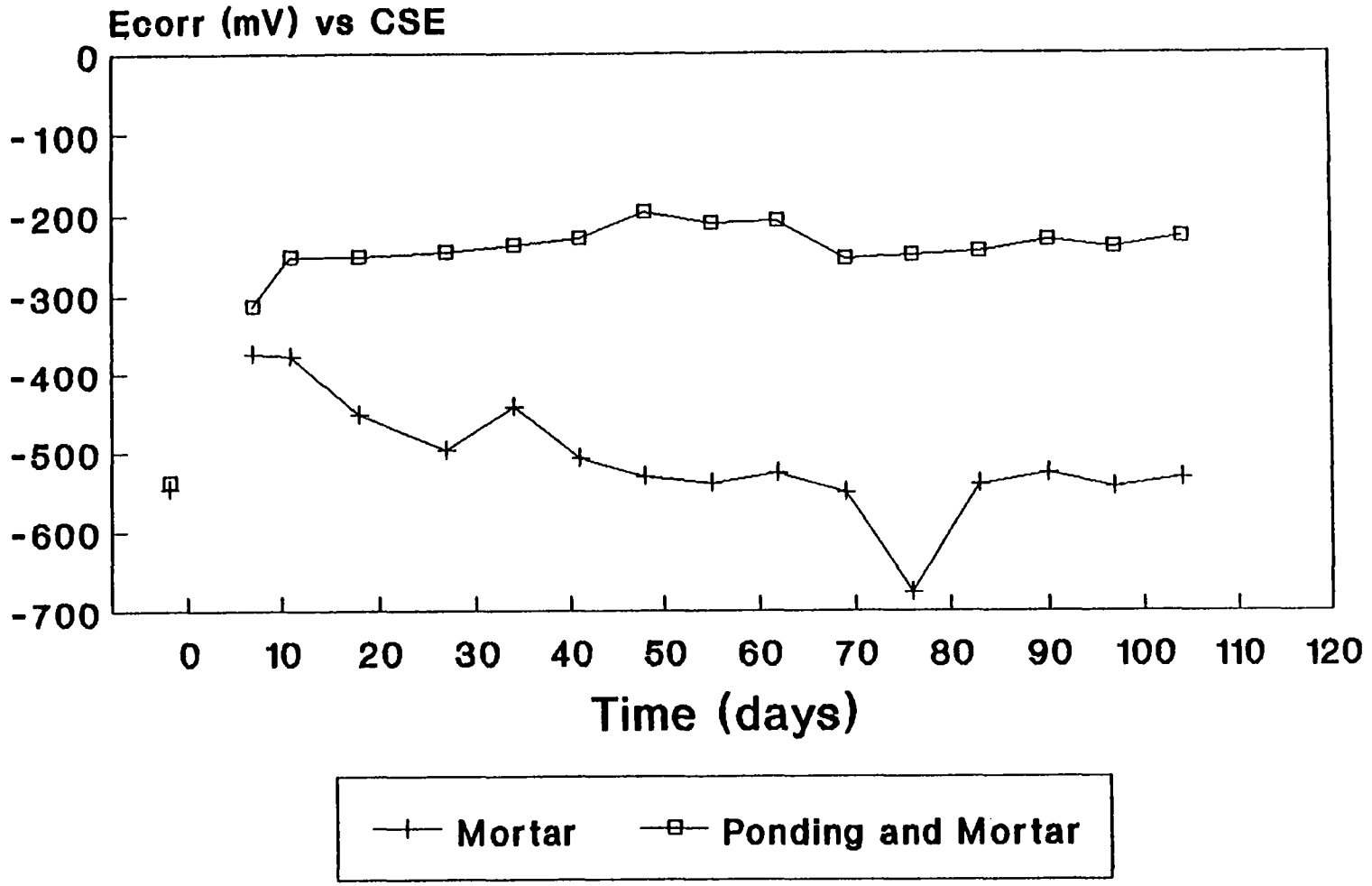

Fig. 19A Mean Half-Cell Potentials for DCI Treated Specimens (B-2, B-3)

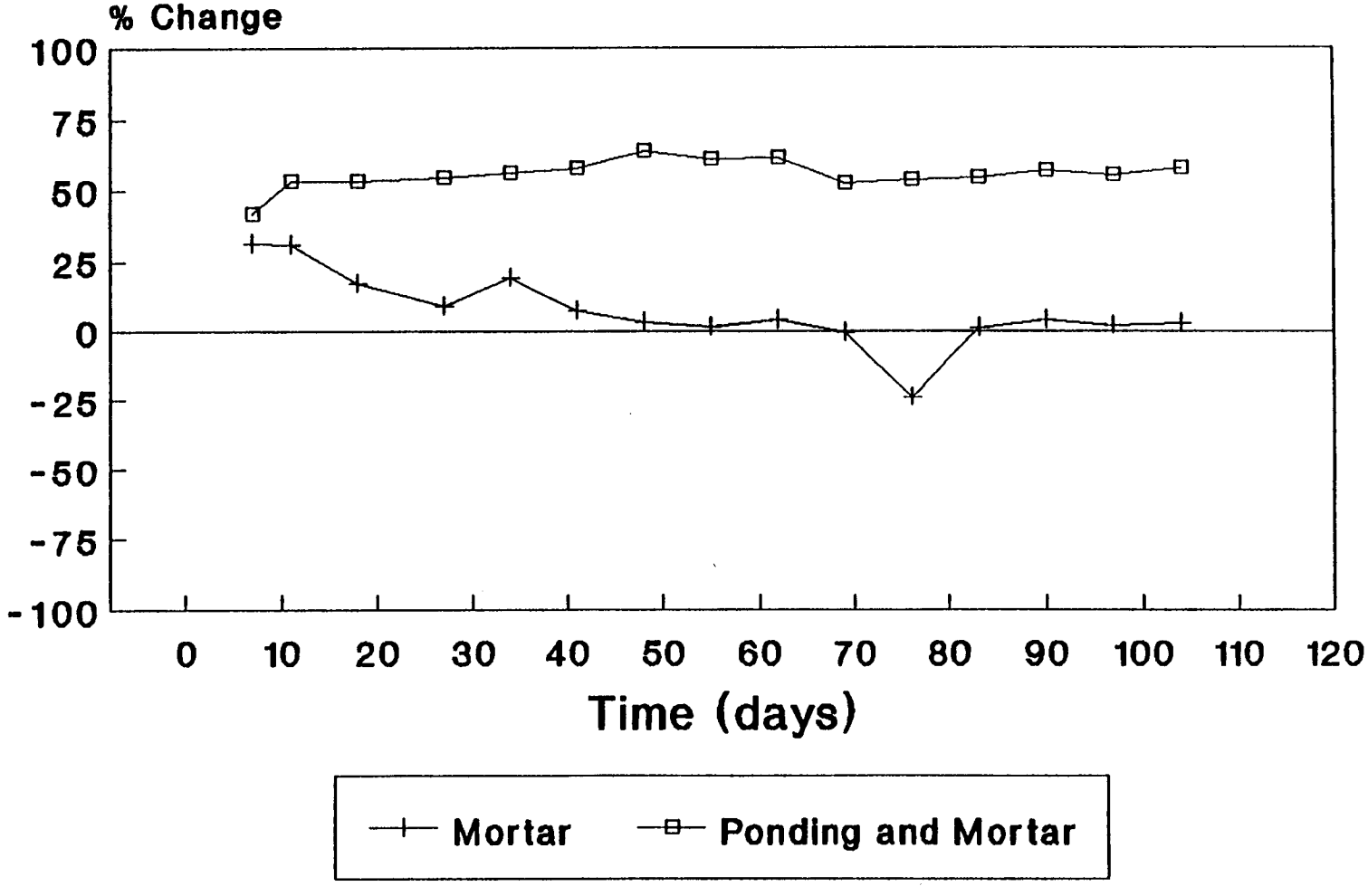

Fig. 19B Post Treatment Percent Change in Half-Cell Potential for DCI Treated Specimens (B-2, B-3)

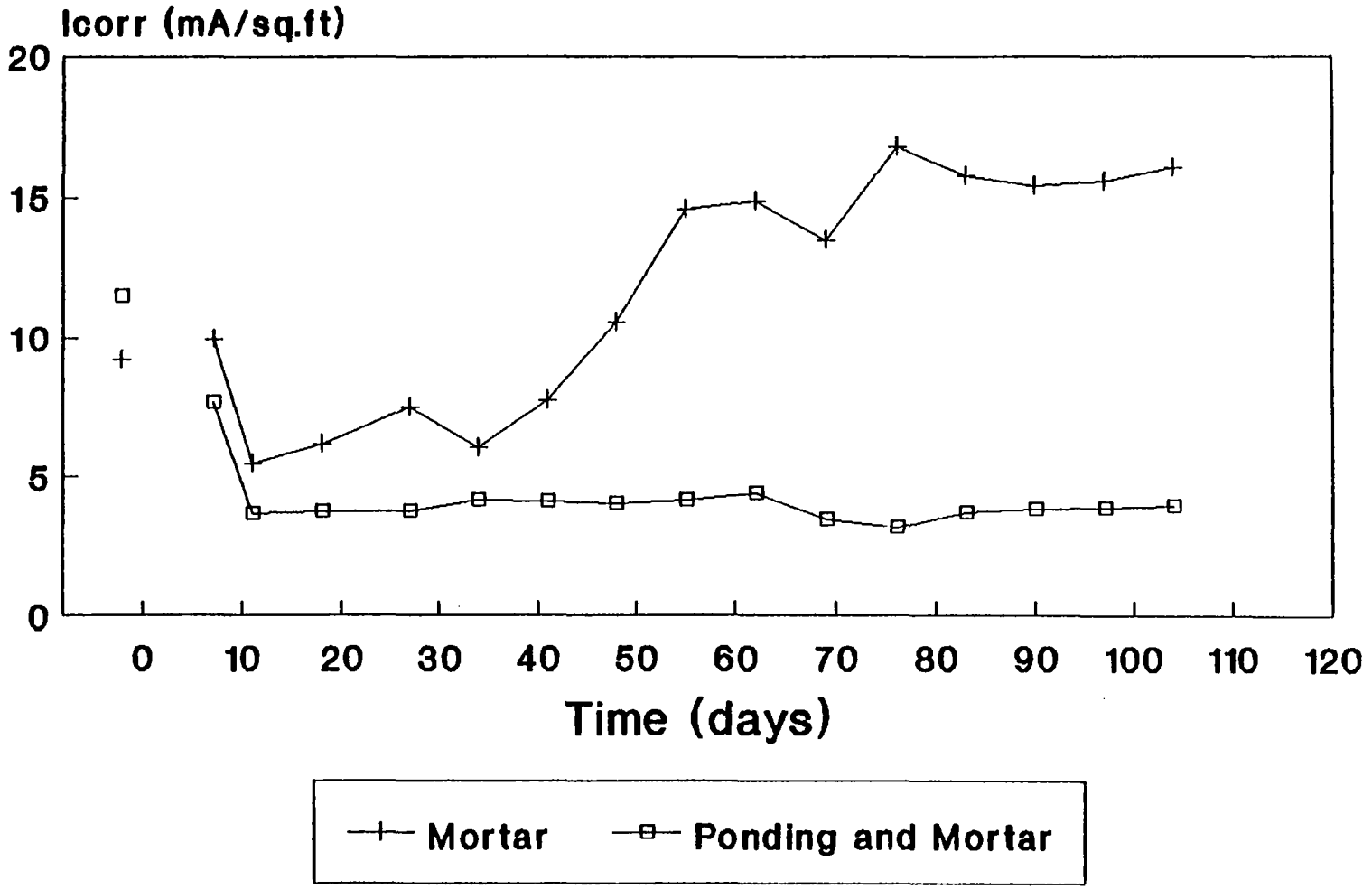

Fig. 19C Mean Corrosion Rates for DCI Treated Specimens (B-2, B-3) NOTE: 1.0 mA/ft^2 = 1.08 $\mu A/m^2$

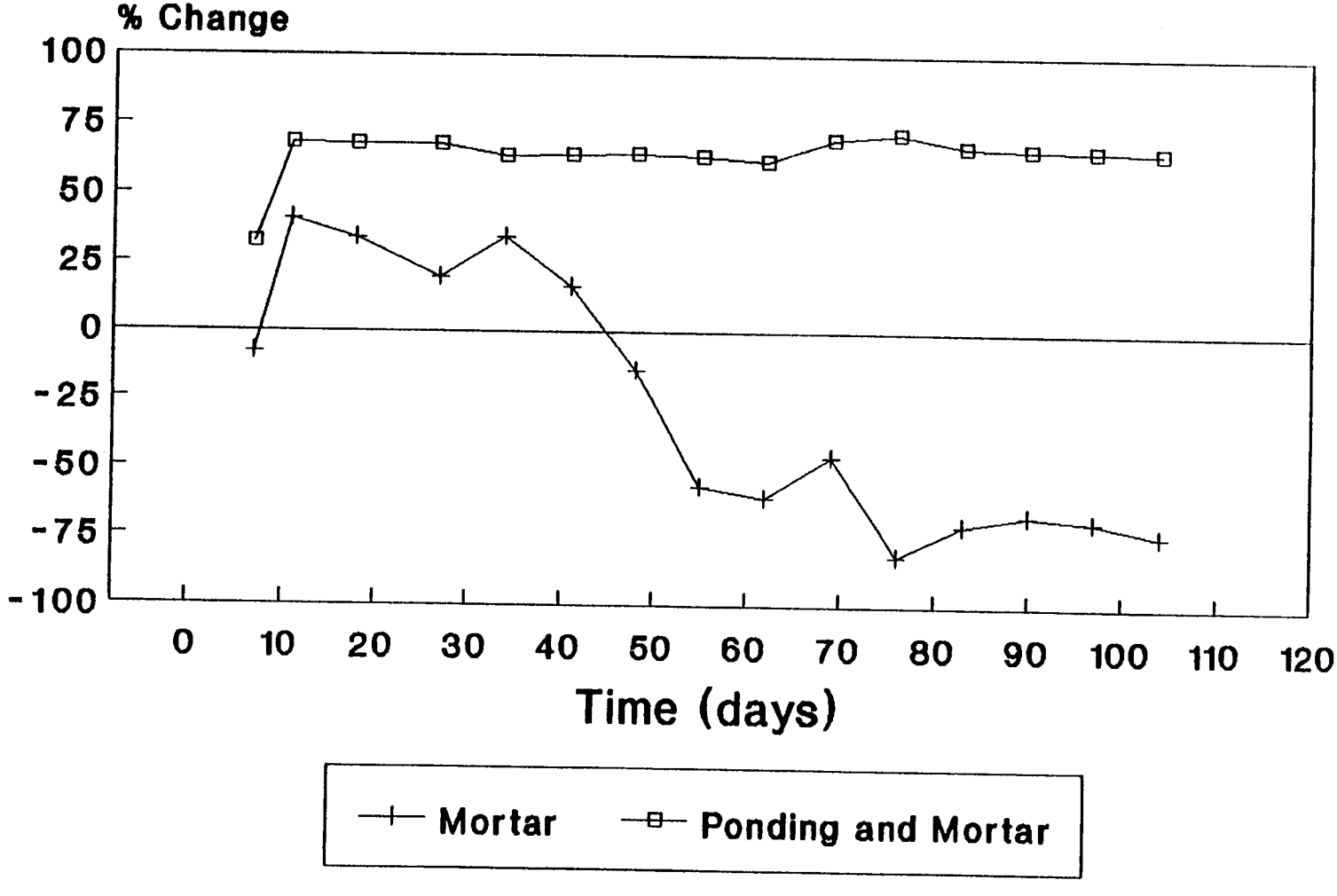

Fig. 19D Post-Treatment Percent Change in Corrosion Rate for DCI Treated Specimens (B-2, B-3)

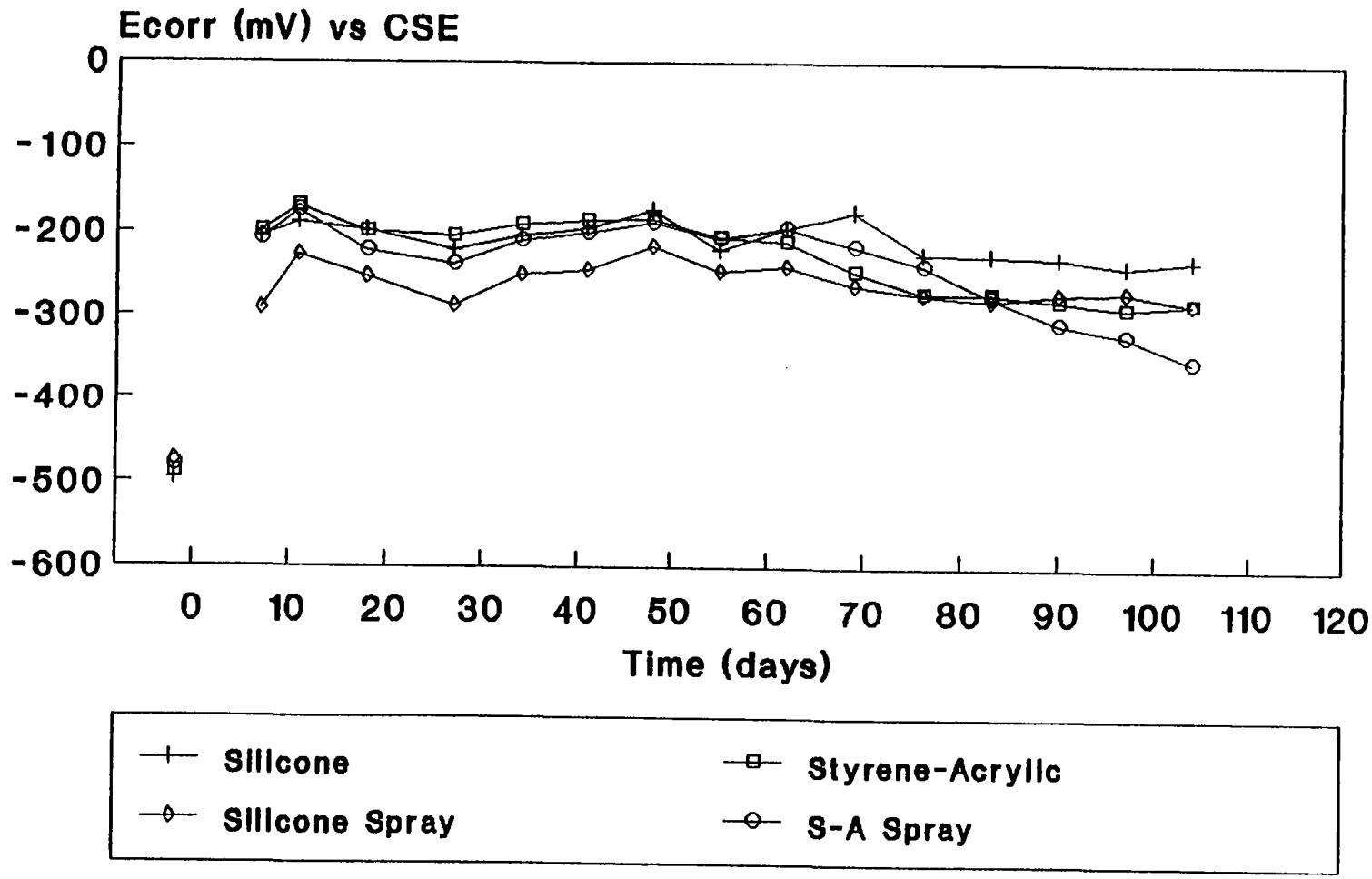

Fig. 19E Mean Half-Cell Potentials for DCI Ponded Specimens with Polymer Sealers (B-13, B-14, B-15)

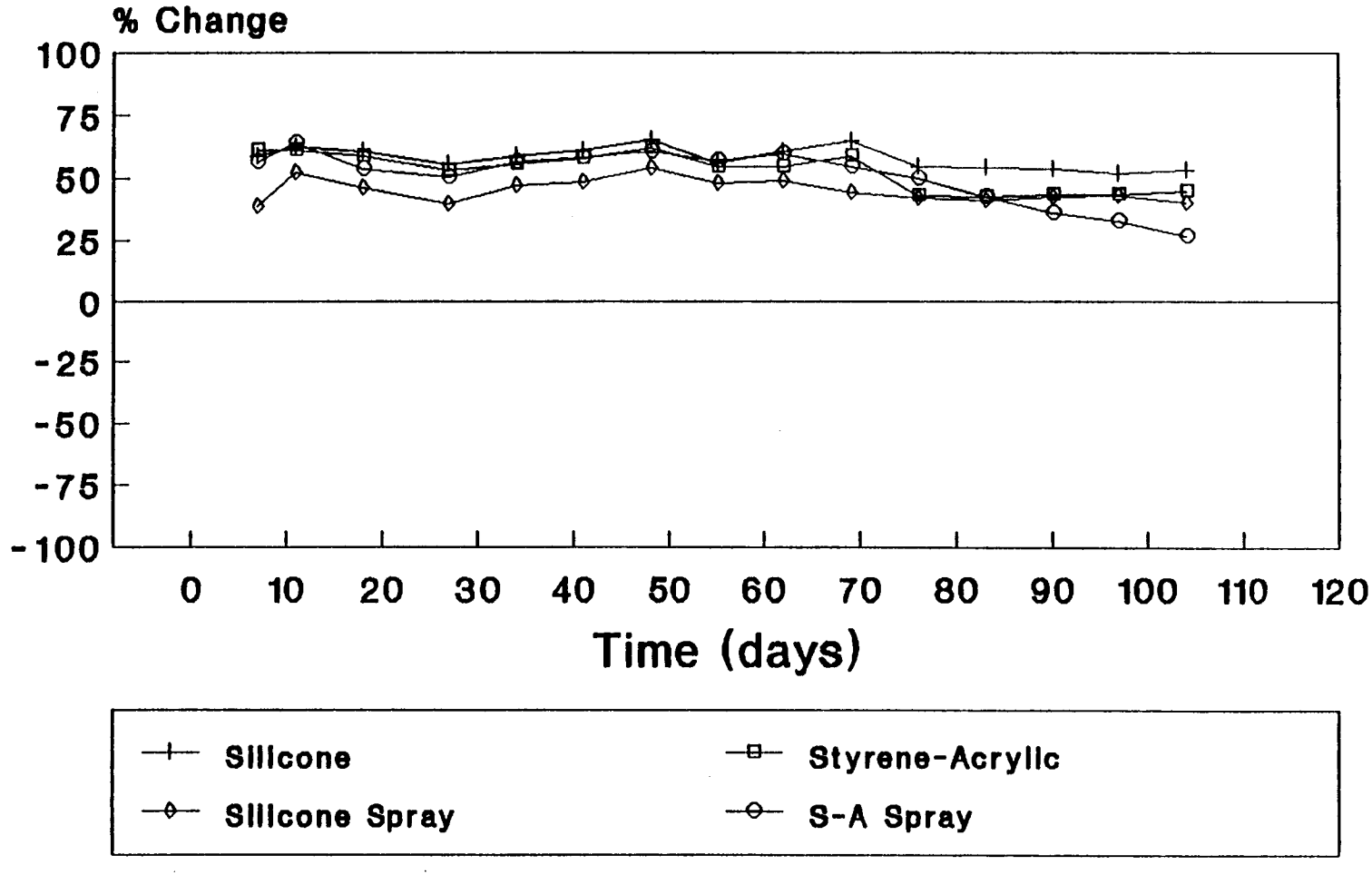

Fig. 19F Post-Treatment Percent Change in Half-Cell Potential for DCI Ponded Specimens with Polymer Sealers (B-13, B-14, B-15)

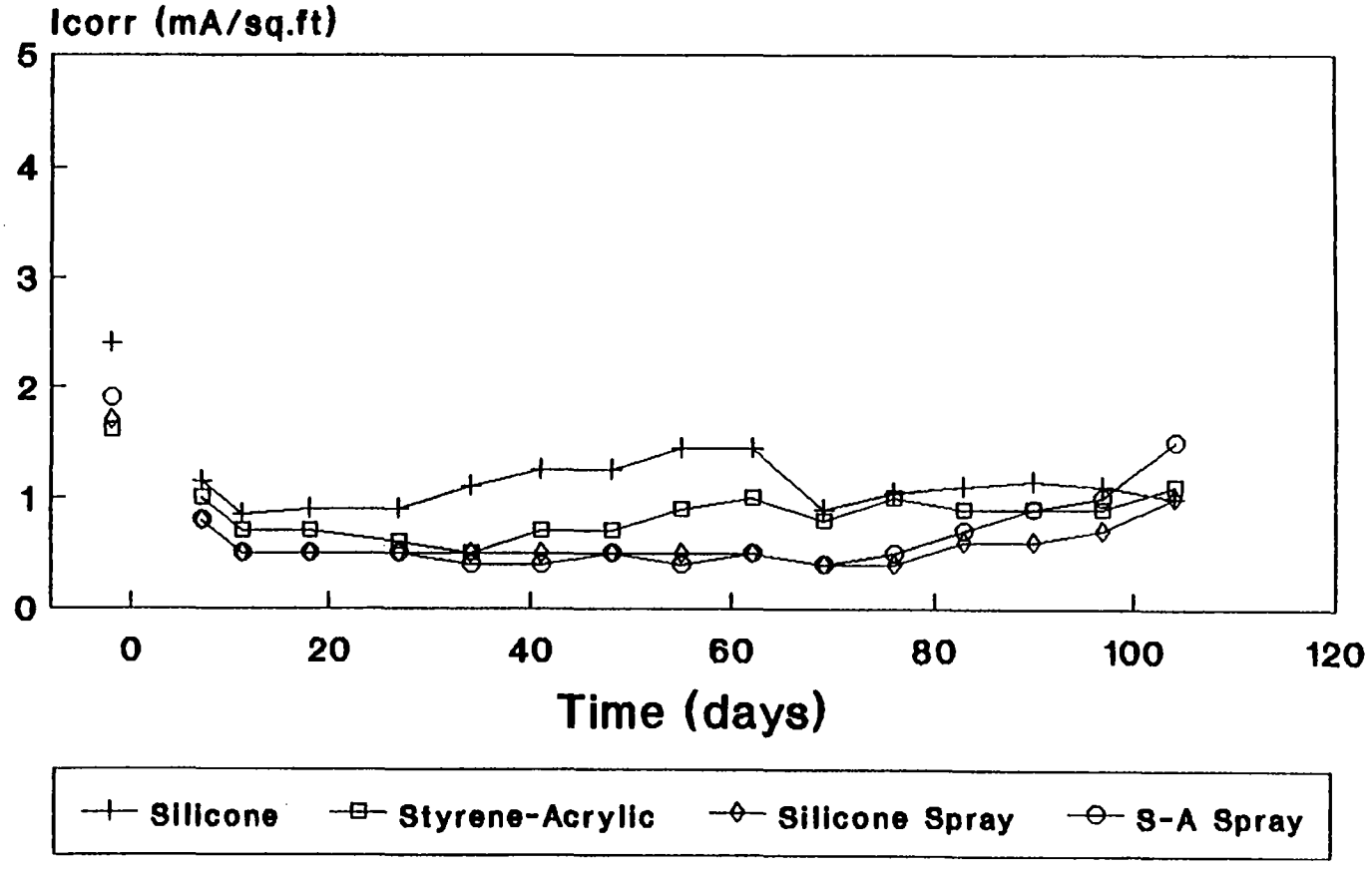

Fig. 19G Mean Corrosion Rates for DCI Ponded Specimens with Polymer Sealers (B-13, B-14, B-15)

NOTE: 1.0 mA/ft^2 = μA/m^2

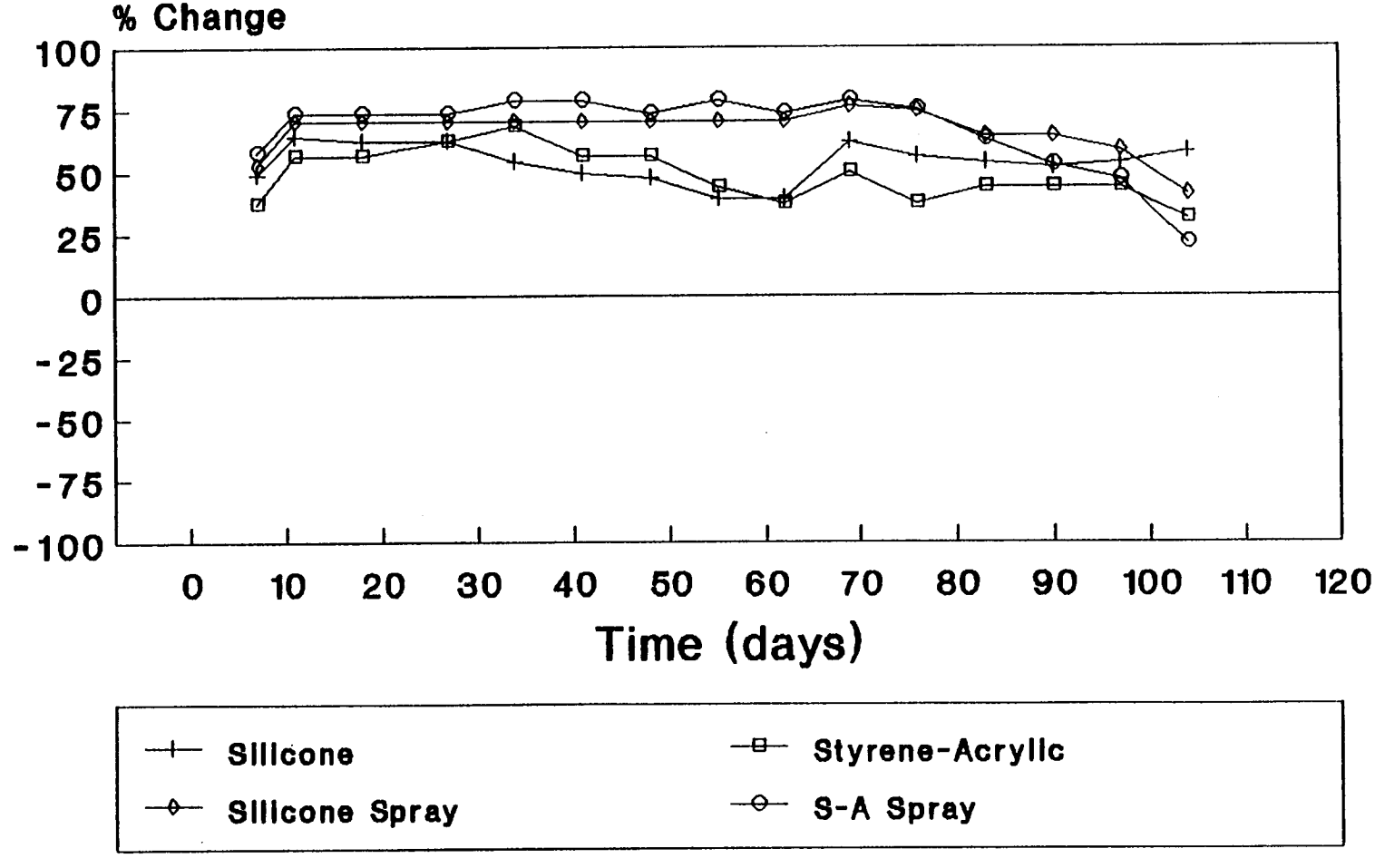

Fig. 19H Post-Treatment Percent Change in Corrosion Rate for DCI Ponded Specimens with Polymer Sealers (B-13, B-14, B-15)

It cannot readily be determined to what degree the polymer sealers play a role in the corrosion abatement process. Since the DCI pond/mortar specimen showed great reduction in both corrosion potential and rate, it is reasonable to expect that the DCI ponding played a major role in the corrosion abatement of the polymer sealer specimens as well. It is possible that the sealers provided an additional physical barrier to chloride ions, moisture, and even oxygen diffusion, which would enhance the effectiveness of the DCI.

The sealers alone probably would not have been effective due to the level of chloride present in the specimens. At the reinforcing steel level, the specimens contained an average of 8.75 lbs Cl^-/yd^3 (5.19 kg/m^3) (see Table 18) of concrete which is more than seven times the accepted level of 1.2 lbs Cl^-/yd^3 (0.71 kg/m^3) needed to initiate corrosion in concrete. Without the DCI to effectively form a passive layer, the reinforcing steels would have still been subjected to this level of chloride underneath the sealant. Since the sealer was only placed in the groove, moisture could still diffuse through the concrete on either side of the groove and around the sealant. The sealers were evaluated in combination with DCI because when used in the field, sealers may be applied in conjunction with an inhibitor treatment.

In comparing the different sealants, no great distinction could be made to determine the most effective between silicone and styrene-acrylic, or between ponding the sealers and spraying them. The spraying of the sealants appeared to be just as effective as applying them through ponding. The advantage to spraying, however, is that it uses less material and takes less time for application.

In the overall evaluation of the DCI-treated specimens, treatment through a combination of ponding and backfilling with treated mortar exhibited the greatest effectiveness in reducing corrosion. Such a treatment provides a sufficient NO_2^-/Cl^- ratio to suppress the anodic reaction and increase the stability of the passive film. The application of sealers may aid in the reduction of corrosion in combination with DCI, but the degree to which they affect the corrosion process could not be determined.

Borate Treatments

The three specimens treated solely with borate-based inhibitors were:

1. B-6, treated with sodium tetraborate placed in the mortar (SB Mortar).

2. B-7, treated with sodium tetraborate ponding and placed in the mortar (SB Pond/Mortar)

3. B-8, treated with zinc borate ponding and placed in the mortar (ZB Pond/Mortar).

The post-treatment corrosion potentials and corrosion rates for each specimen are shown in Figures 20A thru 20D.

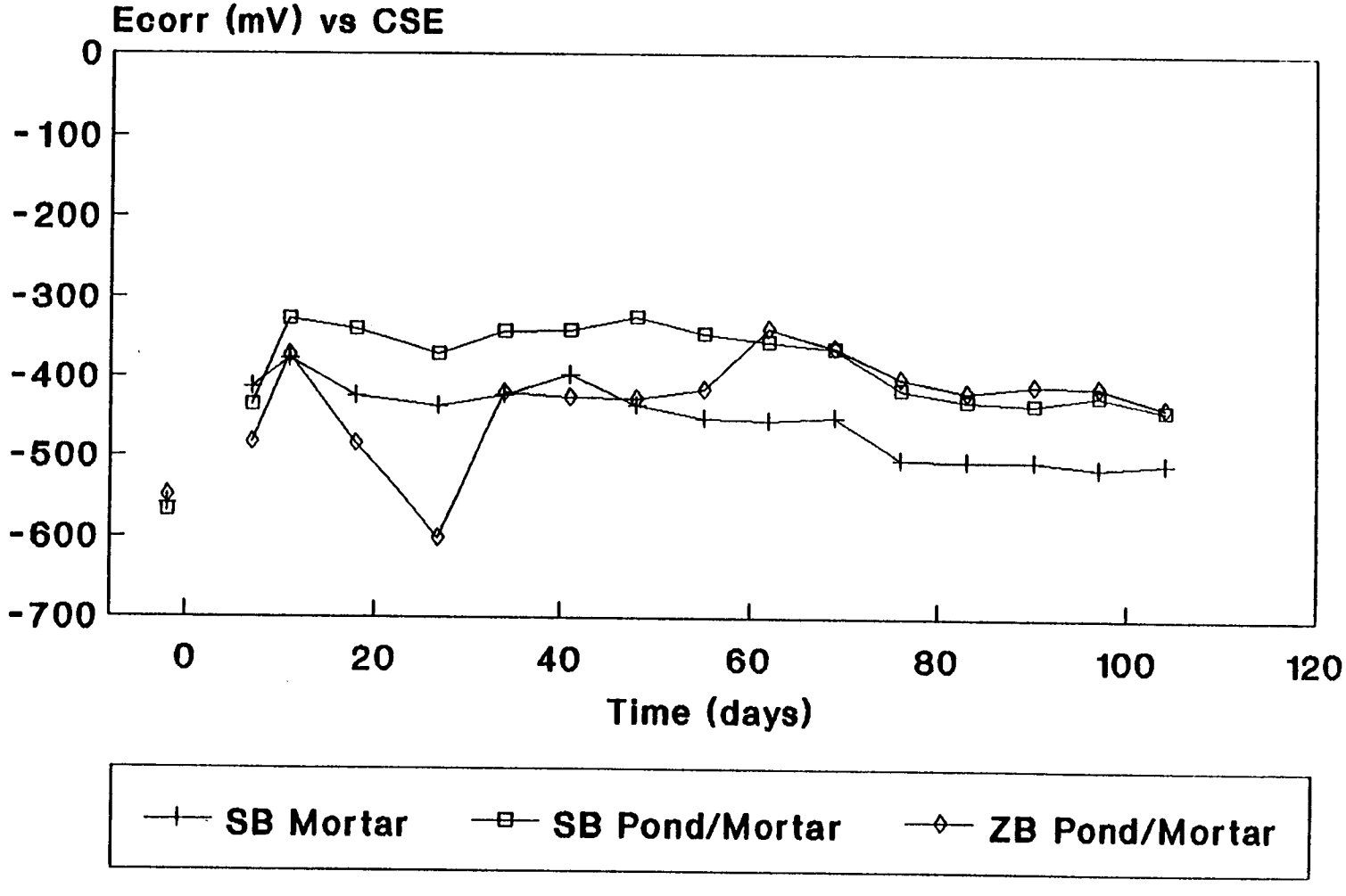

Fig. 20A Mean Half-Cell Potentials for Borate Treated Specimens (B-6, B-7, B-8)

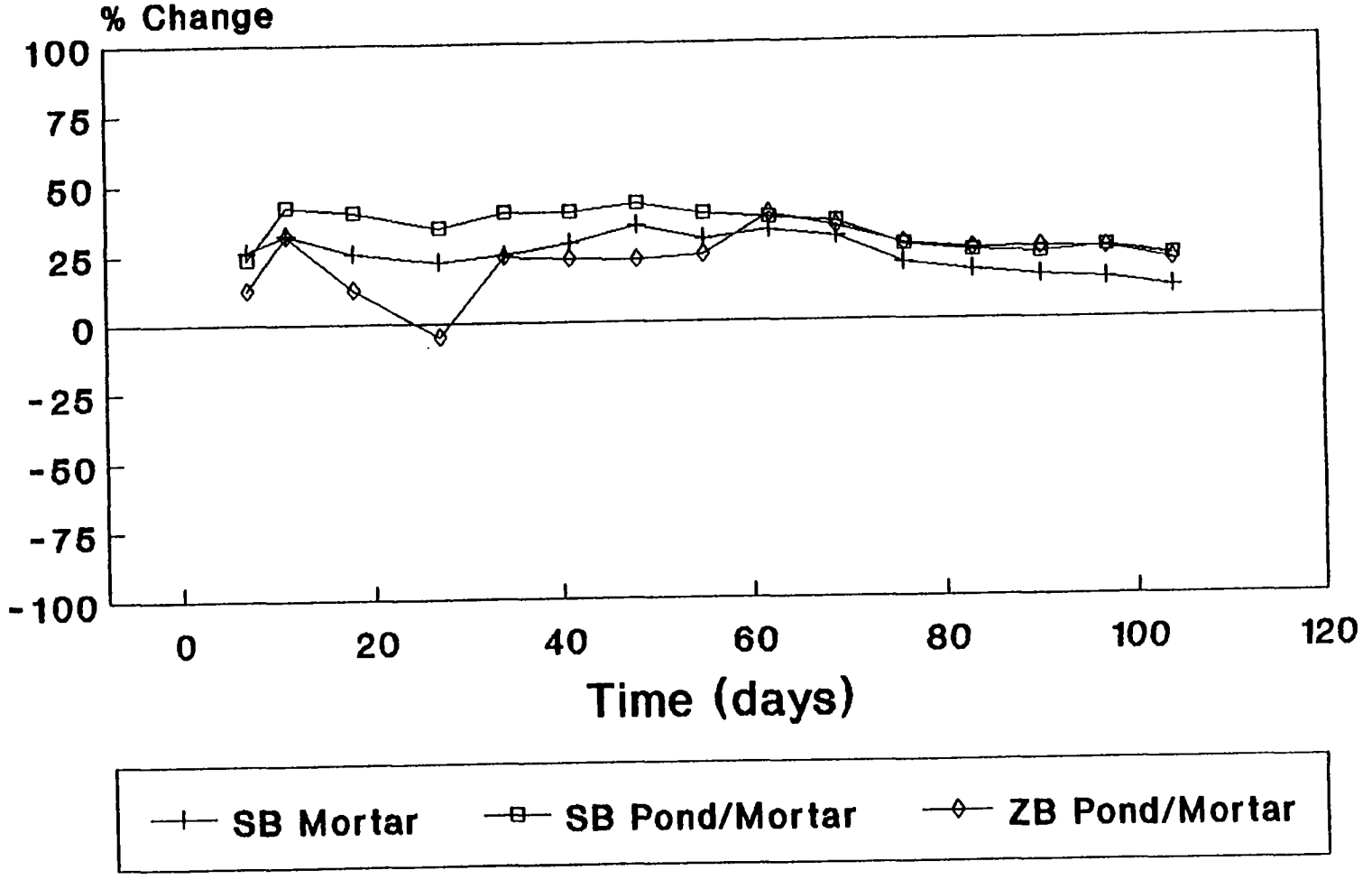

Fig. 20B Post-Treatment Percent Change in Half-Cell Potential for Borate Treated Specimens (B-6, B-7, B-8)

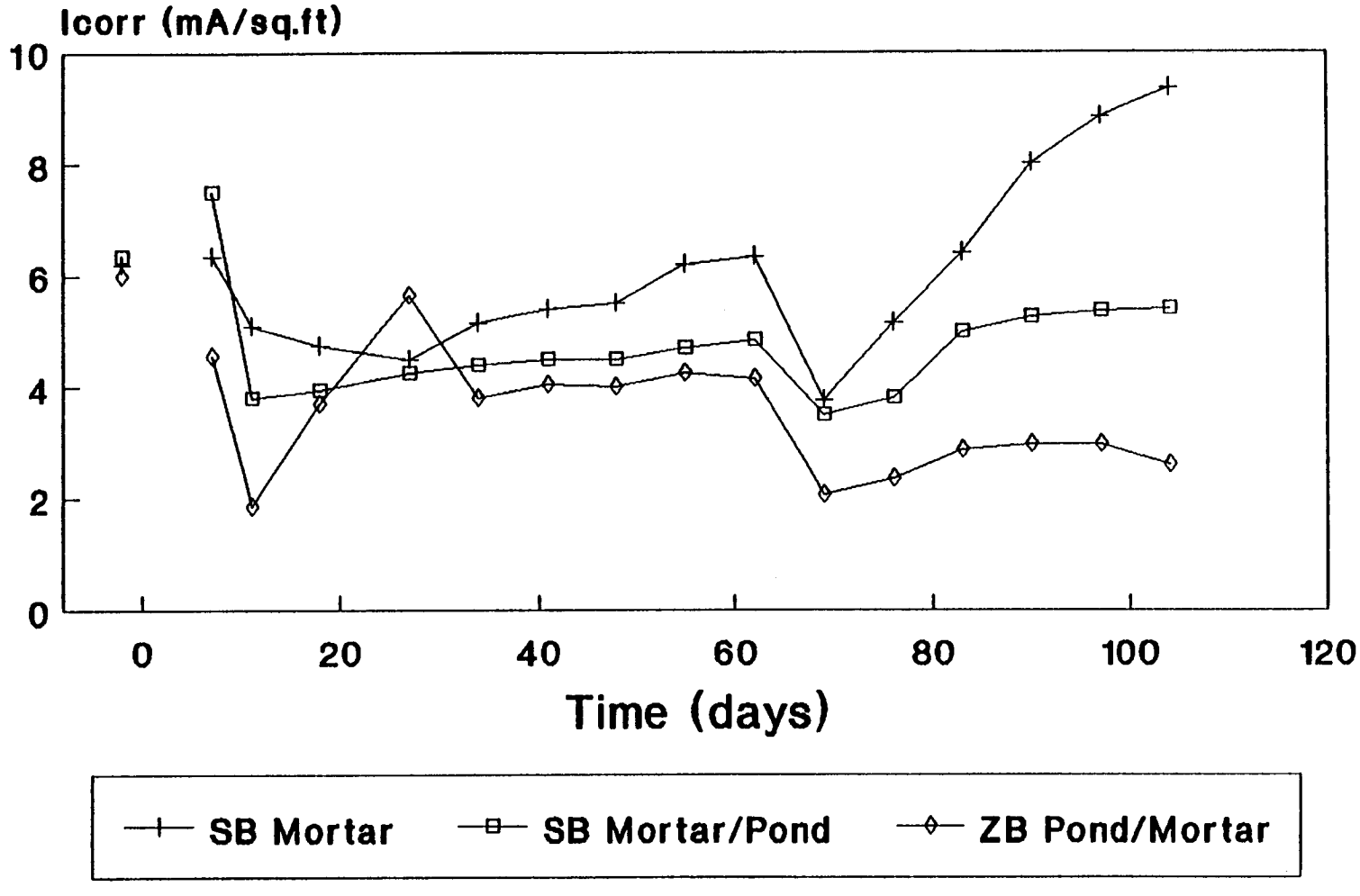

Fig. 20C Mean Corrosion Rates for Borate Treated Specimens (B-6, B-7, B-8)

NOTE: 1.0 mA/ft^2 = 1.08 μA/cm^2

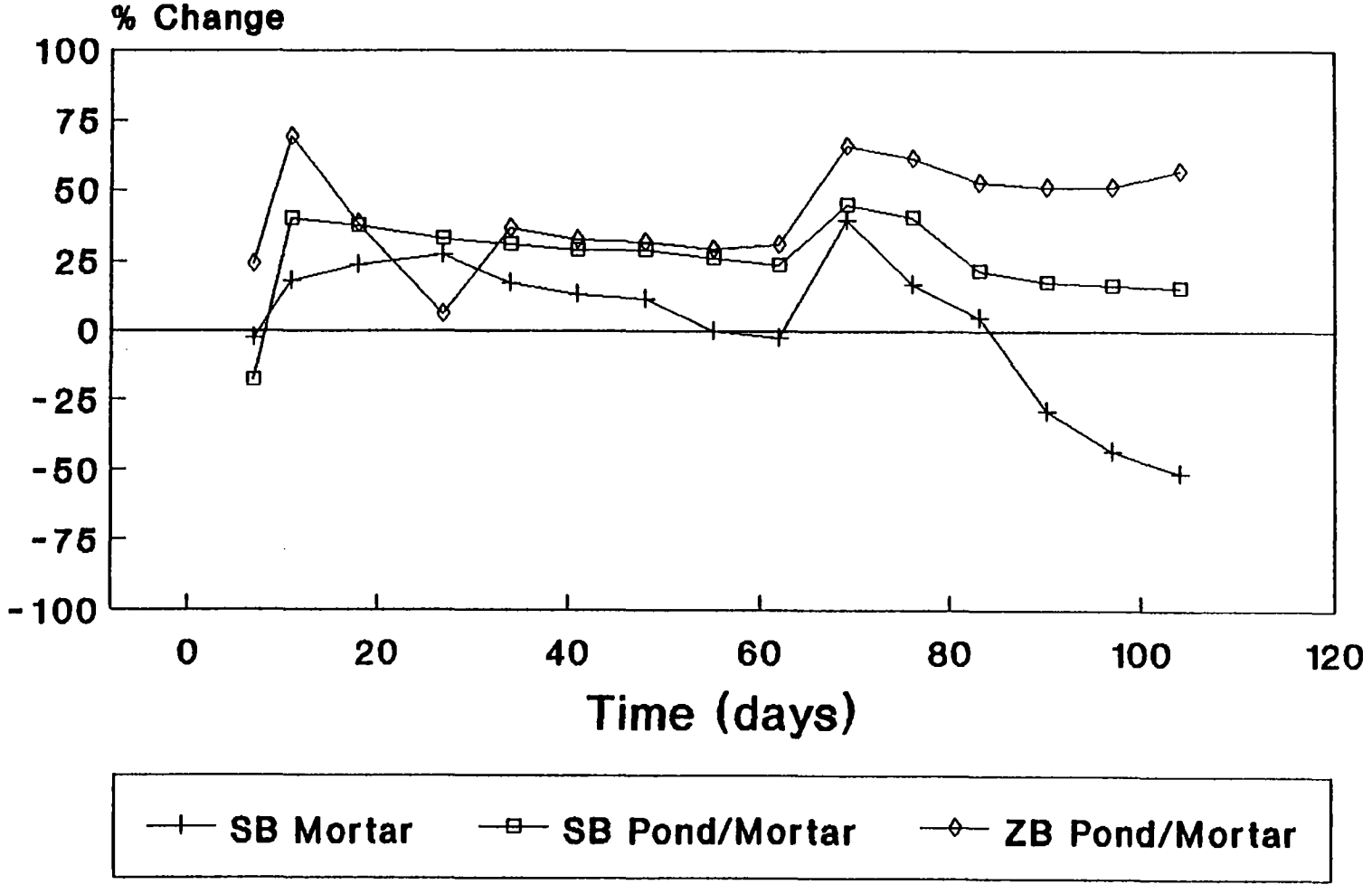

Fig. 20D Post-Treatment Percent Change in Corrosion Rate for Borate Treated Specimens (B-6, B-7, B-8)

All 3 treatments seemed to have had a similar effect on the evolution of E_{corr} for each specimen. More than a 25% increase in potential was experienced by all three specimens for the majority of the exposure duration. The final values were all greater than the pre-treatment values.

A better comparison between the treatments can be made on the basis of the corrosion rates. The SB mortar specimen displayed the least effect of its treatment with a small decrease in corrosion rate between days 10 and 30, with an eventual 50% increase. Both the SB pond/mortar and ZB pond/mortar specimens showed an average 30% reduction in corrosion rate between days 20 and 60. At longer exposure duration the zinc borate treated specimen experienced an actual further decrease in corrosion rate exceeding 50%.

The borate treatments appeared to be effective for a longer duration when applied both as a ponding and in the mortar when simply just added to the mortar. The additional concentration of borate provided via diffusion through the mortar appears to be adequate to extend the time of corrosion abatement. Of the treatments, both the SB and ZB pond/mortar treatments performed equally well initially, but the zinc borate specimen outperformed the SB at the later stages of exposure. This difference in behavior may be related to the rate of diffusion of the inhibitors through mortar. The zinc borate may have a higher rate of diffusion which allows it to better maintain a sufficient concentration at the reinforcing steel surface to stem corrosion.

In the borate-treated specimens involving both ponding and placement in mortar, the concentration of borate at the reinforcing steel level was sufficient to allow the formation of a corrosion inhibiting coating which served as a barrier to increased metal dissolution.

TCI Treatment

The treatment of specimen B-4 with a TCI (sodium monofluorophosphate) ponding appeared to be effective based on corrosion potentials as shown in Fig. 21A. The corrosion potentials remained more noble than the pre-treatment value for the entire exposure period. However, the corrosion rate measurements shown in Fig. 21B, show an example of how E_{corr} measurements can be misleading. The specimen experienced only a slight decrease in corrosion rate for 25 days before it began to increase and exceed the pre-treatment corrosion rate. TCI inhibitor functions as a diffusional inhibitor; however, it does not appear as though it effectively diffused into the concrete surrounding the reinforcing steel to provide any substantial inhibition.

The ineffectiveness of TCI may have been a result of a low treatment concentration, but no standard application concentration has been developed except in conjunction with surface application of de-icing salts (2.5% s/s salt). The concentration used, however, appeared to be high enough to stabilize the corrosion rate between days 35 and 70 at its pre-treatment I_{corr} level before deteriorating. Increased treatment concentrations may yield better results.

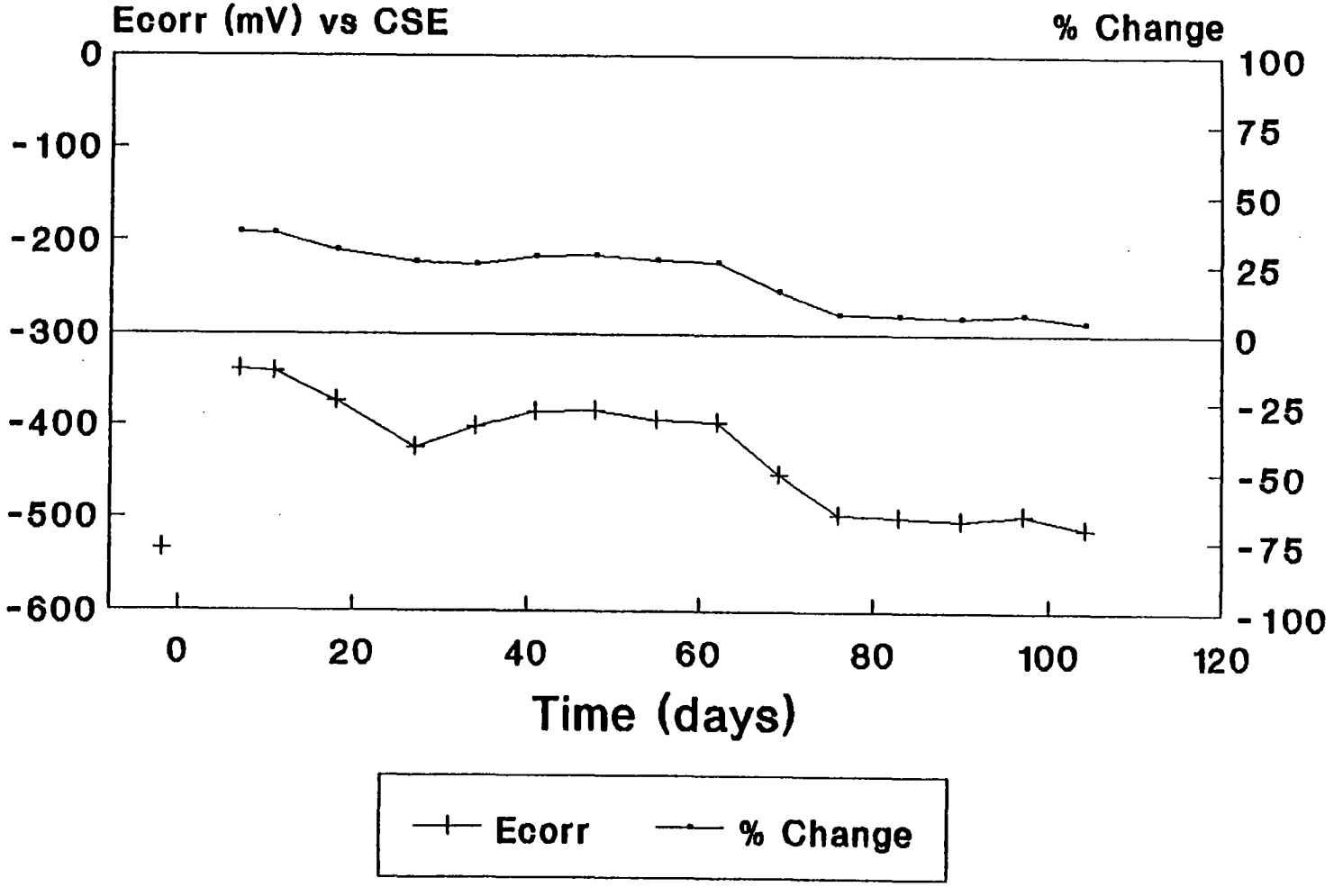

Fig. 21A TCI Ponding Specimen (B-4) Mean Half-Cell Potentials and Post-Treatment Percent Change

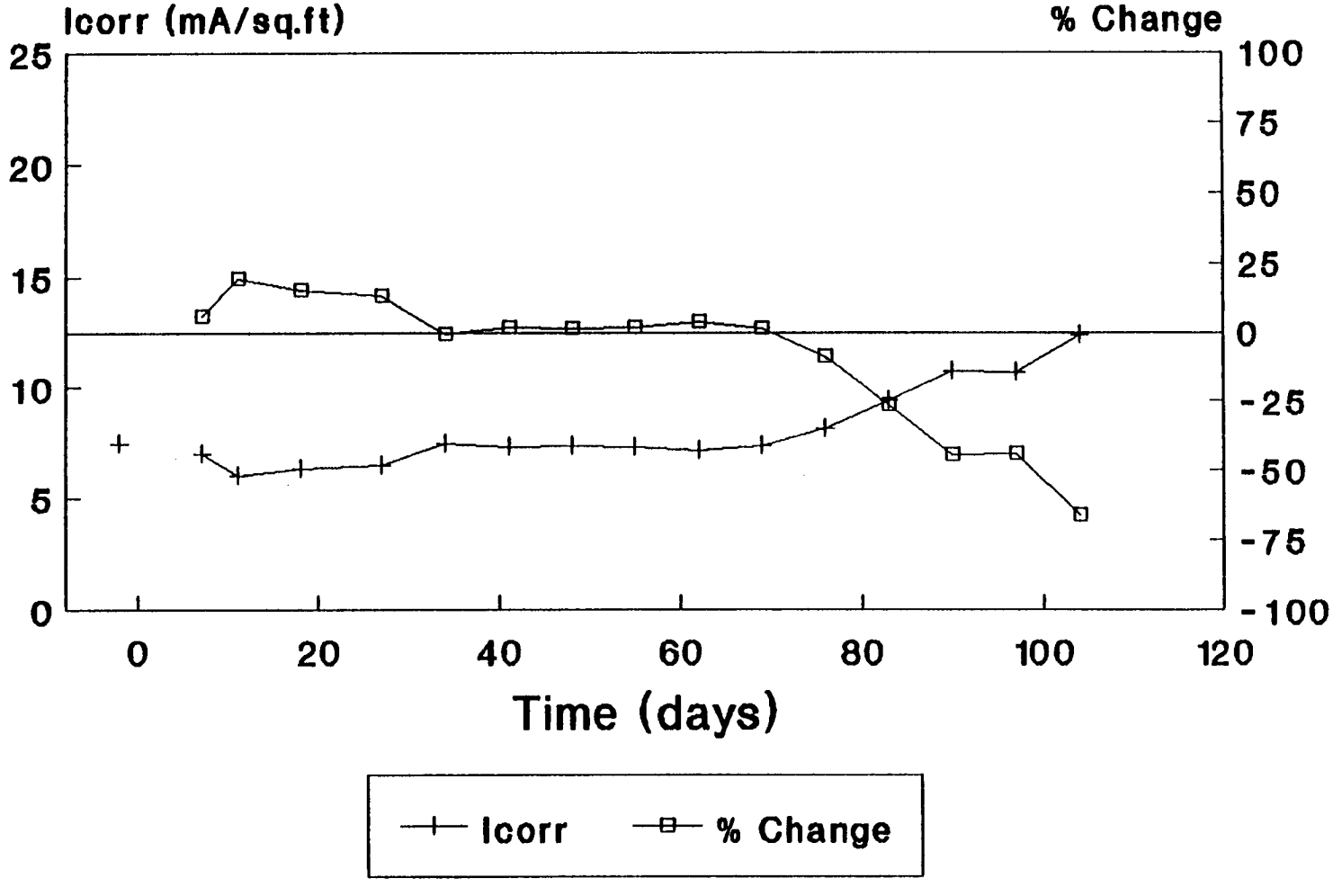

Fig. 21B TCI Ponding Specimen (B-4) Mean Corrosion Rates and Post-Treatment Percent Change

Alox 901 Treatment

The performance of the Alox 901 treatment appeared promising as a possible corrosion inhibitor in concrete. The I_{corr} and E_{corr} measurements shown in Figures 22A and 22B indicate that the treatment was able to keep the corrosion activity from increasing from its initial state for the entire exposure duration. After day 10, the Alox treatment provided an average 40% reduction in corrosion rate for a span of 70 days before decreasing to 9% at day 104.

Although the corrosion rate began to increase over the last 20 days, this is not necessarily a sign of an inhibitor with only a short-term effect. Alox 901 is primarily used as a coating for metallic components exposed to corrosive environments. As a result, it is an extremely viscous liquid which aids in its adhesion to surfaces. In this study, the Alox 901 was dissolved in an ethyl alcohol solvent for ponding because it emulsifies in water. Since there is no known concentration standard for concrete, an equivalent .1M alcohol solution was made for comparison with the other .1M ponding solutions. Therefore, the Alox 901 concentration may not have been the optimum for concrete applications.

The viscous and oily properties of Alox 901 may have caused poor adhesion between the groove and backfilled mortar interface. This could have contributed to the accelerated diffusion of chlorides along this interface, possibly reducing the inhibitor's effectiveness.

Cortec Inhibitor Treatments

The Cortec vapor phase inhibitors were used in several combinations and showed highly effective results both short-term and long term as displayed in Figures 23A through 23D. Two treatments were applied to specimens of Set A (A-13, A-15) which were highly corroded and exhibiting high corrosion rates, while a third treatment was applied to a specimen of Set B (B-16) with an extremely small corrosion rate.

Cortec 1337 is a surface inhibitor while 1609 is used as an admixture. Cortec 1337 was evaluated applied to the surface of a specimen and applied to grooves, while 1609 was evaluated as a possible ponding treatment as well as being put in the mortar. The surface treatment with 1337 and the combination 1337 pond/1609 mortar treatment could only be evaluated for a short period due to the development of cracks in the specimens.

The application of 1337 to a specimen's surface resulted in nearly a 100% reduction in corrosion rate from 23.5 to 0.75 mA/ft^2 (25.3 to 0.81 MA/m^3). However, shrinkage cracks developed during drying after the first ponding cycle. The cracks allowed for the ingress of high concentrations of sodium chloride solution during subsequent pondings. As a result, the performance of the inhibitor as a surface treatment could not adequately be evaluated after 10 days.

The combination of a 1337 ponding and 1609 being admixed into the mortar initially proved

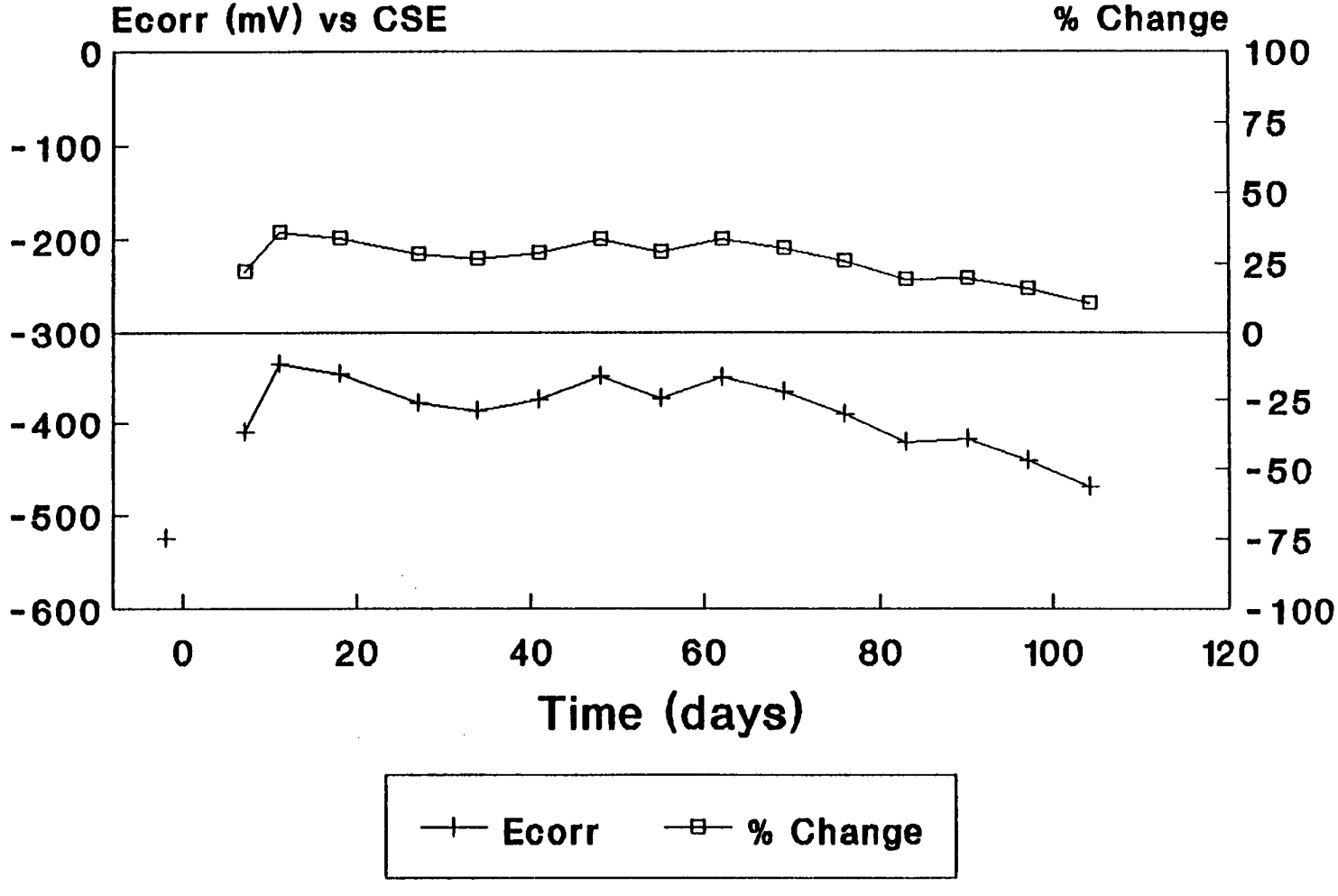

Fig. 22A Alox 901 Ponding Specimen (B-9) Mean Half-Cell Potentials and Post-Treatment Percent Change

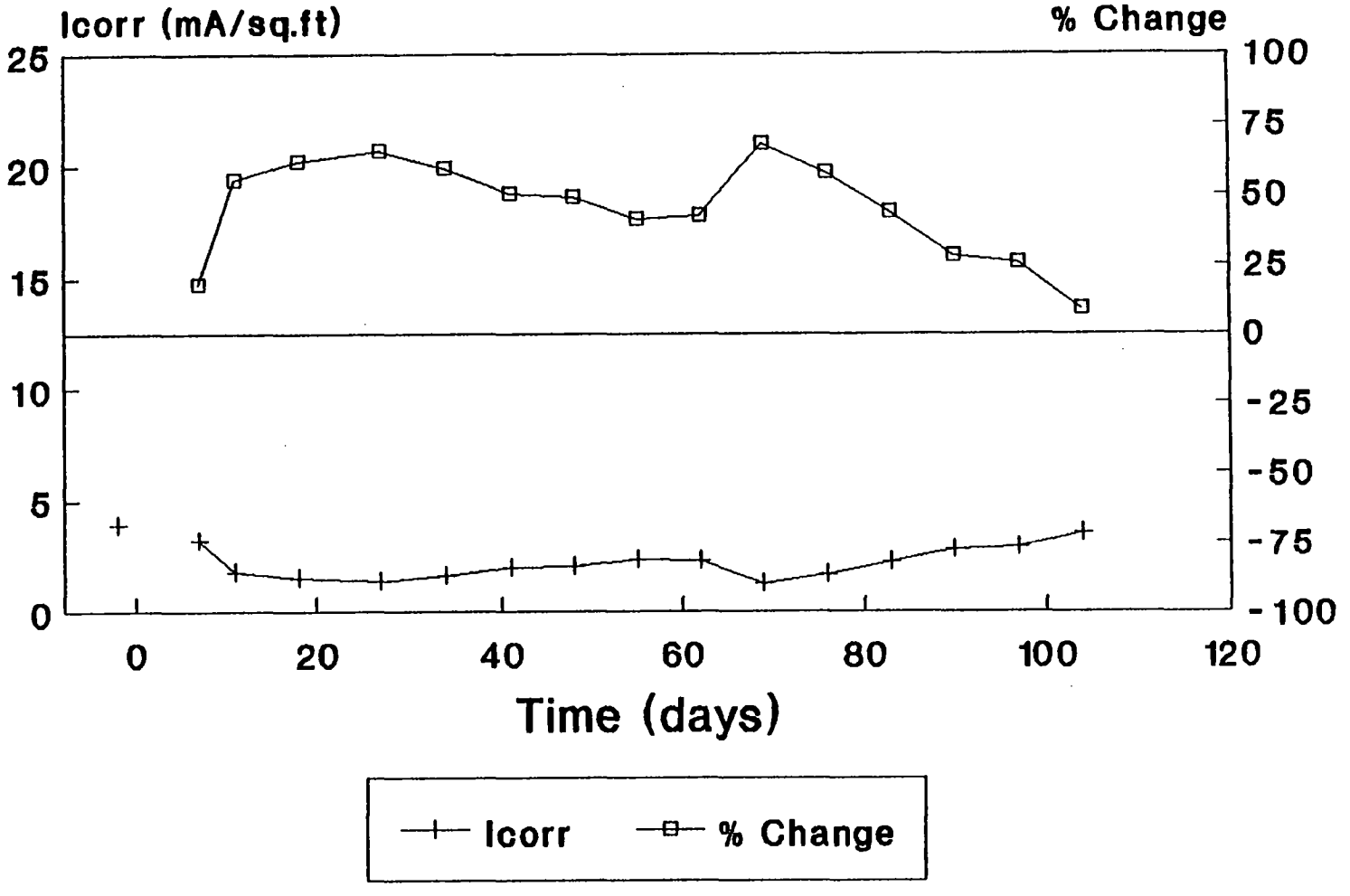

Fig. 22B Alox 901 Ponding Specimen (B-9) Mean Corrosion Rates and Post-Treatment Percent Change

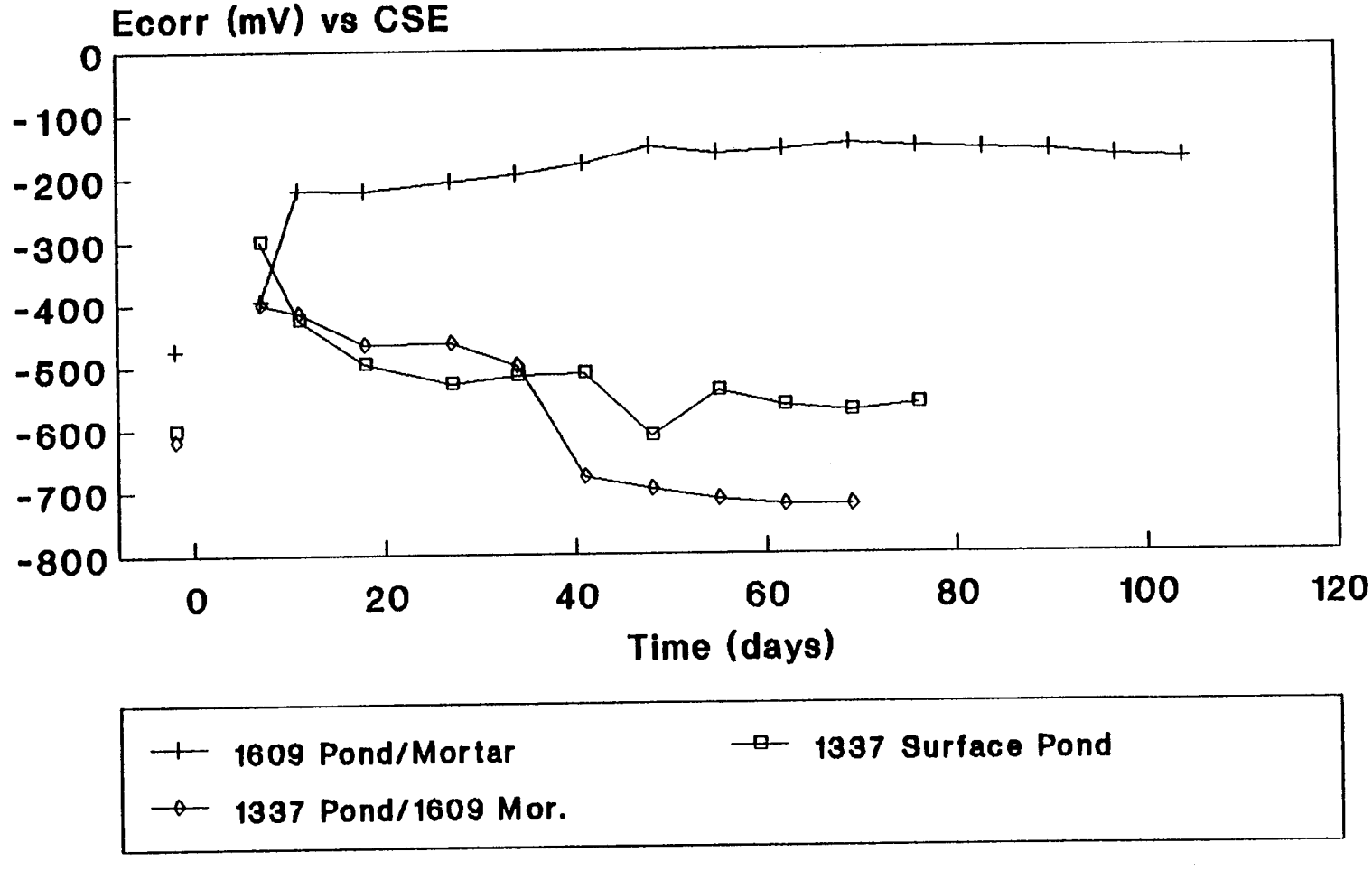

Fig. 23A Mean Half-Cell Potentials for Cortec Inhibitor Treated Specimens (B-16, A-13, A-15)

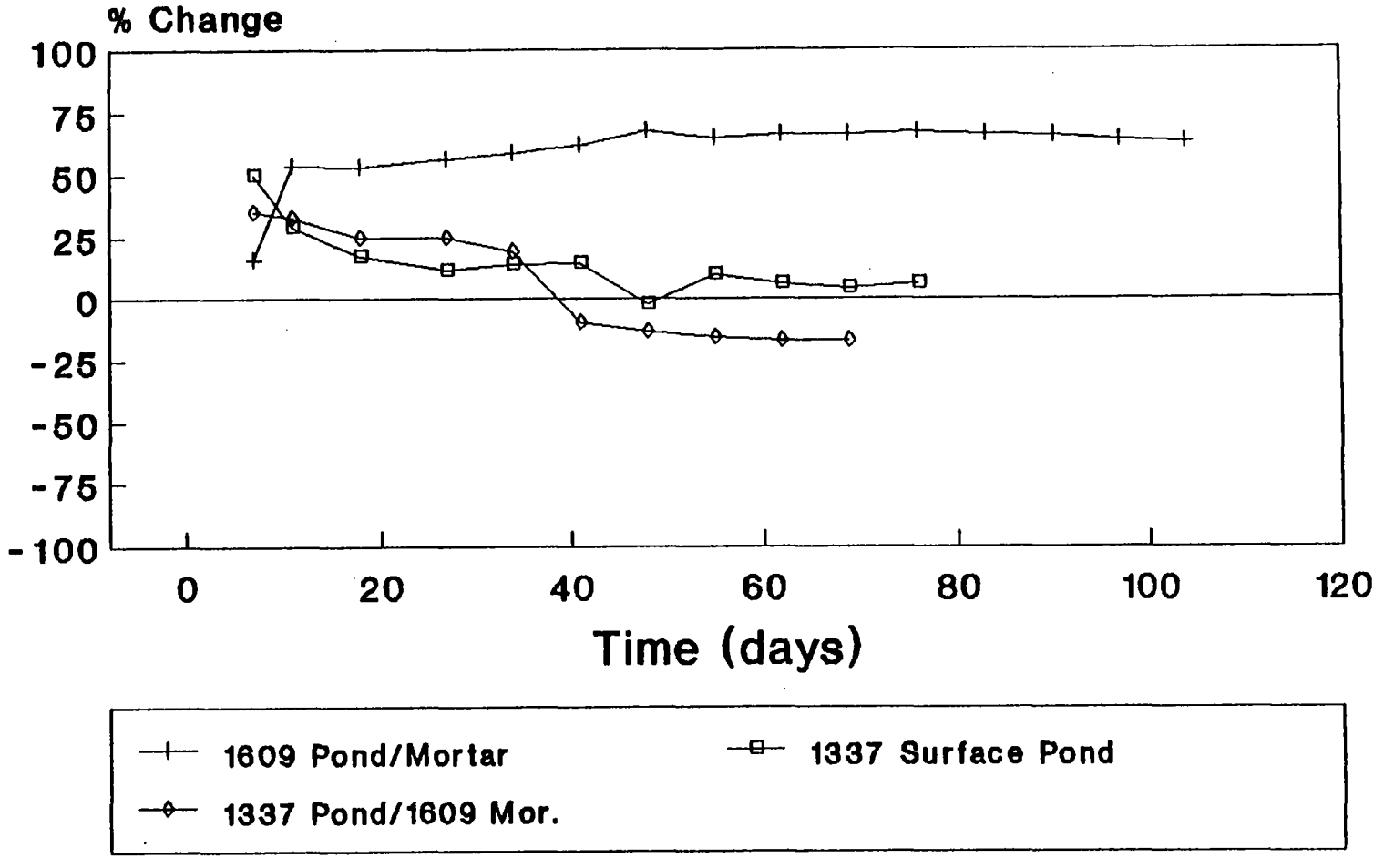

Fig. 23B Post-Treatment Percent Change in Half-Cell Potential for Cortec Inhibitor Treated Specimens (B-16, A-13, A-15)

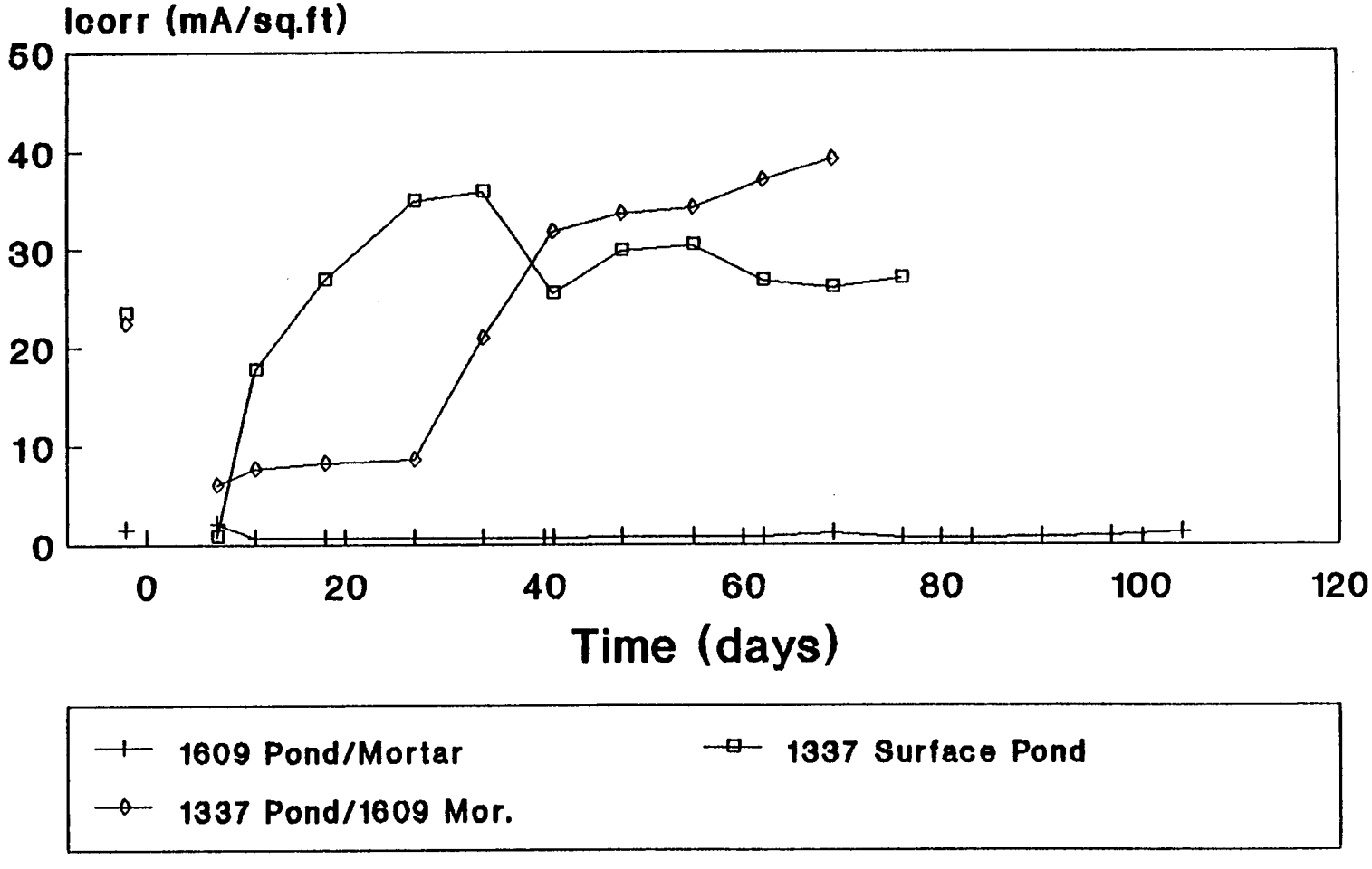

Fig. 23C Mean Corrosion Rates for Cortec Inhibitor Treated Specimens (B-16, A-13, A-15)

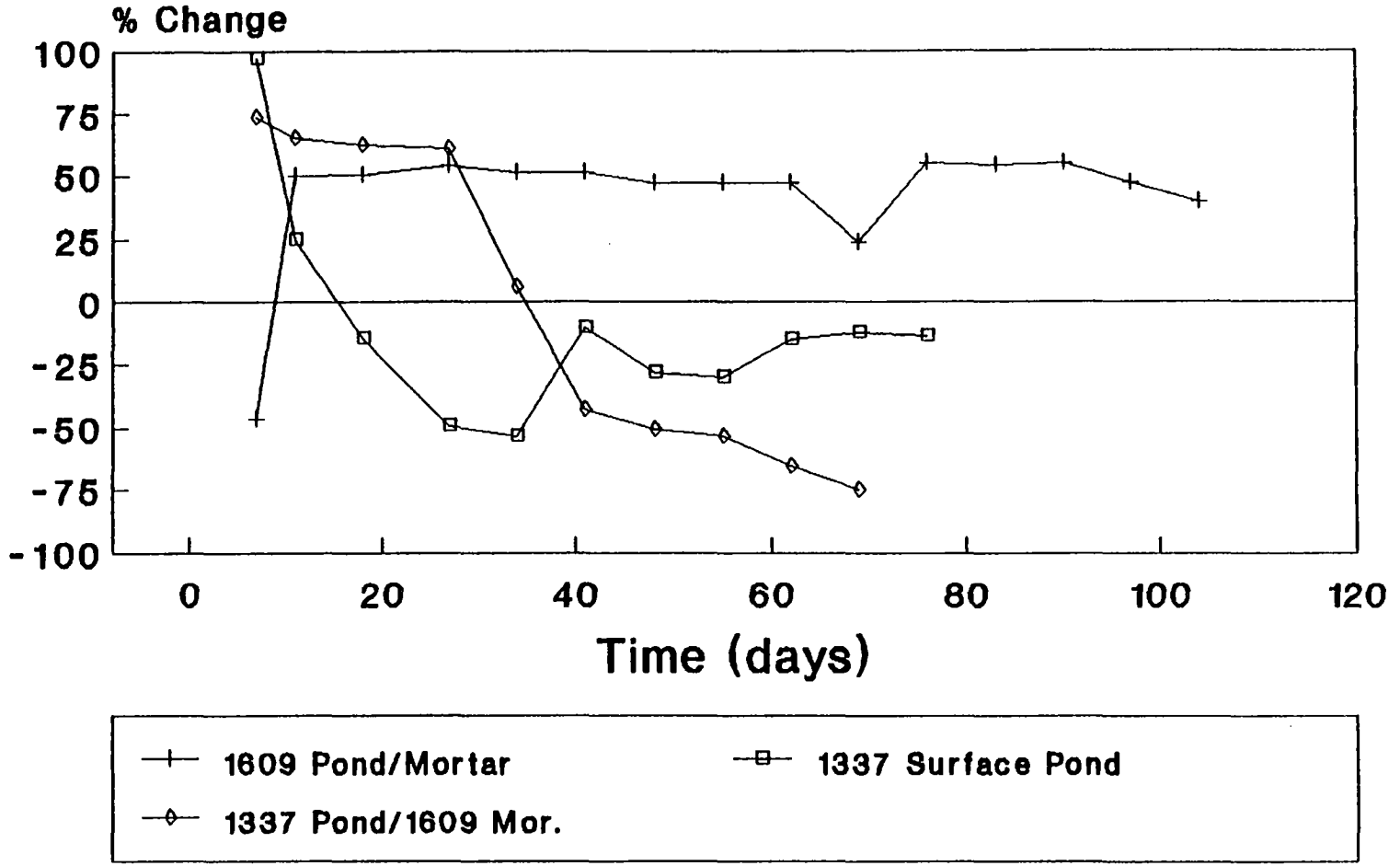

Fig. 23D Post-Treatment Percent Change in Corrosion Rate for Cortec Inhibitor Treated Specimens (B-16, A-13, A-15)

to be a highly effective inhibitor treatment. During the first 30 days of exposure, the treatment resulted in an average I_{corr} decrease of more than 60%. However, the development of shrinkage cracks at the groove/mortar interface over each bar allowed the rapid influx of chlorides and resulted in a rapid increase in corrosion rate.

The use of 1609 as a ponding inhibitor was experimental, but resulted in a stable reduction in both E_{corr} and I_{corr}. The specimen in which 1609 was ponded and placed in mortar had a low pre-treatment corrosion rate of 1.45 mA/ft^2; therefore the magnitude of corrosion reduction was small but the percent change in magnitude was great. It is reasonable to expect better performance because of the low corrosion rate, but the stability of the corrosion rate drop in combination with the large drop in E_{corr} magnitude further supports the treatment's effectiveness.

Over a duration of 104 days, the treatment was able to prevent the corrosion rate from increasing from its low initial value, even though the specimen's chloride concentration was increasing. In addition, the corrosion potential increased (became more noble) more than 60% and remained at this level for the entire exposure duration. No other treatment besides DCI ponding was able to keep the corrosion potentials of a specimen so low for such a duration, regardless of the magnitude of the pre-treatment corrosion rate.

Both Cortec inhibitors appear to be effective corrosion abatement treatments. The ponding of either inhibitor provided adequate reduction in corrosion activity via the vapor phase transport of the inhibitor to the reinforcing steel surface and the resulting formation of a protective monolayer. This monolayer reduced both the anodic and cathodic reaction rates. The long-term effectiveness of 1337 ponding treatments could not be evaluated and the determination of the more effective ponding agent between 1337 and 1609 could not readily be made. However, since 1337 is recommended as a ponding inhibitor by the manufacturer, it is reasonable to expect 1337 to perform better than 1609 when ponded. The degree to which the 1609 admixed in the mortar plays in corrosion abatement could not readily be determined from the treatment combinations.

Hydroxylapatite Treatments

The treatment effects of using hydroxylapatite alone and in combination with inhibitors can be seen in the E_{corr} and I_{corr} measurements shown in Figures 24A through 24D. The admixing of hydroxylapatite (HA Mortar) to the backfilled mortar showed little effect on the corrosion rate of the treated specimen. However, this is not an accurate measure of the mineral's chloride-ion-scavenging ability. The chloride threshold level at the reinforcing steel surface was equivalent to 12.36 lbs Cl^-/yd^3 (see Table 18). Therefore, even with the removal of the grooved concrete, it could be expected that a chloride level sufficient to drive the corrosion process would still exist in the concrete surrounding the unexposed portions of the reinforcing steels. Since hydroxylapatite is insoluble in high pH environments, it has no ability to diffuse to scavenge chloride ions. The only chloride ions that come in contact with hydroxylapatite are those that diffuse through the backfilled mortar.

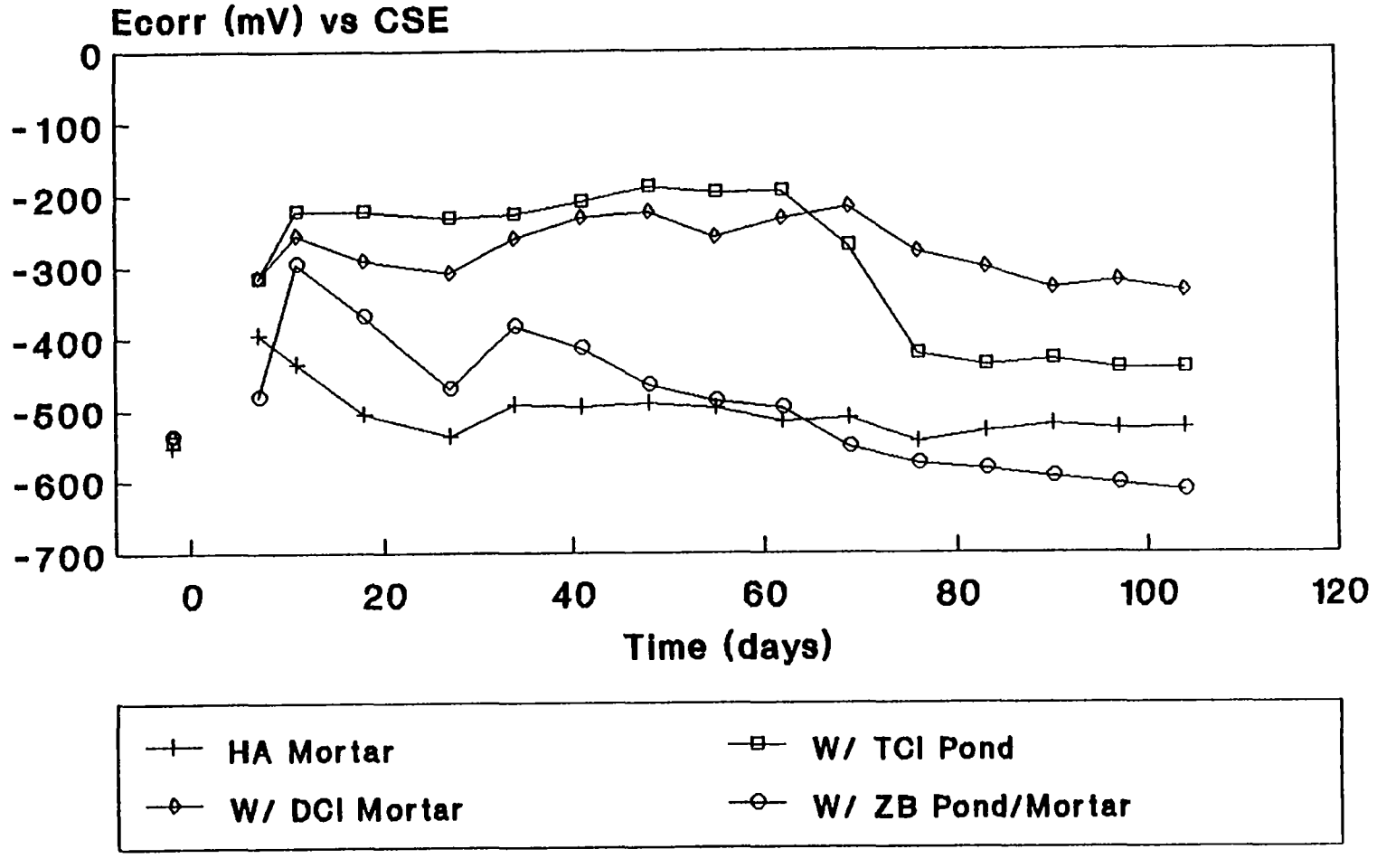

Fig. 24A Mean Half-Cell Potentials for Hydroxylapatite Treated Specimens with Added Inhibitors (B-5, B-10, B-11, B-12)

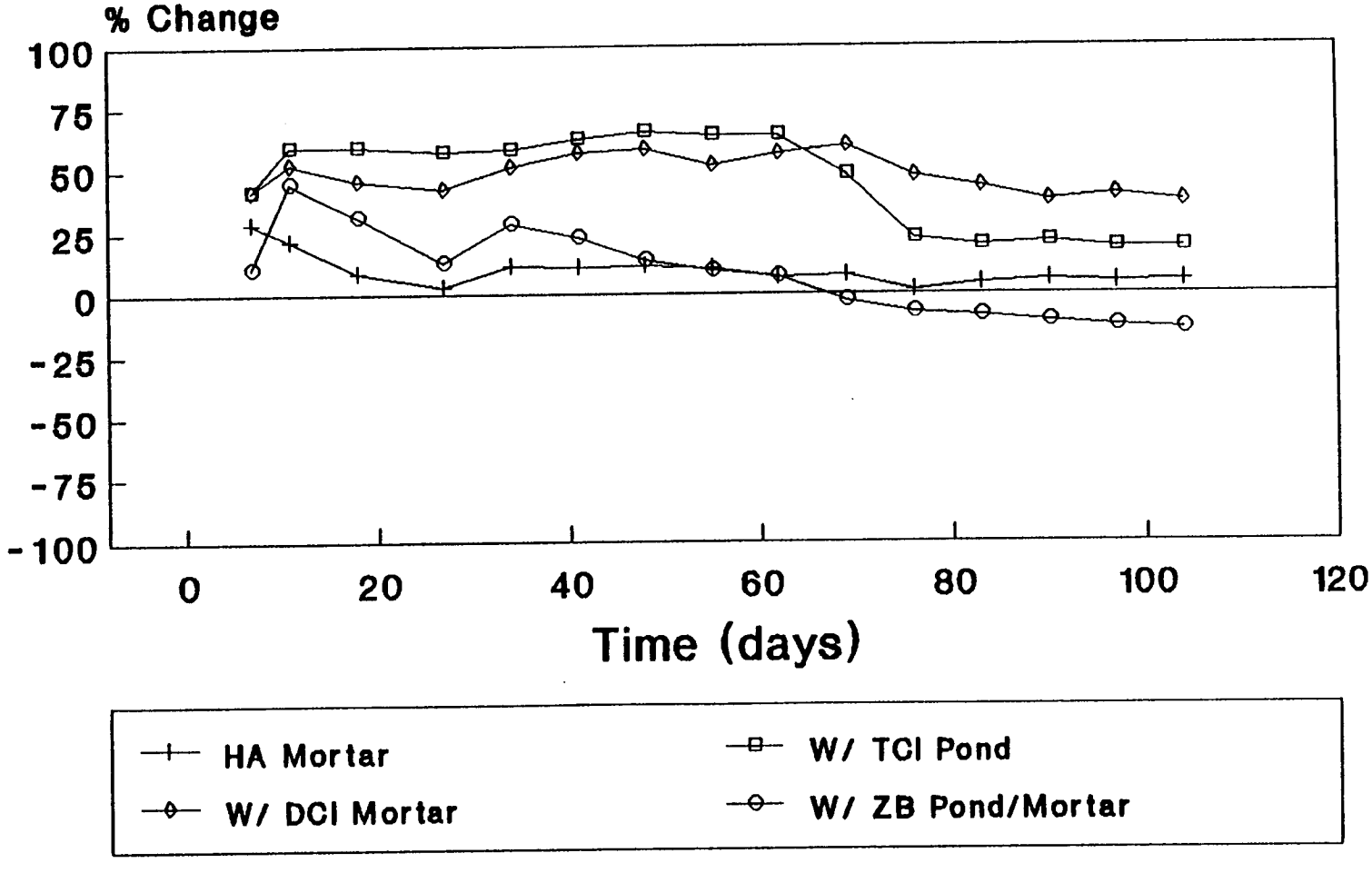

Fig. 24B Post-Treatment Percent Change in Half-Cell Potentials for Hydroxylapatite Treated Specimens with Inhibitor Additions (B-5, B-10, B-11, B-12)

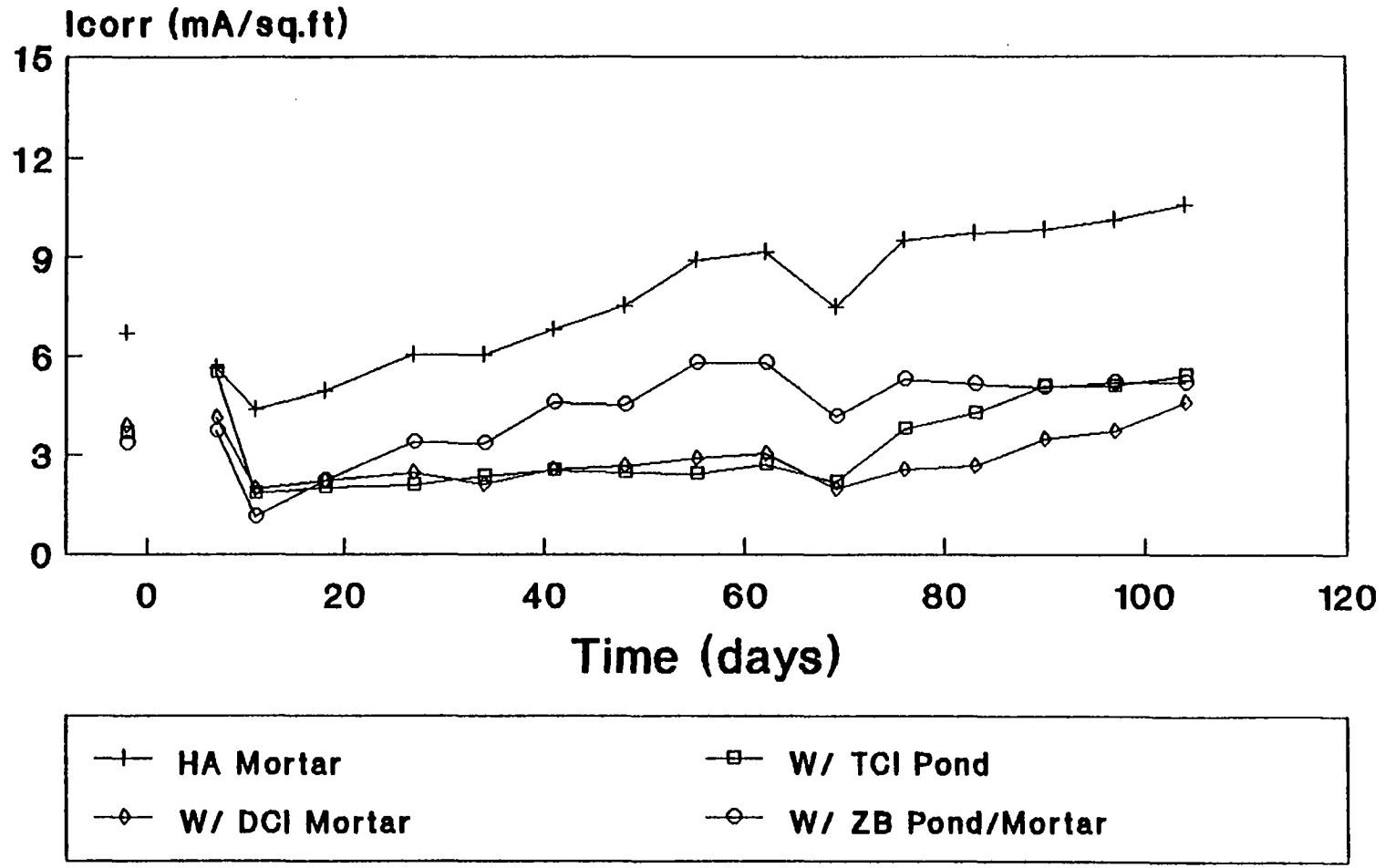

Fig. 24C Mean Corrosion Rates for Hydroxylapatite Treated Specimens with Added Inhibitors (B-5, B-10, B-11, B-12)

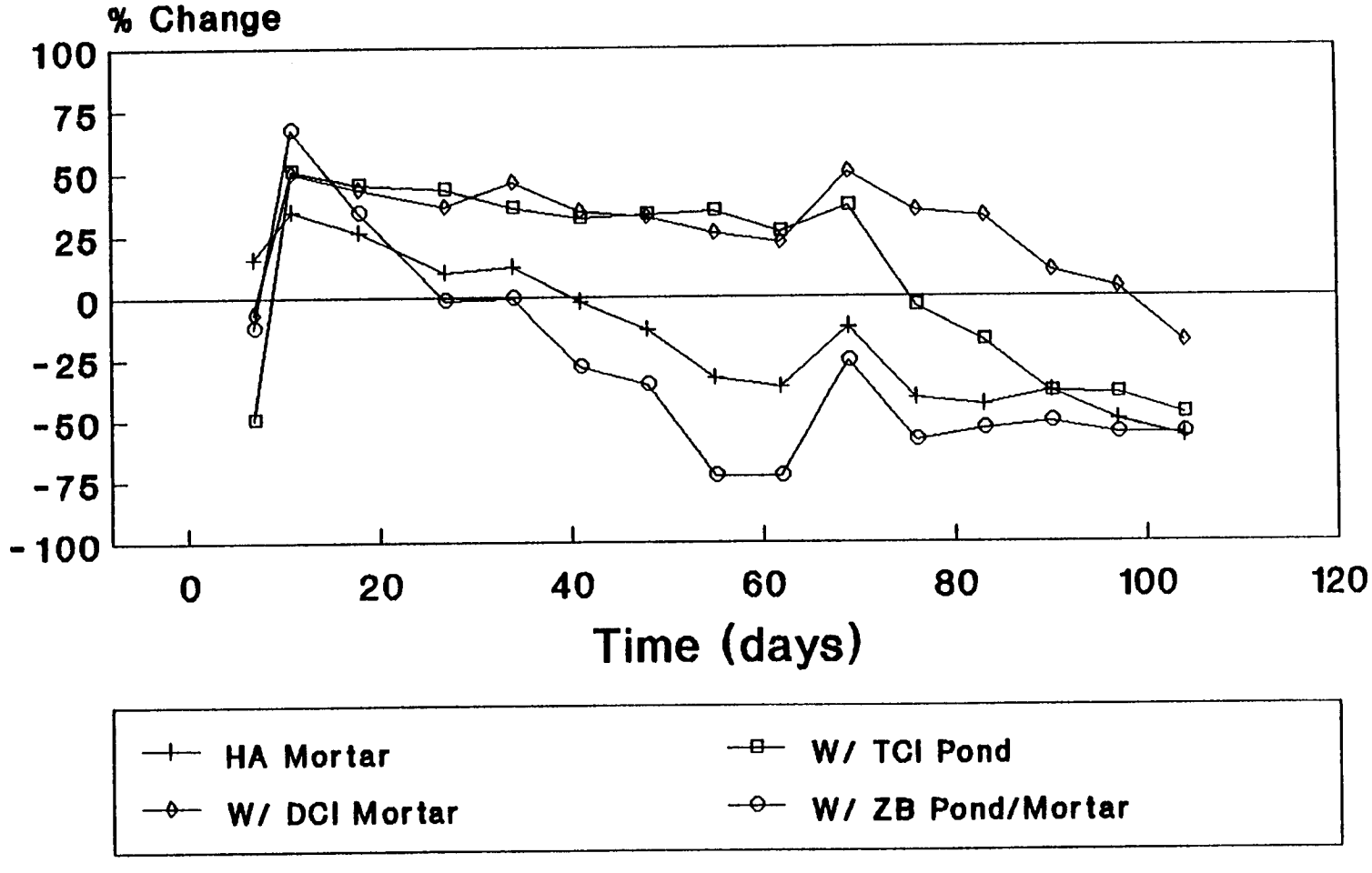

Fig. 24D Post-Treatment Percent Change in Corrosion Rate for Hydroxylapatite Treated Specimens with Inhibitor Additions (B-5, B-10, B-11, B-12)

The use of hydroxylapatite in combination with an inhibitor treatment showed little benefit when used in combination with a zinc borate ponding and mortar admixture. However, when used with TCI ponding or DCI in mortar, there appeared to be some improvement in performance. Both the TCI and DCI specimens with apatite sustained a longer reduction in corrosion rate than the TCI and DCI specimens without apatite. This could possibly be due to chloride scavenging, synergistic effects, or the fact that the apatite specimens with TCI and DCI had pre-treatment corrosion rates lower than the corresponding specimens without apatite. Despite this improvement, the 30-40% reduction in corrosion rate for both specimens lasted only for a duration of 60 days before increasing to rates higher than pre-treatment.

Hydroxylapatite does not appear to be an effective treatment in itself after removal of chloride contaminated concrete.

Selection of Most Effective Treatments

In determining the most effective corrosion abatement treatments based solely on corrosion measurements, the treatments were evaluated in terms of greatest % improvement in I_{corr}, I_{corr} improvement at selected days during exposure, and length of I_{corr} improvement. The comparison of the best treatment or treatments from each experimental group is detailed in Table 20.

All the following treatments have indicated effectiveness in abating corrosion based on electrochemical measurements and are possible candidates for reinforced concrete treatment after removal of chloride contaminated concrete:

1. DCI ponding and in mortar
2. Alox 901 ponding
3. Cortec 1337 ponding and Cortec 1609 in mortar
4. Cortec 1609 ponding and Cortec 1609 in mortar
5. Zinc borate or sodium tetraborate ponding and in mortar

Of the above treatments, DCI showed the greatest effectiveness based on the level in which a high pre-treatment corrosion rate was reduced and the duration of its effectiveness. The borate based treatments also proved effective for the same duration but at an average corrosion rate reduction of 30-40% compared to DCI's 50-60%. The other three treatments appeared effective, but due to a low pre-treatment corrosion rate or the formation of cracks, their electrochemical data is not as well defined as for the DCI and borate treatments.

Mortar Strength and Resistivity Evaluation

Mortar cube strength and resistivity was evaluated to determine any deleterious effects that

Table 20. Treatment effectiveness comparison measures

Treatment	Percent Change in I_{corr}				Final I_{corr} < Pre-Treatment I_{corr} ?
	Greatest	Day 11	Day 55	Day 104	
DCI pond/mortar	71.7	67.8	63.3	65.5	Yes
TCI pond	19.4	19.4	2.0	-66.2	No
Zinc Borate pond/ mortar	69.2	69.2	29.5	57.0	Yes
Sodium Borate pond/mortar	40.6	40.1	25.9	15.3	Yes
Alox 901 pond	65.4	55.2	41.3	9.0	Yes
Hydroxylapatite w/ DCI mortar	50.0	50.0	25.7	-18.0	No
Cortec 1609 pond/ 1609 mortar	55.1	49.8	47.4	39.7	Yes
Cortec 1337 pond/1609 mortar	74.0	65.5	-53.7	-75.0	No[1]

[1]Cracks formed in specimen allowing chloride ingress, therfore, values at days 55 and 104 are not representative of treatment corrosion abatement.

treatments or level of treatments may have on cement mortar properties. The compressive strength measurements would indicate hydration retarding or accelerating properties of the treatments used as admixtures. The resistivity would also indicate retardation or acceleration of set based on the fact that resistivity is a function of permeability which increases with higher degrees of hydration. In addition, the resistivity measurements could possibly detect the contribution of ionic species to the mortar which may contribute to increased current flow. An increase in the ability of current to flow through the mortar would increase the rate of corrosion of reinforcing steel embedded in the mortar.

Treatment Effects on Mortar Compressive Strength

Compressive strength measurements taken over a span of 20 days indicated little difference in strength between the control group and those cubes treated with Cortec 1609 or hydroxylapatite. Fig. 25 presents a comparison of the control cube strengths with the strengths of the cubes containing the highest concentrations of Cortec 1609 (0.45% l/s cement) and hydroxylapatite (25.00% s/s cement). There was also no observed effect of the concentration level within the Cortec 1609 and hydroxylapatite specimens. The compressive strength data for all the cubes are tabulated in Appendix C, Table C-6.

DCI (calcium nitrite) is a known set accelerator and, at low concentrations, can increase the compressive strength of concrete [24]. This is evident in Fig. 26 which compares the control group strength with those of the different DCI concentration groups. For every DCI concentration, the mortar strength was greater than the untreated control cubes and the difference in magnitude increased with increased curing time. At 20 days, each DCI concentration had increased the mortar strength by more than 20% over untreated mortar. Strength increase was also a function of increasing DCI concentration. It should be noted that a small amount of set retarder was added to the 5% and 10% DCI concentration cubes to combat rapid setting.

The calcium nitrite and small amounts of calcium nitrate in DCI serve as an accelerating admixture. The presence of the strong NO_2^- anion in DCI tends to accelerate the solubility of calcium ions from the cement compounds, resulting in more calcium ions to participate in the aluminate and silicate hydration reactions. An increase in the hydration rate of the cement translates into higher compressive strengths in shorter time. However, long-term strengths may be sacrificed because accelerated hydration produces hydration products of larger particle size which have less strength than smaller particles of a slower hydration process.

Unlike calcium nitrite, both borate based inhibitors exhibited set retarding properties as seen in Figs. 27 and 28. Sodium tetraborate so heavily retarded the set of the mortar that cubes of 2.0% s/s cement concentration did not have sufficient set strength at 24 hours to be removed from their molds. Even the 0.5% and 1.0% concentration showed heavy retardation as their compressive strengths were 75% and 96% lower than the control group strength after one day. The 0.5% concentration cubes reduced the strength difference in

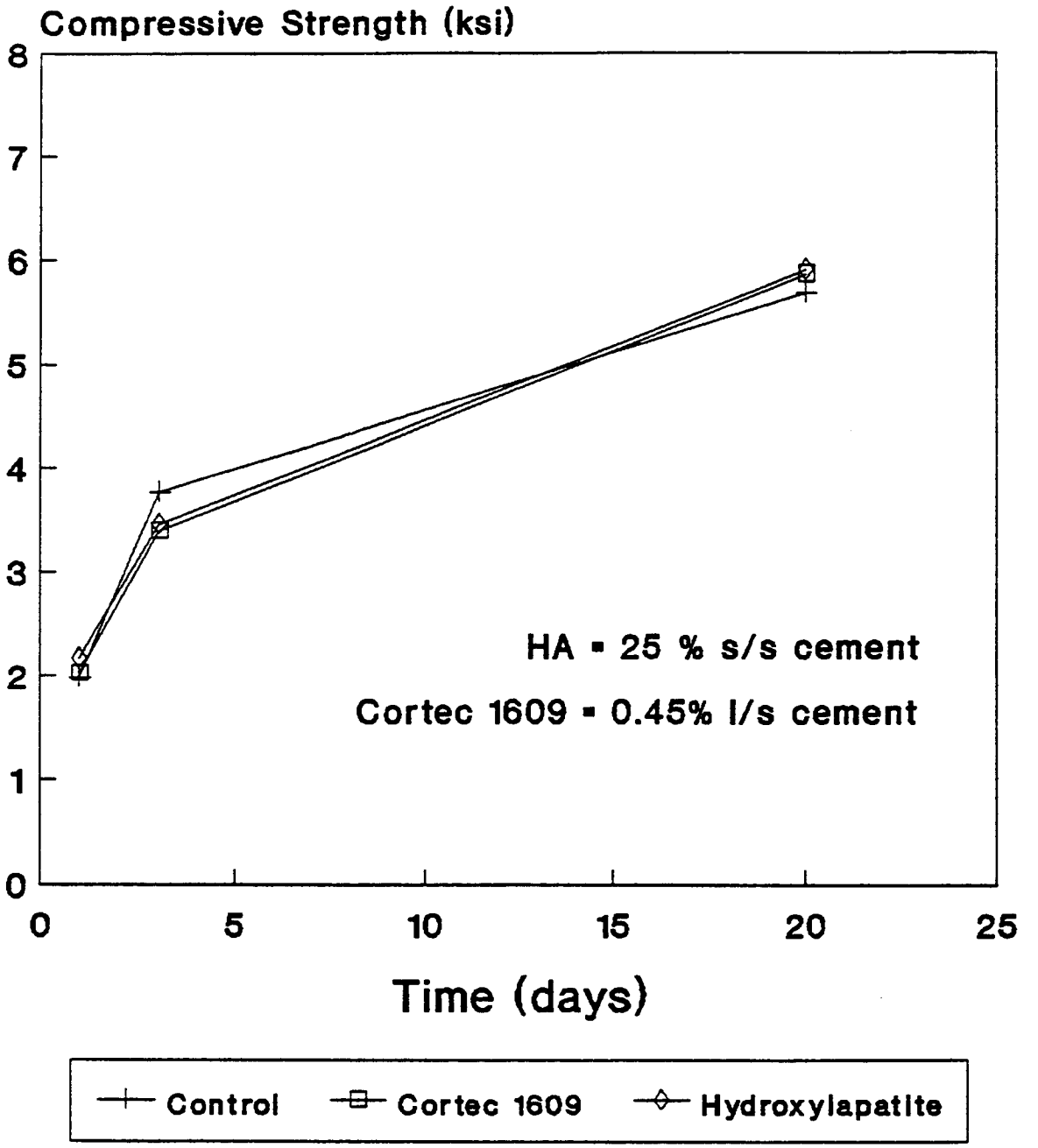

Fig. 25 Mortar Cube Strength vs Time for Highest Concentration Cortec 1609 (0.15%) and Hydroxylapatite (25%) Cubes

NOTE: 1 ksi = 6.895 MPa

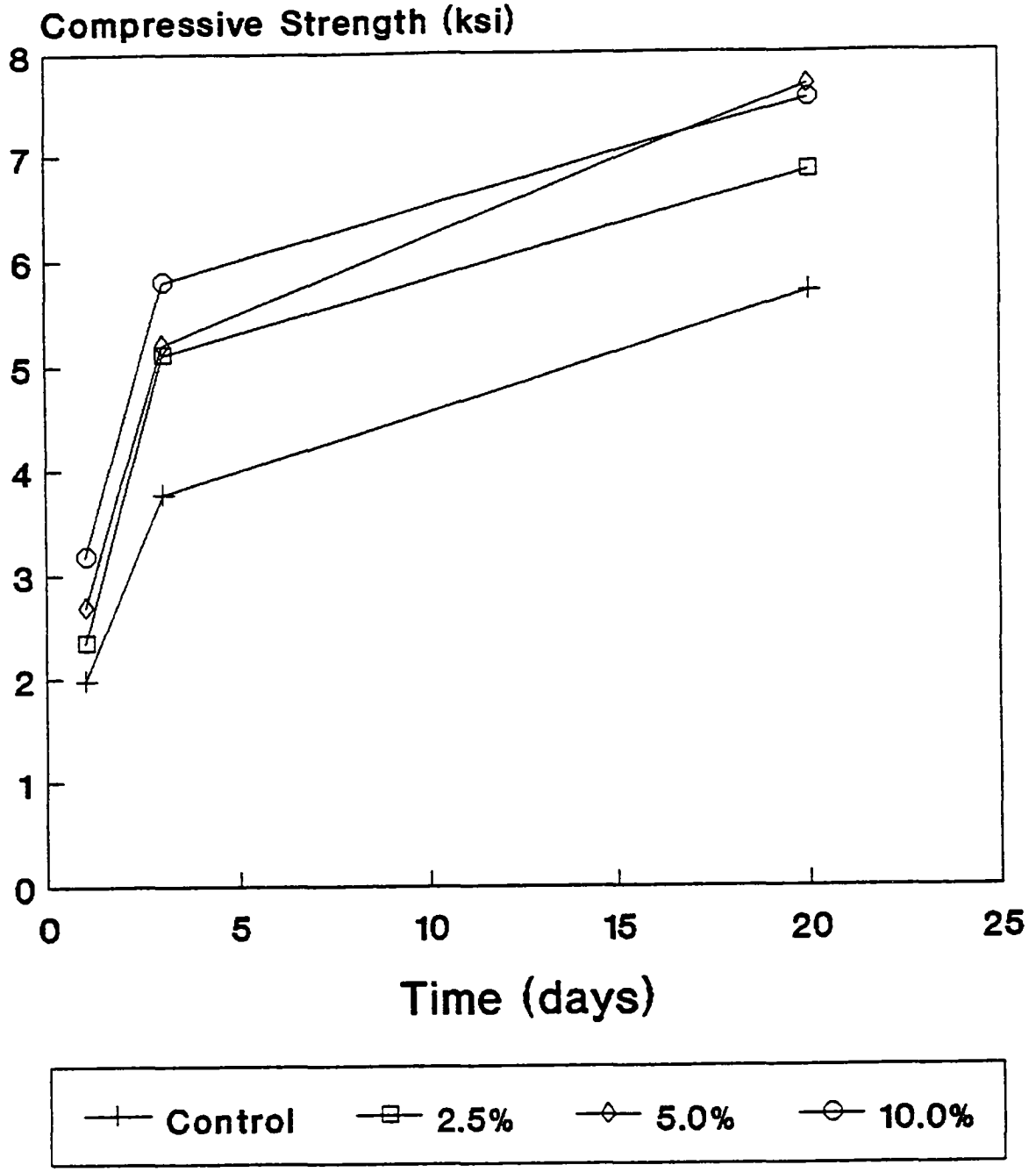

Fig. 26 Mortar Cube Strength as a function of DCI Concentration (% s/s Cement)

NOTE: 1 ksi = 6.895 MPa

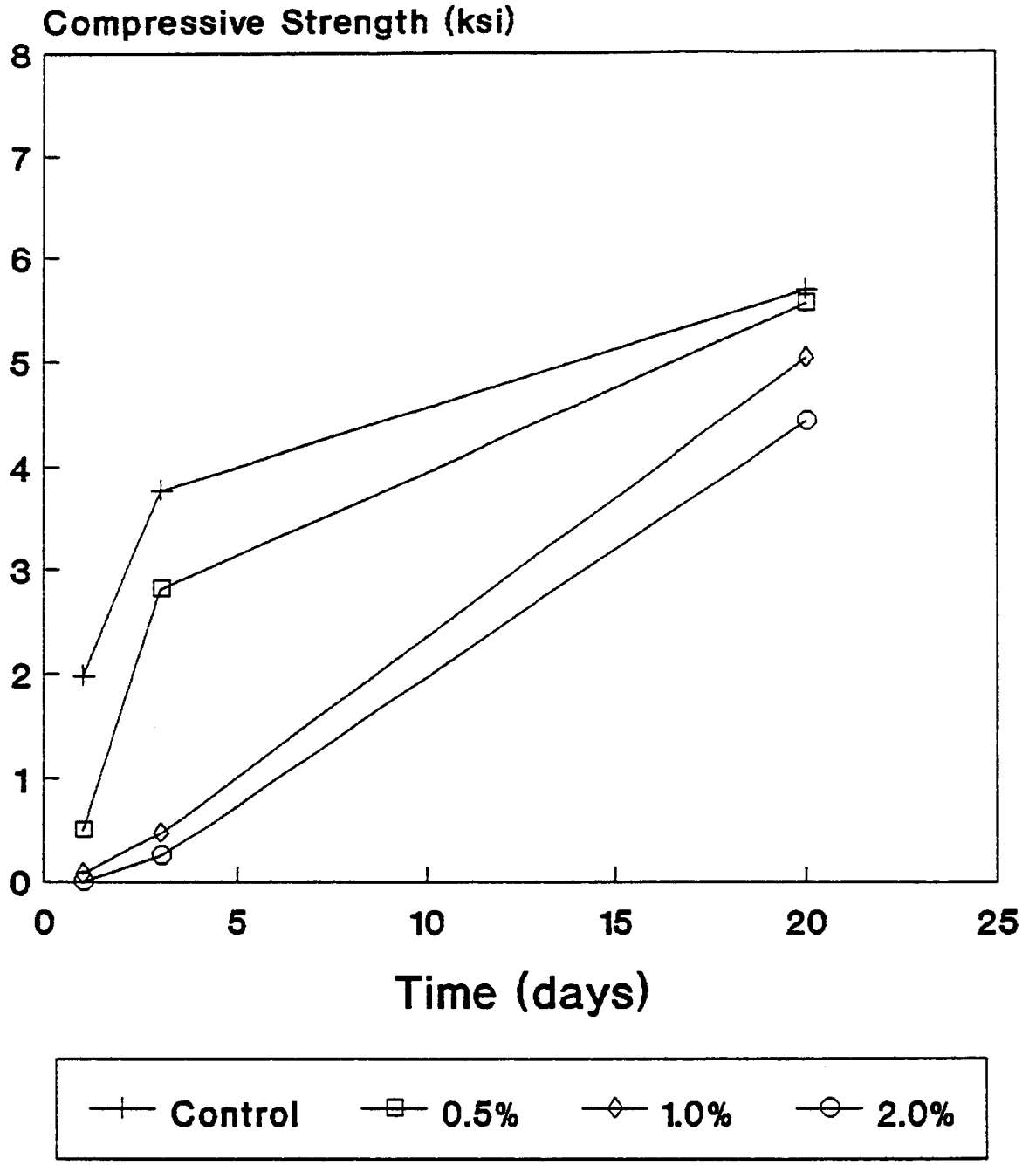

Fig. 27 Mortar Cube Strength as a Function of Sodium Tetraborate Concentration (% s/s Cement)

NOTE: 1 ksi = 6.985 MPa

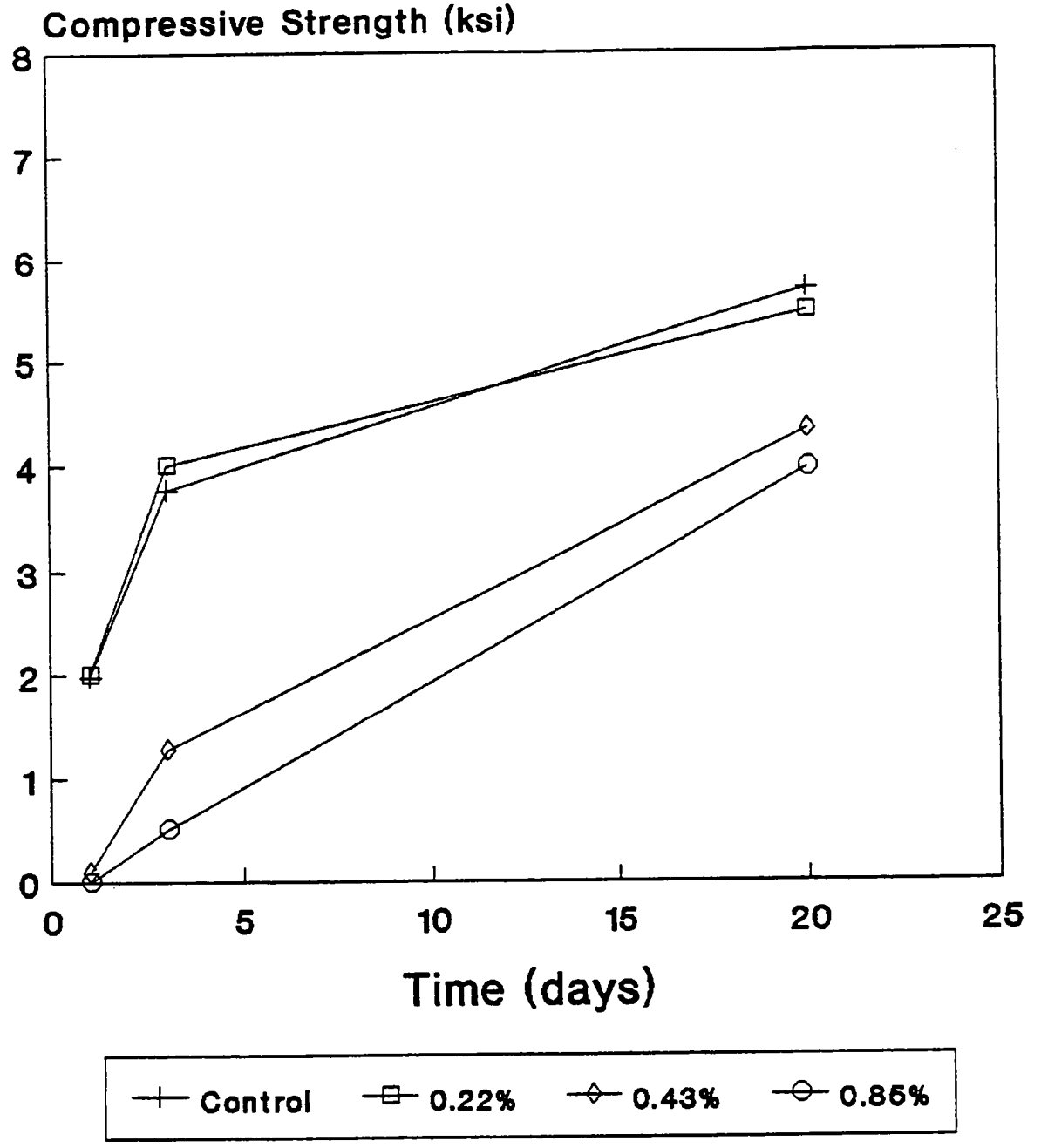

Fig. 28 Mortar Cube Strength as a Function of Zinc Borate Concentration (% s/s Cement)

NOTE: 1 ksi = 6.895 MPa

relation to the controls with time to point of only a 2% difference after 20 days. The two higher concentrations still had extremely low strengths after 3 days, but rapidly increased between days 3 and 20.

Zinc borate exhibited the same type of behavior as the sodium tetraborate but to a higher degree. Original concentrations of 1.7% and 3.4 % s/s cement did not have sufficient set strength at days 1 or 3 to be removed from the mold, therefore, lower concentrations of 0.22%, 0.43%, and 0.85% were used. The 0.22% concentration showed little effect on strength as shown in Fig. 28. However, almost doubling the concentration to 0.43% resulted in a 95% reduction in strength after 24 hours and a 66% reduction after 3 days. The 0.85% concentration strength was even lower, with no set strength after 24 hours. However, after 20 days, the 0.22% and 0.43% concentrations had compressive strengths within 30% of the control group. The two highest concentrations eventually set within 20 days with compressive strengths equal to 3.25 and 2.46 ksi respectively.

Both sodium tetraborate and zinc borate showed the same set retarding characteristics. The high concentration mortar cubes began to set in a characteristic manner for both borate treatments. The setting process was most rapid at the open surface of the cube molds and then progressed downward along the outer edges of the cube, with the slowest set being at the bottom surface of the cube in contact with the mold. Also characteristic of the borate treatments was the evolution of the strengths. High concentrations showed drastic reduction in initial strengths, but a rapid increase between days 3 and 20.

Borates are classified under Type B set retarding admixtures and were popular in the 1930's [41] but are rarely seen in use today. The borates form insoluble calcium borate salts which tie up calcium ions needed for the hydration process. The zinc borate may have had a greater set retardation effect because one molecule of zinc borate provides six boride ions while a molecule of sodium tetraborate provides only four boride ions. In addition to the borate effects, the presence of Na^+ and Zn^{2+} reduces the solubility of calcium ions, thus reducing the rate of hydration even further.

The long-term strengths of set retarded mortars tend to reach and even exceed normally cured mortar strengths [41]. The slower rates of hydration product formation allows greater alignment of the hydration products in the cement paste which produces higher later strengths. This may account for the great increase in strength magnitude between days 3 and 20 for the higher borate concentrations.

Based on the mortar cube strength study, only the borates have a deleterious effect. However, the set retardation effect may be overcome the use of a set accelerating admixture. The admixing of DCI tends to only improve compressive strength which further supports its use a corrosion treatment after removal of chloride-contaminated concrete. Both hydroxylapatite and Cortec 1609 showed no positive or negative effects on mortar strength.

Treatment Effects on Mortar Resistivity

Effects on resistivity were only found in those treatments that produced compressive strength effects due to a change in hydration rate. Since resistivity is a function of permeability which is dictated by the degree of hydration, it is reasonable to expect that set retardation would decrease resistivity and set acceleration would increase it. This is reflected in Figs. 29 through 31 which display resistivity as a function of inhibitor concentration for sodium tetraborate, zinc borate, and DCI respectively. The average resistivity values for each treatment and concentration group are tabulated in Appendix C, Table C-7.

For sodium tetraborate and zinc borate, the higher concentrations which produced a higher degree of set retardation also exhibited lower resistivity values than the control specimens. Since set retardation means a slower formation of hydration products, the reduction in permeability of the system also proceeds slower. The lower concentration zinc and sodium borate specimens which exhibited strengths more similar to the control cubes, also exhibited like resistivity values. One day resistivity values could not be measured on the two higher zinc and sodium borate concentration specimens because their low set strengths made them too fragile to handle.

The DCI mortar cubes behaved opposite of the borate cubes. Since DCI accelerated the hydration process, the permeability reduction of the cubes was also accelerated due to the rapid formation of hydration products. As a result, increasing DCI concentrations yielded higher resistivity values and all resistivities were greater than the control group resistivities. The difference in resistivities is small after 24 hours but gradually increased with the rapid set of the cubes.

None of the specimens were determined to contribute highly conductive ionic species to the mortar cubes. Hydroxylapatite and Cortec 1609 exhibited resistivities similar to the control, while the rest of the treatments' resistivities were dictated by the change in setting rate.

Chloride-Ion Scavenging Ability of Hydroxylapatite

The apatite series, all of which has the same type of hexagonal crystal structure, includes hydroxylapatite ($Ca_{10}(PO_4)_6(OH)_2$) and chlorapatite ($Ca_{10}(PO_4)_6Cl_2$). The nature of apatite's structure renders it particularly prone to substitution. Studies have shown that hydroxylapatite readily undergoes an OH^-/F^- substitution in which the product is fluorapatite ($Ca_{10}(PO_4)_6F_2$) [42] and the ion exchange was found to be irreversible. The possible irreversible substitution of Cl^- for OH^- in concrete would provide a means of scavenging the chloride ions and simultaneously releasing hydroxyl ions which would enhance the pH of the concrete. However, three tests were conducted to evaluate the possibility of hydroxylapatite scavenging chloride, and the results reflected little if any scavenging ability.

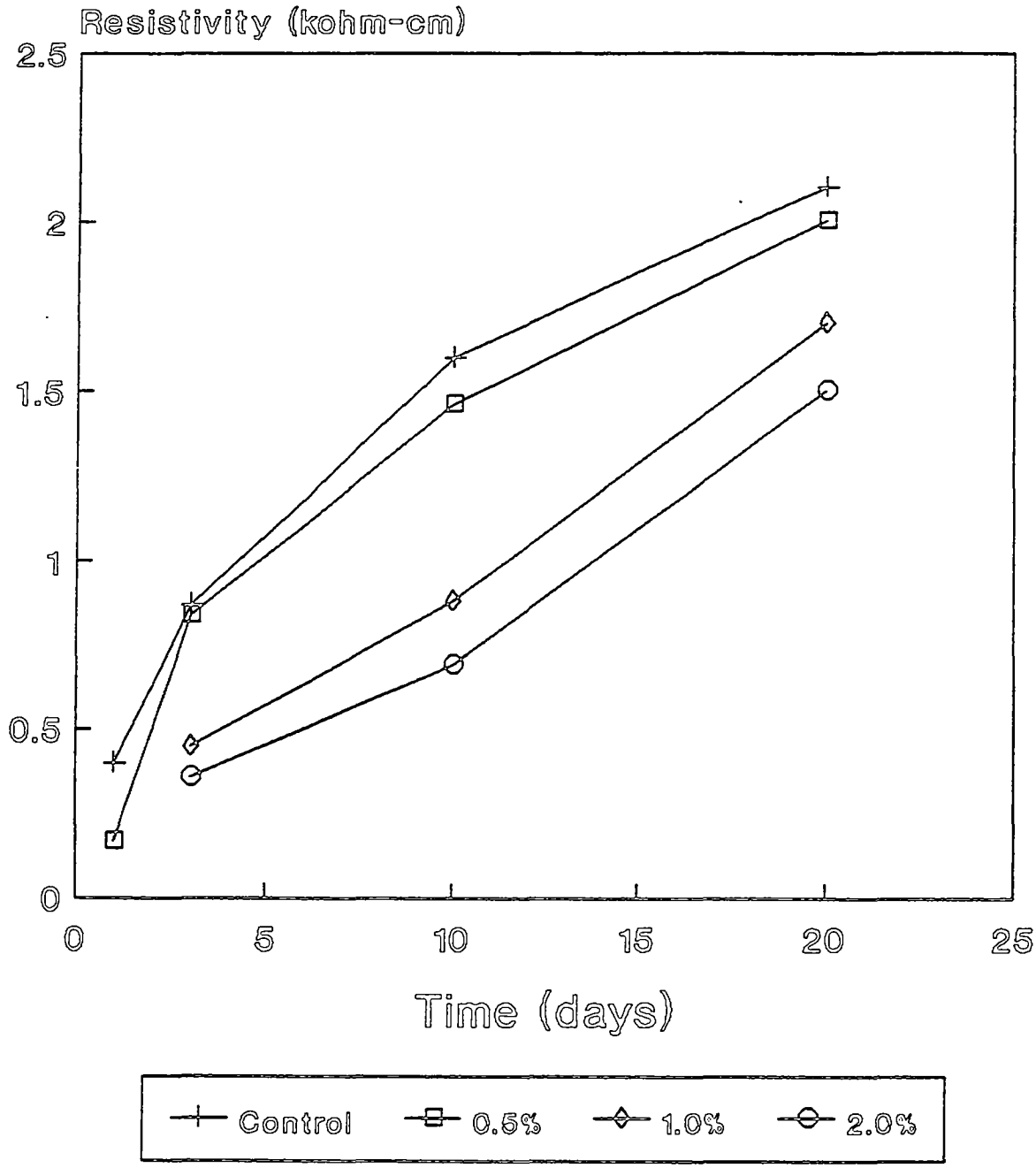

Fig. 29 Resistivity as a Function of Sodium Tetraborate Concentration

NOTE: 1 kohm - cm = 0.39 kohm - in

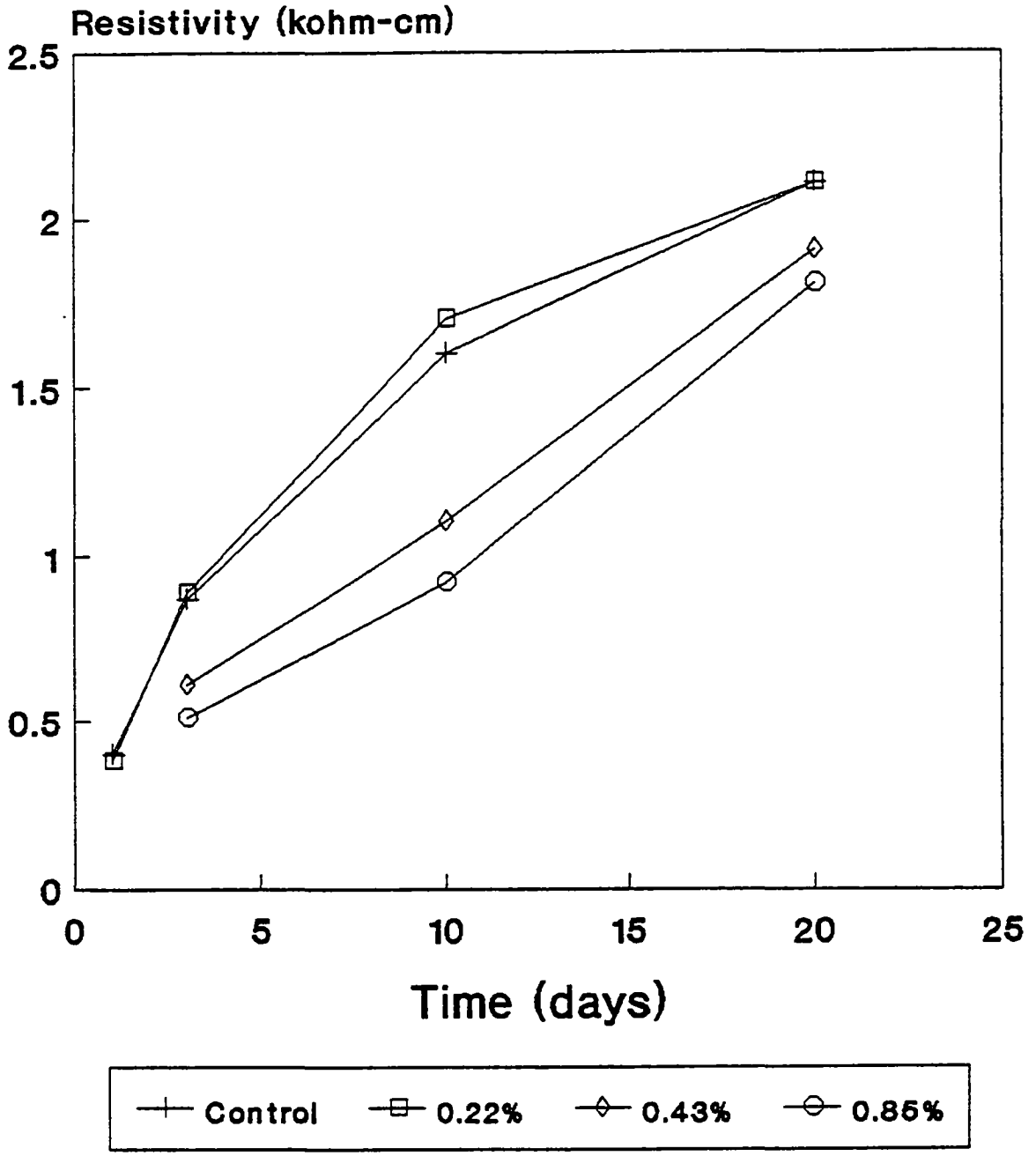

Fig. 30 Resistivity as a Function of Zinc Borate Concentration

NOTE: 1 kohm - cm = 0.39 kohm - in

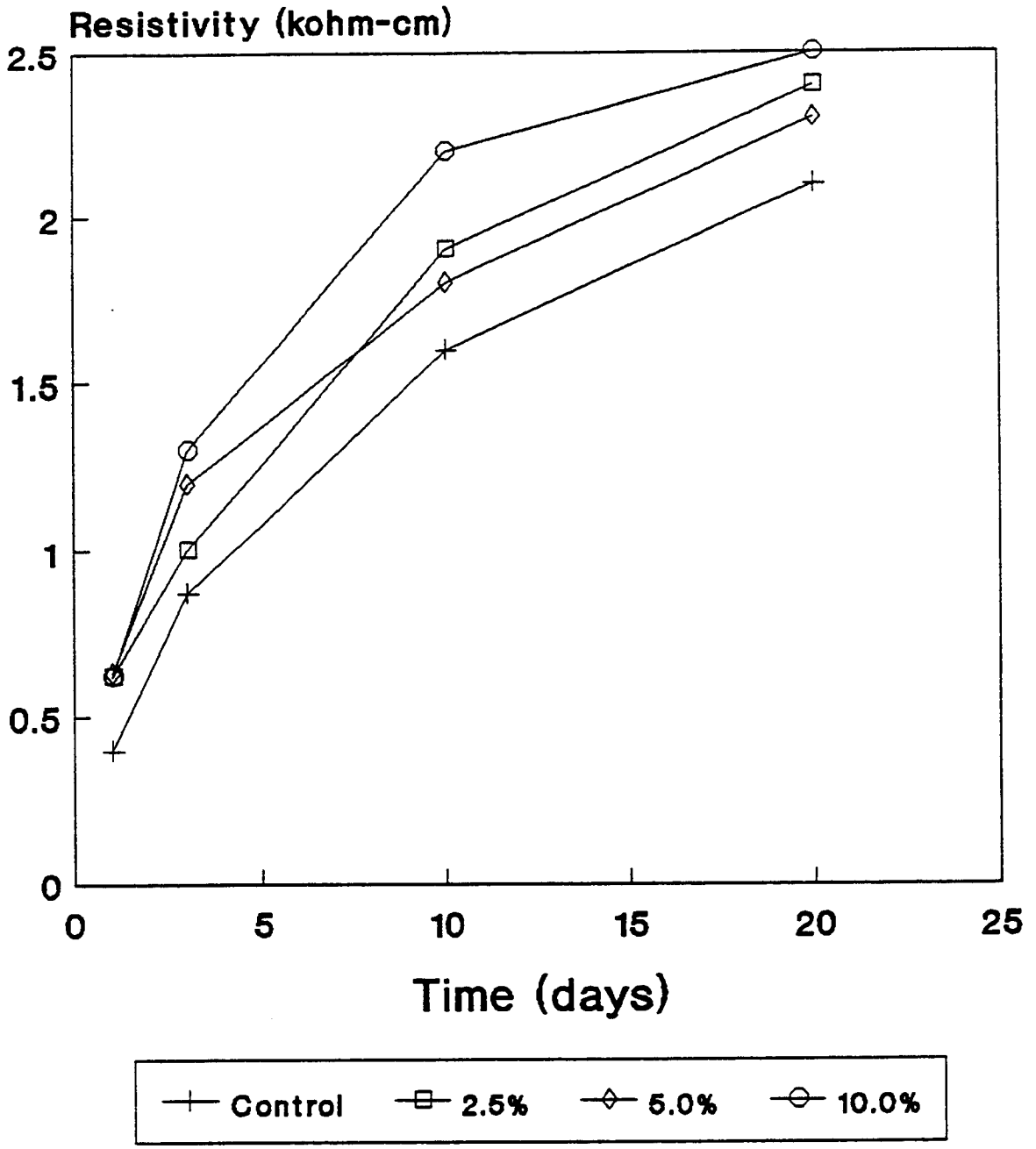

Fig. 31 Resistivity as a Function of DCI Concentration

NOTE: 1 kohm - cm = 0.39 kohm - in

pH Measurements

The results of a pH monitoring test to detect the release of hydroxyl ions as a result of chloride ion substitution are presented in Table 21. Theoretically, if chloride ions substitute for the hydroxyl ions in the apatite molecule, the release of hydroxyl ions should cause a pH increase. Based on a 25 g sample of apatite, 97 ozs. (200 ml) of solution, and a water/apatite pH of 7.5, a 100% exchange would result in a pH of 13.40 which is an approximate pH increase of 6 units of magnitude. However, results from pH measurements taken at room temperature and at 150 °F (65.5° C) for a 5% by weight NaCl solution with 25 g of apatite showed minimal change in pH over a 24 hour period. The difference in minimum and maximum pH measured was only 0.07 pH at room temperature and 0.12 at 150 °F (65.5° C). In addition, the minimal change was not linear with time.

If a direct substitution of chloride for hydroxyl ion was done for every hydroxyl group, the 25 g of apatite would have theoretically released 0.85 grams of hydroxyl ions which should have been detected with an increase in pH to 13.40. However, no pH change was detected to support this at either room temperature or 150°F (65.5°C). In addition, the highest pH measurement for both tests never exceeded the pH value of 7.50 measured for hydroxyl apatite in distilled water.

Specific Ion Electrode Measurements

An attempt was made to determine the extent of hydroxylapatite's chloride ion scavenging ability by measuring chloride content via a specific ion probe. In order to determine a baseline value for comparison, the chloride ion concentration of untreated hydroxylapatite was evaluated. However, the specific ion probe system is calibrated to a lower threshold value of .016% Cl^- for a 3 g sample. All measurements of untreated hydroxylapatite and hydroxylapatite exposed to various % NaCl solutions yielded values below this threshold, therefore, the exact chloride contents could not be determined.

Since the exposed hydroxylapatite samples yielded values less than .016% Cl^-, it is reasonable to assume the maximum chloride concentration an exposed sample could have is .016%. If this is assumed, a 3g sample of exposed apatite would contain 0.00048 g of Cl^-. However, if enough apatite is desired to scavenge a nominal 10 lbs Cl^-/yd^3 of concrete (4536 g) at a level of 0.00048g Cl^-/3g of hydroxylapatite, 12,859 lbs (2.83×10^7 g) of hydroxylapatite/yd^3 of concrete would be needed. This unreasonable and infeasible amount is twenty times the average amount of cement put in a yd^3 of concrete. Based on this analysis, hydroxylapatite is ineffective in scavenging the necessary degree of chloride ions to warrant its feasibility in concrete.

Differential Thermal Analysis

If the Cl^-/OH^- substitution readily takes place, differential thermal analysis (DTA) could detect the loss of the hydroxyl groups in the apatite molecule. A DTA scan of an untreated

Table 21. Measurement of pH as a function of time for hydroxylapatite treated NaCl solution (5% by weight)

Time	pH Measurement[1]	
	Room Temperature	150 °F
0	7.38	7.30
1 min	7.42	7.35
10 min	7.45	7.35
30 min	7.40	7.32
1 hr	7.42	7.30
2 hr	7.39	7.31
5 hr	7.42	7.39
10 hr	7.45	7.37
24 hr	7.43	7.42

[1]pH measurements of:
distilled water = 6.72
distilled water and apatite (R.T.) = 7.50
distilled water and apatite (150°F) = 7.44
5% by weight NaCl solution (R.T.) = 7.31
5% by weight NaCl solution (150°F) = 7.20

Note: 150°F = 65.5°C.

hydroxylapatite specimen is shown in Fig. 32. The initial valley at 257°F (125°C) is due to the release of water from the specimen. The valley at 1832°F (1000°C) corresponds to a dehydration of the specimen in which the hydroxyl groups are released. Studies have shown that hydroxyapatite does not readily lose OH^- from its crystal lattice, which is stable up to at least 1832°F (1000°C) [42] which correlates with the DTA scan.

If chloride ions substitute for hydroxyl groups within the hydroxylapatite molecule, the magnitude of the valley at 1832°F (1000°C) would decrease with increasing loss of OH^-. DTA scans of hydroxylapatite specimens exposed to varying concentrations of NaCl solution showed no indication of ion substitution. All DTA scans of the samples showed minimal to no change from the reference sample scan shown in Fig. 32.

The substitution of chloride ion for hydroxyl ion in hydroxylapatite may possibly be inhibited by the size of the chloride ion. The fluoride ion readily substitutes but has an ionic radius 25% smaller than the chloride ion. Studies have indicated that structural requirements preclude site-by-site substitution such as Cl^- for F^- [37]. This may be the case in the Cl^-/OH^- substitution as well.

Conclusions

The removal of chloride-contaminated concrete is an effective means through which corrosion abatement treatments can be applied. Several treatments and treatment combinations were found effective and are recommended for further evaluation in large-scale and field experimentation.

When chloride-contaminated concrete is removed, the combination of DCI (calcium nitrite) inhibitor ponded and placed in backfilling mortar proved to be the most effective corrosion treatment under investigation. The treatment exhibited the greatest sustained reduction in corrosion rate. The effectiveness of the DCI is dependent upon an adequate nitrite-to-chloride-ion ratio. This ratio dictates the degree to which the nitrite ions can compete with the chloride ions for the Fe^{2+} ions in solution. Higher nitrite levels result in the enhanced stability of the passive film due to the reformation of Fe_2O_3. It was also reconfirmed that DCI acts as a set accelerator and increases the compressive strength of the mortar at least in measurements up to 20 days.

The experimental inhibitors sodium tetraborate and zinc borate showed adequate effectiveness in reducing corrosion when applied as both a ponding and mortar admixture. The borate ion's ability to produce a protective layer on steel resulted in a effective reduction in the corrosion activity by acting as a barrier to increased metal dissolution. However, the borate compounds act as cement set retarders with zinc borate having a greater effect at similar concentrations.

Commercial inhibitors Alox 901, Cortec 1337, and Cortec 1609, are potentially effective treatments for reinforced concrete after removal of chloride-contaminated concrete.

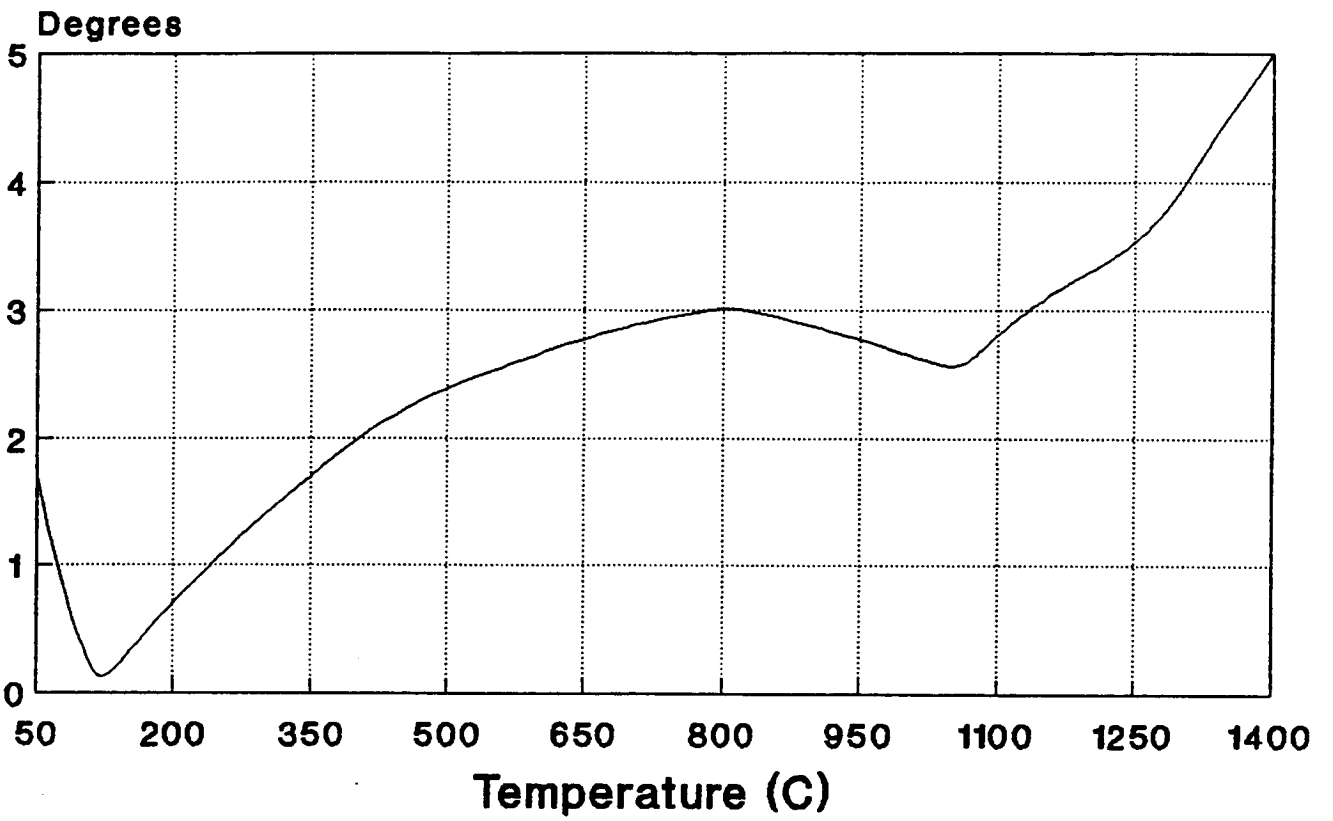

Fig. 32 Differential Thermal Analysis of Hydroxylapatite

NOTE: °F = 9/5°C + 32

However, due to their proprietary nature, the exact mechanism of their corrosion inhibition ability is not known.

In general, it was determined that the ponding of treatment solution is more effective in corrosion abatement than solely backfilling with treated mortar. The ponding allows for the diffusion of the inhibitor not only through the concrete but also possibly through the reinforcing steel/concrete interface. However, the removal of chloride-contaminated concrete above a reinforcing bar and subsequent replacement with fresh mortar has little effect on the corrosion activity when the chloride ion concentration at the reinforcing steel level is high. Without the presence of a corrosion inhibiting agent, the concrete surrounding a corroding reinforcing steel would still have a sufficient chloride concentration to spur the continuation of corrosion.
The evaluation of hydroxylapatite as a chloride ion scavenging mineral showed no indication of chloride ion scavenging ability in aqueous tests or when placed alone in mortar.

Recommendations

Based on the limitations encountered through the course of this study, the following recommendations can be made for further research:

1. Long term evaluation of treated specimens should be addressed to aid in estimating treatment life-cycles in bridge deck systems.

2. Tests should be conducted to determine the optimum treatment concentration based on the volume of chloride contaminated concrete removed.

3. In order to aid in the diffusion of treatment chemicals, the concrete should be dried prior to ponding treatment.

4. The removal of all concrete to the reinforcing steel level as opposed to solely grooving above the reinforcing steel is an enhanced treatment.

5. Economic feasibility studies should be performed on effective treatments.

6. Surface analysis on the reinforcing steel should be conducted after the termination of the exposure period to detect the presence of passive films or adsorbed species.

7. Evaluation of the chloride ion scavenging ability of other apatite forms should be performed. Other minerals, such as sodalite, should also be evaluated.

4

Part III: Evaluation of Polyaphrons As Corrosion Inhibitors

Introduction

A polyaphron is a small oil drop that has been encapsulated by a soapy aqueous film layer, in which water is the continuous phase. Polyaphrons are formed by first dissolving surfactants in both the separate oil and aqueous phases. Then, slowly, the oil phase is added to the aqueous phase. The mixture must be well shaken between additions of the oil in order to break the oil into very small drops and allow the aqueous phase to encapsulate it. This process is continued until all the oil has been added. Factors contributing to the size distribution of the resulting aphron include surfactant concentration and water-to-oil ratio (PVR). The resulting size distribution can vary from only a few microns up to 30 or 40 microns in size. The general relationship between size distribution and PVR is the higher the PVR, the smaller the aphrons will be.

Research Objectives

The objectives of this part of the study is two-fold: 1) To investigate the feasibility of reducing corrosion using polyaphrons of different compositions, and 2) study the movement rate of liquid core aphrons through cement paste, mortar, and concrete.

Experiment Program

Corrosion Reduction Using Polyaphrons

The commercial inhibitors, primarily, sulfonated petrochemicals such as Petromix HL and CR, Petromix #9 and Arguard 2C-75 were dissolved in the oil phase. A non-ionic surfactant, 15-A-9, which is a polyethylene glycolether of a secondary alcohol, was commonly used as a surfactant in the aqueous. Petromix #9 and Petronate CR were also used as the aqueous phase surfactant. Table 22 presents aphron types used in the corrosion reduction tests.

Once a particular composition of aphron was chosen and made, corrosion reduction tests were performed on 0.25 x 1.0 x 3.0 inch, 1040 carbon steel coupons placed in various solutions. Prior to testing, the steel coupons were first washed in soap and water by scrubbing each sample with a soft nylon brush, then dried, and soaked in hexane to further remove any remaining loose rust or oil. The coupons were then weighed, submerged in an aphron solution, and placed in an oven at 95°F (35°C) to accelerate corrosion. After a given amount of time, usually 4 to 7 days, the samples were removed from the aphron solution, cleaned using the same pre-immersion procedure, visually inspected for corrosion, and weighed. When the samples underwent general corrosion only, the corrosion rate was calculated as:

$$\text{Rate} = (K \times W)/(A \times T \times D) \quad (3)$$

where

K = constant (3,450,000)
W = weight loss due to corrosion
A = surface area of the coupon, cm^2
T = immersion time, hours
D = coupon density, 8.28 g/cm^3

All the solutions used in the immersion tests were based on 0.3% NaCl combined with a particular polyaphron such that the resulting solution was 10 parts saline solution and 1 part polyaphrons. The variations to the saline solution included buffering the pH from 7 to 11; introducing potassium hydroxide, (KOH); sodium hydroxide, (NaOH); and calcium hydroxide, ($Ca(OH)_2$). Another variation on the immersion solution included adding sodium sulfite ($NaSO_3$) as an oxygen scavenger.

For all immersion tests performed, a representative number of coupons was always immersed in a solution with no aphrons present to provide a means of comparison to those containing aphrons. This was essential to compare weight losses due to general corrosion and was helpful in providing visual comparisons with samples treated with aphrons. The aphron corrosion reduction results, mean and standard deviation, for the various test conditions of solution type, aphron composition, number of coupons, test time and solution pH are presented in Table 23. The general results and observations are as follows:

Table 22. Aphron Types Used in the Corrosion Reduction Tests

Aphron Type	PVR	Water Surfactant	Concentration (mL/L)	Oil Surfactant	Concentration (g/L)	Ionic Character
A-2	10	15-S-9	5	Petronate L	1.0	Anionic
C-1	10	15-S-9	5	Petronate CR	1.5	Anionic
C-2	10	15-S-9	10	Petronate CR	3	Anionic
C-3	10	Petronate CR	15	Petronate CR	5	Anionic
D-1	10	15-s-9	5	Petromix #9	1.5	Anionic
D-2	10	Petromix #9	10	Petromix #9	1.5	Anionic
D-3	10	Petromix #9	5	Petromix #9	1.5	Anionic
D-4	10	Petromix #9	5	Petromix #9	---	Anionic
D-6	10	15-S-9	10	Petromix #9	10	Anionic
D-7	10	15-S-9	10	Petromix #9	3	Anionic
G-1	10	15-S-9	10	Arquad 2C-75	40	Cationic

Table 23. Aphron Corrosion Reduction Results

Solution	Aphron	Weight Loss (g) x		n	Time (h)	pH
0.3% NaCl	A-2	.0051	.0008	5	48	8
"	C-1	.0168	.0012	6	96	8
"	C-2	.0304	.0004	4	96	8
"	C-3	.0040	.0009	10	96	8
"	D-1	.0147	.0020	6	96	8
"	D-2	.0036	.0006	5	96	8
"	D-3	.0022	.0010	4	96	8
0.3% NaCl 500 ppm Na_2SO_3	D-3	.0003	.0007	13	72	8
"	D-3	.0051	.0005	4	139	8
"	D-3	.0049	.0006	7	144	10
0.3% NaCl	D-3	.0007	.0003	4	119	11
*Pore Sol'n 500 ppm Na_2SO_3	D-3	.0048	.0009	4	256	13
0.3% NaCl	D-4	.0193	.0011	5	96	8
"	D-6	.0134	.0010	5	96	8
"	D-7	.0199	.0016	7	96	8
Pore Sol'n	G-1	.0106	.0012	4	173	13
"	G-1	.0011	.0004	5	191	13
"	G-1	.0074	.0010	4	240	13

- The aphrons which were made using Petromix #9 as the oil phase surfactant showed the most promise in preventing general corrosion (D-1 through D-7).

- Pitting corrosion was a common occurrence, however, it was believed to be caused primarily due to the orientation of the steel coupon in the solutions.

- Aphrons made with the cationic surfactant, Arquad 2C-75, were by far the most stable in the heat and salt/pore solution environment. All other aphrons broke very shortly after being added to the salt/pore solutions.

- Lower pH solutions (7-8) showed a higher tendency for general corrosion, while higher pH solutions (13) showed a greater tendency towards scale corrosion. Solutions with a pH in the range of 9-10 appeared to minimize both types of corrosion.

- The addition of excess amounts of sodium sulfite as an oxygen scavenger clearly reduced the amount of general corrosion as well as pitting corrosion. However, it was suspected that the oil/aphron layer that would form on the top of the solutions provided a barrier to prevent further oxygen from ingressing into solution.

Movement of Aphrons Through Concrete

The second aspect of the research was aimed at investigating how polyaphrons diffuse through concrete when subjected to a potential gradient. Aphrons which showed the most promise for corrosion protection were predominantly used.

Three separate mixtures were used for the tests: concrete, mortar and cement paste. All three mixtures were cast with a water to cement ratio of 0.47 and were cured in a moist room for 28 days prior to testing. Once the specimens had been cured, they were cut into small discs with dimensions of approximately 3/4 in. (1.91 cm) in diameter by 1/8 in. (0.32 cm) thick. The samples were then placed in a glass cell (See Fig. 33), using a silicon rubber sealant to prevent leaks around the edges of the specimens. Once the sealant was allowed adequate time to dry, one side of the glass cell was filled with an aphron solution while the other was filled with distilled water. The electrodes were then placed in each side according to the ionic character of the aphron, and an electric potential of 110 volts DC was applied to the cell.

It was usually noticed, while performing these experiments, that after some time, the electrode on the water side of the cell would begin bubbling and the current across the cell would often rise above the scale limits of the apparatus, (5mA). At that point, the experiment was usually terminated, or observed for a short period of time and then terminated. The sample was then removed from the cell and cut in half. The extent of penetration of the aphrons into the cell was visually determined due to the "wetting" of the cement by the aphrons. Table 24 presents the results of the aphron diffusion tests.

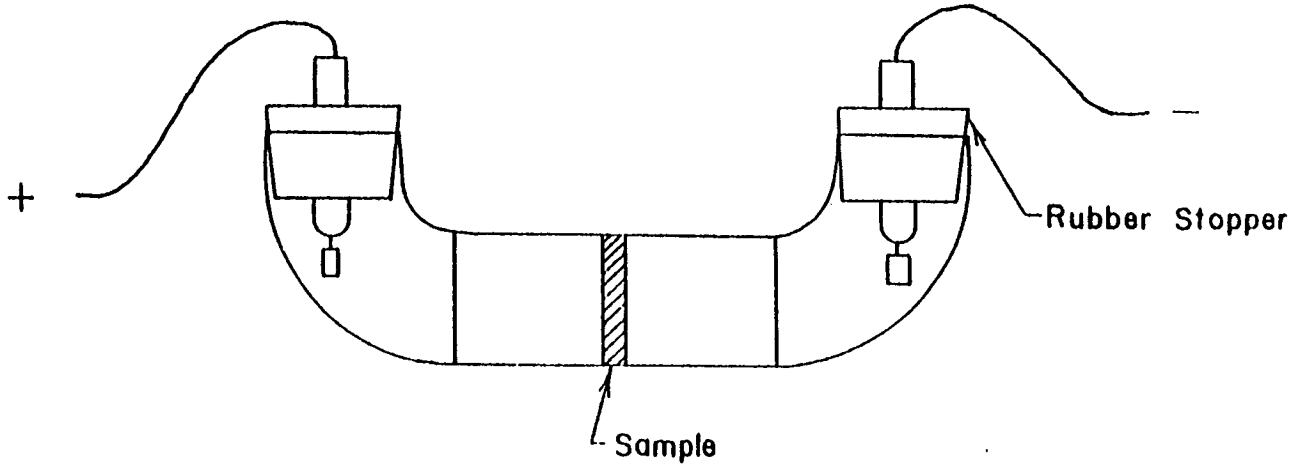

Electrodes connected to an amp. meter and variable voltage supply.

Fig. 33 Electrophoretic Apparatus

Table 24. Aphron Electrically Induced Diffusion Test Results

Trial #	Aphron Type	Mixture *	Rate (in/hr)
1	D-7	F.A.	0.00179
6	D-7	F.A.	0.00610
7	D-7	C.P.	0.00205
8	D-7	C.P.	0.00540
20	D-7	C.A.	0.00120
22	G-1	C.A.	0.00164
23	G-1	C.A.	0.00246
24	G-1	F.A.	0.00239
25	G-1	F.A.	0.00492
26	G-1	F.A.	0.00328
28	G-1	C.P.	0.00514

Mixture*	Mean Rate (in/Hr)	Standard Deviation
C.A.	0.00179	0.00060
F.A.	0.00370	0.00179
C.P.	0.00420	0.00186

C.A. - concrete
F.A. - mortar
C.P. - cement paste

The diffusion rates of the polyaphrons through the various types of cement mixtures were very slow, even with the addition of the driving force provided by an electric potential. It was also observed that most aphrons would begin breaking down after several hours under the effect of the electric current. Once this occurred, the water and oil separated, any salts that were dissolved in the water caused the water to be drawn through the cement and not the oil containing the inhibitor.

The results show that the diffusion rates of polyaphrons through the various mixtures are very slow even with an additional electrical driving force, and the mean rate and standard deviation significantly increased with increasing aggregate content. In addition, most aphrons broke down after several hours under the effect of the electric current. Once the aphrons broke down, the water and oil separated and any salts dissolved in the water caused the water to be drawn through the cement leaving the oil containing the inhibitor behind. The water being drawn through the concrete would decrease the specimen's resistance and the current would increase under a constant potential and the water would begin to bubble at which time the test was stopped.

Findings and Conclusions

Based on the results of this study, the following findings were obtained.

- Aphrons made using Petromix #9 showed promising results in preventing general corrosion.
- Aphrons made with cationic surfactant were the most stable in heat and salt.
- Solution with a pH of 9-10 minimized corrosion.
- Increasing sodium sulfite, as an oxygen scavenger, reduced corrosion.
- The diffusion rate of polyaphrons through concrete are very slow.
- Using electrical current as a driving force to increase the polyaphrons diffusion rate in concrete led to breaking the aphrons down after several hours.

This study concluded that polyaphrons are not practical inhibitors due to the fact of their very low diffusion rate.

APPENDIX A

Concrete and Mortar

Table A-1. Gradations of coarse (CA) and fine (FA) aggregates

Sieve Size	CA % Passing	FA % Passing
1/2"	100	100
3/8"	93	98
No. 4	17	91
No. 8	9	73
No. 16	1	52
No. 30	---	32
No. 50	---	8
No. 100	---	2
No. 200	---	0.2

Table A-2. Characteristic properties of coarse (CA) and fine (FA) aggregates

Property	CA (3/8" limestone)	FA (natural sand)
Dry Unit Weight	89.3 lbs/ft^3	----
Specific Gravity	2.73 g/cc	2.66 g/cc
Absorption	1.36%	0.36%
Fineness Modulus	----	3.39

Table A-3. Concrete mix design for specimen set A

Component	Quantity (SSD) in lb
Cement	39.04
Water	19.72
Coarse Aggregate	68.50
Fine Aggregate	107.91
AEA (Microair)	2.89 ml
WR-R	92.45 ml
Total	235.17 lbs

Table A-4. Concrete properties for specimen set A

Property	Batch 1	Batch 2	Batch 3	Batch 4
Slump	2.25"	2.50"	2.50"	2.25"
Air	6%	5.7%	5.3%	6.2%
Unit Wt. (pcf)	141.4	141.8	141.9	141.6
Temperature	59 °F	61 °F	62 °F	61 °F
Strength (ksi)				
7-day	4.97	5.37	5.09	4.93
28-day	6.57	5.97	6.45	6.41

Table A-5. Concrete mix design for specimen set B

Component	Quantity (SSD) in lb
Cement	39.04
Water	19.73
Coarse Aggregate	68.47
Fine Aggregate	107.93
AEA (Microair)	2.43 ml
WR-R	80.89 ml
Total	235.17 lbs

Table A-6. Concrete properties for specimen set B

Property	Batch 1	Batch 2	Batch 3	Batch 4
Slump	3.5"	4.0"	3.75"	3.75"
Air	6.9%	6.6%	7.0%	6.8%
Unit Wt. (pcf)	141.4	141.8	141.9	141.6
Temperature	63 °F	60 °F	60 °F	62 °F
Strength (ksi)				
7-day	5.01	4.87	5.12	5.05
28-day	6.72	6.34	6.43	6.27

Table A-7. Backfill mortar mix design with treatment variations

Basic mix used to fill two grooves:

Cement	1.75 lbs
Fine Aggregate (dry)	5.28 lbs
Water	0.61 lbs

List of treatments placed in mortar, amount of additional water needed to obtain adequate workability, and resulting w/c ratio based on 0.36% FA absorption:

Treatment	Additional Water	w/c Ratio
Blank (B-1,B-4,B-9 B-13, B-14, B-15)	20.5%	.42
DCI (B-2,B-3)	18.0%	.41
Sodium Tetraborate (B-6,B-7)	25.8%	.44*
Zinc Borate (B-8)	29.3%	.45*
Apatite (B-5, B-10)	30.9%	.45*
Zinc Borate/Apatite (B-12)	32.5%	.46*
DCI/Apatite (B-11)	29.3%	.45*
CORTEC 1609 (B-16,A-15)	21.0%	.42

*These water/cement ratios may be high due to the fact that that apatite and both the borates are applied as powders into the mixing water; therefore, they may have absorbed or adsorbed some of the water, taking it away from the hydration process.

Table A-8. Mortar cube mix design with treatment variations

Basic mortar cube mix (9 cubes):

Cement	740 g
Fine Aggregate (dry)	2035 g
Water	369 ml*

*10 ml of additional water were needed above the ASTM C 109 standard (359 ml) due to the use of the dry sand.

The following treatments required additional water or the addition a set retarder:

Treatment	Addition
DCI 5% s/s cement	Set retarder 0.3% s/s cement
DCI 10% s/s cement	Set retarder 0.6% s/s cement
Apatite 25% s/s cement	10 ml of water for workability
Cortec 1337	No additions
Sodium tetraborate	No additions
Zinc borate	No additions

APPENDIX B

Measurement Procedures

Resistivity Measurements Using a Soil Resistance Meter

The resistivity of the 2" mortar cubes was found through the use of a modified Nilsson soil resistance meter. Two metal filled copper rings secured to an insulative backing were soldered onto the two contact cables of the resistance meter. These circular metallic surfaces, 1 in^2, served as the two contact surfaces between which current was passed.

Based on Ohm's Law,

$$R = V/I \qquad (9)$$

where,

R = resistance in Ω

V = potential in Volts

I = current in Amperes

resistance can be expressed as:

$$R = \rho L/A \qquad (10)$$

where,

ρ = resistivity in Ω-in.

L = length in in.

A = cross sectional area in in^2

From this, resistivity can be expressed in terms of centimeters:

$$\rho = A \times R/L \qquad (11)$$

$$= 0.997 \times R$$

where A and L have been converted to centimeters and the units of resistivity are ohms-cm. Based on equation eleven, the resistance readings from the meter can be directly converted to resistivity.

The resistance measurements were taken between all three opposite faces of each cube. Electroconductive gel was used to assure a conductive contact with the mortar cube surfaces. The metal contacts were clamped down over the opposite surfaces and a current was applied. A resistance dial was turned until the current was nulled and the dial reading was taken as the resistance across the mortar cube. The rough surface of each mortar cube that corresponded to the open surface of the mortar molds appeared to affect the resistivity measurements. The resistivity across this surface always appeared higher than the other surfaces. This is probably due to the rough surface affecting the contact area. As a result, only the two resistivity measurements taken across the smooth surfaces was recorded for each cube.

Differential Thermal Analysis Procedure

The differential thermal analysis conducted on hydroxylapatite was performed using a Perkin Elmer high temperature differential thermal analysis system in combination with a thermal analysis controller and data station.

Samples were weighed and placed in a small platinum crucible which was positioned in the DTA heating chamber next to the standard reference sample. The following parameters were used in controlling the thermal analysis:

Final temperature = 1400 °C
Minimum temperature = 30 °C
Temperature increment = 140 °C
Y-range = 20
Heating rate = 20 °C/min
Cooling rate = 30 °C/min

After completion of the thermal analysis, the DTA scan was plotted and evaluated for any noticeable peaks or valleys indicating a thermally induced reaction.

APPENDIX C

Experimental Data

Table C-1. Pre-Treatment Half-Cell Potentials of Set A and B in Reference to Copper-Copper Sulfate Electrode

		Half-Cell Potential (-mV)								
Specimen	Bar	Day 1	Day 8	Day 15	Day 22	Day 29	Day 36	Day 43	Day 50	Day 57
A-1	A	480	480	441	377	401	444	446	433	445
	B	482	492	436	384	399	437	452	440	444
A-2	A	494	498	452	400	412	462	468	438	441
	B	475	487	447	440	443	476	498	489	500
A-3	A	492	488	462	465	471	522	533	520	499
	B	486	489	452	433	466	497	512	510	497
A-4	A	490	488	435	404	415	444	480	442	436
	B	488	480	458	399	410	456	478	452	447
A-5	A	488	498	450	412	415	437	446	412	420
	B	488	494	465	460	462	476	476	480	492
A-6	A	491	490	462	432	438	461	475	455	462
	B	487	484	453	421	419	444	452	432	435
A-7	A	491	491	447	450	451	499	504	510	515
	B	486	496	450	439	423	487	503	487	492
A-8	A	518	428	406	333	350	392	420	395	400
	B	499	507	469	365	390	442	445	438	449
A-9	A	473	479	435	378	398	454	461	435	440
	B	469	477	428	388	401	481	492	467	469
A-10	A	498	506	465	440	440	493	501	500	498
	B	510	510	472	381	414	451	466	462	468
A-11	A	484	497	472	398	422	472	480	453	452
	B	509	521	489	412	431	488	495	482	481
A-12	A	496	520	480	409	416	456	463	412	420
	B	490	502	475	354	360	410	430	414	423
A-13	A	480	503	462	405	436	466	470	448	450
	B	491	510	500	493	511	544	544	523	522
A-14	A	506	514	491	478	487	533	552	500	495
	B	511	531	501	501	526	550	543	523	523
A-15	A	490	522	503	501	517	537	504	475	482
	B	488	504	474	472	485	513	536	535	520
A-16	A	495	516	494	494	522	545	563	543	548
	B	500	512	478	470	487	533	565	551	560

Table C-1. Pre-Treatment Half-Cell Potentials of Set A and B in Reference to Copper-Copper Sulfate Electrode (continued)

Specimen	Bar	Day 64	Day 71	Day 78	Day 85	Day 92	Day 99	Day 106	Day 113
A-1	A	448	443	469	488	490	520	520	545
	B	450	452	498	509	512	543	567	572
A-2	A	446	445	467	498	499	516	522	542
	B	498	488	515	512	503	507	515	564
A-3	A	515	492	522	533	545	526	543	552
	B	512	489	513	507	508	517	546	558
A-4	A	442	441	463	476	479	482	512	584
	B	452	438	449	480	483	503	545	601
A-5	A	433	428	435	488	490	523	568	610
	B	490	462	488	507	511	523	555	584
A-6	A	455	452	475	483	490	513	547	579
	B	444	438	451	513	541	558	606	639
A-7	A	521	503	542	506	538	589	623	641
	B	493	476	482	507	522	580	604	623
A-8	A	400	410	428	417	451	498	532	572
	B	450	444	453	480	498	513	541	584
A-9	A	452	452	457	507	505	525	569	590
	B	466	448	466	496	505	537	536	575
A-10	A	509	462	512	560	564	592	600	622
	B	477	452	476	489	503	545	564	584
A-11	A	460	468	465	488	501	548	571	599
	B	491	468	493	507	521	537	568	602
A-12	A	433	432	472	508	512	516	554	588
	B	433	441	446	468	488	524	578	613
A-13	A	452	461	464	462	488	512	566	592
	B	533	520	545	560	572	612	642	611
A-14	A	502	511	545	552	566	574	611	625
	B	541	501	523	548	542	555	584	622
A-15	A	497	481	497	545	550	559	599	607
	B	533	498	568	572	575	589	623	631
A-16	A	559	539	562	558	562	581	605	624
	B	575	562	588	598	603	601	635	647

Table C-1. Pre-Treatment Half-Cell Potentials of Set A and B in Reference to Copper-Copper Sulfate Electrode (continued)

Half-Cell Potential (-mV)

Specimen	Bar	Day 1	Day 8	Day 15	Day 22	Day 29	Day 36	Day 43	Day 50	Day 57	Day 64	Day 71	Day 78
B-1	A	266	284	329	354	404	458	470	461	460	491	566	588
	B	249	266	312	348	395	439	429	448	433	441	512	534
B-2	A	266	289	351	388	423	445	462	447	445	462	518	542
	B	255	288	334	369	413	448	444	444	441	447	469	498
B-3	A	254	289	326	337	391	445	475	438	442	448	465	470
	B	258	266	317	341	399	436	436	446	438	455	504	523
B-4	A	249	278	322	347	392	442	451	448	435	466	547	571
	B	251	285	328	355	407	450	469	458	448	472	556	587
B-5	A	261	298	354	360	404	443	451	433	437	447	490	505
	B	246	269	309	375	422	458	460	448	451	482	553	567
B-6	A	278	311	336	366	423	461	448	452	439	461	503	524
	B	267	310	347	363	418	444	451	425	433	458	519	524
B-7	A	256	287	307	338	387	434	438	439	438	442	493	516
	B	245	270	313	346	393	426	440	435	430	449	511	530
B-8	A	240	261	312	333	385	429	452	440	442	468	514	542
	B	234	255	316	324	384	421	426	426	427	443	524	533
B-9	A	237	254	307	333	378	453	469	452	451	477	534	567
	B	253	286	321	348	391	440	425	433	430	457	509	543
B-10	A	279	309	334	367	422	466	462	451	461	491	544	566
	B	274	300	333	381	433	452	468	452	426	454	490	517
B-11	A	244	281	307	338	377	407	409	408	410	435	489	499
	B	249	278	316	356	420	464	455	438	433	452	517	524
B-12	A	255	281	329	360	396	445	458	443	411	438	488	503
	B	266	272	322	354	390	390	406	414	421	434	481	497
B-13	A	251	290	331	374	411	451	466	448	441	469	511	534
	B	259	279	330	362	412	458	481	453	436	448	491	520
B-14	A	245	276	326	353	404	434	457	451	437	436	472	487
	B	248	288	326	349	395	447	454	458	448	477	533	523
B-15	A	215	248	295	332	384	433	488	448	444	482	546	540
	B	224	252	303	337	386	439	444	439	438	452	496	511
B-16	A	236	253	310	341	397	442	452	450	440	449	481	496
	B	237	250	308	337	384	450	449	431	433	441	478	487

Table C-2. Post Treatment Half-Cell Potential as a Function of Time in Reference to Copper-Copper Sulfate Electrode

Half-Cell Potential, Ecorr (-mV)

Specimen	Bar	Pre-Treat	Day 7	Day 11	Day 18	Day 27	Day 34	Day 41	Day 48
B-1	A	546	399	431	497	519	492	499	496
	B	521	399	432	504	525	490	495	491
B-2	A	542	368	378	446	488	431	492	513
	B	550	380	375	460	506	455	521	547
B-3	A	540	301	240	243	239	234	225	192
	B	533	325	263	259	252	240	231	197
B-4	A	548	326	345	363	408	393	370	371
	B	521	354	340	385	440	408	401	397
B-5	A	561	402	431	498	529	486	489	479
	B	545	388	437	511	546	495	498	501
B-6	A	558	419	370	411	434	424	392	369
	B	559	407	386	426	440	421	406	359
B-7	A	562	447	314	322	346	328	330	295
	B	571	422	342	359	398	359	353	357
B-8	A	547	482	373	490	626	418	413	400
	B	552	484	374	478	575	421	436	454
B-9	A	530	398	315	324	355	370	355	325
	B	519	422	355	368	401	403	392	373
B-10	A	542	299	224	225	233	233	191	196
	B	545	334	219	219	228	221	218	181
B-11	A	534	314	255	292	318	269	226	218
	B	537	313	254	287	299	252	236	227
B-12	A	545	480	301	373	489	393	429	491
	B	528	480	290	364	450	373	397	438
B-13	A	494	191	192	203	230	220	208	187
	B	503	220	183	190	210	189	181	158
B-14	A	488	199	169	198	204	191	185	183
	B	484	269	224	242	274	265	296	371
B-15	A	475	291	227	254	287	251	245	217
	B	480	208	174	222	238	210	200	188
B-16	A	477	408	222	229	210	202	179	146
	B	470	381	218	214	201	189	180	161
A-13	A	592	305	432	507	536	515	518	649
	B	611	294	419	485	522	518	507	577
A-15	A	607	409	430	478	479	507	679	702
	B	631	391	400	451	448	492	677	694

Table C-2. Post-Treatment Half-Cell Potential as a Function of Time in Reference to Copper-Copper Sulfate Electrode (continued)

		Half-Cell Potential, Ecorr (-mV)							
Specimen	Bar	Day 55	Day 62	Day 69	Day 76	Day 83	Day 90	Day 97	Day 104
B-1	A	500	497	502	542	572	645	650	662
	B	501	485	502	544	592	623	666	711
B-2	A	515	502	550	640	543	520	548	535
	B	562	549	549	712	537	531	537	529
B-3	A	211	188	239	262	249	241	250	230
	B	209	225	271	237	242	220	230	223
B-4	A	381	358	419	465	472	465	440	480
	B	406	436	484	527	526	540	551	542
B-5	A	484	502	498	529	520	501	517	523
	B	507	528	523	558	540	540	537	527
B-6	A	396	382	379	450	472	470	490	490
	B	386	372	402	442	451	477	469	507
B-7	A	317	308	312	350	367	388	379	408
	B	377	404	418	482	490	480	465	474
B-8	A	390	315	333	362	367	370	366	380
	B	448	364	396	439	453	449	455	492
B-9	A	346	325	331	364	384	401	412	446
	B	399	374	400	415	466	444	469	492
B-10	A	196	208	278	482	475	456	462	441
	B	198	182	285	361	400	404	423	444
B-11	A	256	254	220	333	382	440	422	459
	B	260	211	214	224	221	222	219	210
B-12	A	520	500	512	592	601	633	651	653
	B	454	494	591	561	567	558	559	574
B-13	A	223	224	202	282	283	280	280	273
	B	217	165	148	170	172	179	200	193
B-14	A	205	211	247	272	272	280	289	283
	B	407	409	407	446	451	466	472	472
B-15	A	247	241	263	274	280	272	270	283
	B	207	194	217	240	276	308	322	353
B-16	A	160	156	146	150	152	150	158	165
	B	170	162	153	160	167	173	183	184
A-13	A	532	593	601	567				
	B	551	537	549	561				
A-15	A	750	735	749					
	B	680	712	700					

Table C-3. Percent Change in Half-Cell Potential After Treatment, CSE Reference

Positive (+) % = increase to more noble potential
Negative (-) % = decrease to more active potential

Percent Change in Potential Magnitude

Specimen	Bar	Day 7	Day 11	Day 18	Day 27	Day 34	Day 41	Day 48	Day 55
B-1	A	26.9	21.1	9	5	9.9	8.6	9.2	8.4
	B	23.4	17.1	3.3	-0.8	6	5	5.8	3.8
B-2	A	32.1	30.3	17.7	10	20.5	9.2	5.4	5
	B	30.9	31.8	16.4	8	17.3	5.3	0.6	-2.2
B-3	A	44.3	55.6	55	55.7	56.7	58.3	64.4	60.9
	B	39	50.7	51.4	52.7	55	56.7	63	60.8
B-4	A	40.5	37	33.8	25.6	28.3	32.5	32.3	30.5
	B	32.1	34.7	26.1	15.6	21.7	23	23.8	22.1
B-5	A	28.3	23.2	11.2	5.7	13.4	12.8	14.6	13.7
	B	28.8	19.8	6.2	-0.2	9.2	8.6	8.1	7
B-6	A	24.9	33.7	26.3	22.2	24	29.8	33.9	29
	B	27.2	31	23.8	21.3	24.7	27.4	35.8	31
B-7	A	20.5	44.1	42.7	38.4	41.6	41.3	47.5	43.6
	B	26.1	40.1	37.1	30.3	37.1	38.2	37.5	34
B-8	A	11.9	31.8	10.4	-14.4	23.6	24.5	26.9	28.7
	B	12.3	32.3	13.4	-4.2	23.7	21	17.8	18.8
B-9	A	24.9	40.6	38.9	33	30.2	33	38.7	34.7
	B	18.7	31.6	29.1	22.4	22.4	24.5	28.1	23.1
B-10	A	44.8	58.7	58.5	57	57	64.8	63.8	63.8
	B	38.7	59.8	59.8	58.2	59.5	60	66.8	63.7
B-11	A	41.2	52.3	45.3	40.5	49.6	57.7	59.2	52.1
	B	41.7	52.7	46.6	44.3	53.1	56.1	57.7	51.6
B-12	A	11.9	44.8	31.6	10.3	27.9	21.3	9.9	4.6
	B	9.09	45.1	31.1	14.8	29.4	24.8	17.1	14
B-13	A	61.3	61.1	58.9	53.4	55.5	57.9	62.2	54.9
	B	56.3	63.6	62.2	58.3	62.4	61	68.6	56.9
B-14	A	59.2	65.4	59.3	58.2	60.9	62.1	62.5	58
	B	44.4	53.7	50	43.4	45.3	38.8	23.4	15.9
B-15	A	38.7	52.2	46.5	39.6	47.2	48.4	54.3	48
	B	56.7	63.8	53.8	50.4	56.3	58.3	60.1	56.9
B-16	A	14.5	53.5	52	56	57.7	62.5	69.4	66.5
	B	18.9	53.6	54.5	57.2	59.8	61.7	65.7	66.8
A-13	A	48.5	27	14.4	9.5	13	12.5	-9.6	10.1
	B	51.9	31.4	20.6	14.6	15.2	17	5.6	9.8
A-15	A	32.6	29.2	21.3	21.1	16.5	-11.9	-15.7	-23.6
	B	38	36.6	28.5	29	22	-7.3	-10	-7.8

Table C-3. Percent Change in Half-Cell Potential After Treatment, CSE Reference (continued)

Positive (+) % = increase to more noble potential
Negative (-) % = decrease to more active potential

Percent Change in Potential Magnitude

Specimen	Bar	Day 62	Day 69	Day 76	Day 83	Day 90	Day 97	Day 104
B-1	A	9	8.1	0.7	-4.8	-18.1	-19.1	-21.3
	B	6.9	3.7	-4.4	-13.6	-19.6	-27.8	-36.5
B-2	A	7.4	-1.5	-18.1	-0.2	4.1	-1.1	1.3
	B	0.2	0.2	-29.5	2.4	3.5	2.4	3.8
B-3	A	65.2	55.7	51.5	53.9	55.4	53.7	57.4
	B	57.8	49.2	55.5	54.6	58.7	56.9	58.2
B-4	A	34.7	23.5	15.2	13.9	15.2	19.7	12.4
	B	16.3	7.1	-1.2	-1	-3.7	-5.8	-4
B-5	A	10.5	11.2	5.7	7.3	10.7	7.8	6.8
	B	3.1	4	-2.4	0.9	0.9	1.5	3.3
B-6	A	31.5	32.1	19.4	15.4	15.8	12.2	12.2
	B	33.5	28.1	20.9	19.32	14.7	16.1	9.3
B-7	A	45.2	44.5	37.7	34.7	30.1	32.6	27.4
	B	29.3	26.8	15.6	14.2	15.9	18.6	17
B-8	A	42.4	39.1	33.8	32.9	32.7	33.1	30.5
	B	34.1	28.3	20.5	17.9	18.7	17.6	10.9
B-9	A	38.7	37.6	31.3	27.6	24.3	22.3	15.9
	B	27.9	22.9	20	10.2	14.5	9.6	5.2
B-10	A	61.6	48.7	11.1	12.4	15.6	14.8	18.6
	B	66.6	47.7	33.8	26.6	25.9	22.4	18.5
B-11	A	52.4	58.8	37.6	28.5	17.6	21	14
	B	60.7	60.2	58.3	58.9	58.7	59.2	60.9
B-12	A	8.3	6.1	-8.6	-10.3	-16.2	-19.5	-19.8
	B	6.4	-11.9	-6.3	-7.4	-5.7	-5.9	-8.7
B-13	A	54.7	59.1	42.9	42.7	43.3	43.3	44.7
	B	67.2	70.6	66.2	65.8	64.4	60.2	61.6
B-14	A	56.8	49.4	44.3	44.3	42.6	40.8	42
	B	15.5	15.9	7.9	6.8	3.7	2.5	2.5
B-15	A	49.3	44.6	42.3	41.1	42.7	43.2	40.4
	B	59.6	54.8	50	42.5	35.8	32.9	26.5
B-16	A	67.3	69.4	68.6	68.1	68.6	66.9	65.4
	B	65.5	67.5	66	64.5	63.2	61.1	60.9
A-13	A	-0.2	-1.5	4.2				
	B	12.1	10.2	8.18				
A-15	A	-21.1	-23.4					
	B	-12.8	-10.9					

Table C-4. Post-Treatment Corrosion Current as a Function of Time

		Corrosion Current, Icorr (mA/sq.ft)							
Specimen	Bar	Pre-Treat	Day 7	Day 11	Day 18	Day 27	Day 34	Day 41	Day 48
B-1	A	8.7	8.2	8.5	9.2	10.3	10.5	9.9	10.1
	B	8.2	8.6	7	7.4	7.4	8	9.7	10.2
B-2	A	9.1	9.4	5.8	6.3	7.3	6.23	7.6	9.1
	B	9.3	10.5	5.1	5.9	7.5	5.9	7.8	12
B-3	A	12	8.1	4.1	4.1	3.9	4.3	4	4
	B	11	7.2	3.2	3.3	3.5	4	4.2	4.1
B-4	A	7.5	6.1	4.9	5.8	6.3	6.9	6.8	6.8
	B	7.4	7.9	7.1	6.8	6.6	8	7.8	7.9
B-5	A	6.5	5.6	3.9	4.4	5.3	6.4	7	7.2
	B	6.9	5.7	4.9	5.5	6.8	5.3	6.6	7.9
B-6	A	6.1	6.9	4.4	4.5	4.5	5.2	5.5	5.6
	B	6.3	5.8	5.8	5	4.5	5.1	5.3	5.4
B-7	A	6.2	7.1	3.9	4.1	4.4	4.2	4.5	4.4
	B	6.5	7.9	3.7	3.8	4.1	4.6	4.5	4.6
B-8	A	5.9	4.3	1.9	3.3	5.7	3.8	3.5	3.6
	B	6.1	4.8	1.8	4.1	5.6	3.8	4.6	4.6
B-9	A	4	3.4	1.8	1.6	1.3	1.9	2.2	2.4
	B	3.8	3	1.7	1.4	1.4	1.3	1.7	1.6
B-10	A	3.5	4.6	1.5	1.9	2.1	1.8	2.1	2.1
	B	3.8	6.4	2.1	2.1	2	2.9	2.9	2.8
B-11	A	3.9	4.2	1.8	2.2	2.4	2.3	2.8	2.6
	B	3.9	4.1	2.1	2.2	2.5	1.9	2.3	2.7
B-12	A	3.4	3.5	1.3	2.1	3.4	3	4	4.8
	B	3.3	4	0.9	2.3	3.4	3.7	4.6	4.3
B-13	A	2.3	1.1	0.8	0.9	0.9	1.1	1.4	1.3
	B	2.5	1.3	0.9	0.9	0.9	1.1	1	1.2
B-14	A	1.6	1	0.7	0.7	0.6	0.5	0.7	0.7
	B	1.4	1.1	0.6	0.6	0.7	0.8	1	0.9
B-15	A	1.7	0.8	0.5	0.5	0.5	0.5	0.5	0.5
	B	1.9	0.8	0.5	0.5	0.5	0.4	0.4	0.5
B-16	A	1.3	2.1	0.9	0.8	0.7	0.7	0.7	0.8
	B	1.6	2.1	0.5	0.6	0.6	0.7	0.7	0.7
A-13	A	25	1.3	19.4	28.7	36.7	37.3	22	29
	B	22	0.2	15.9	25	33.2	34.5	29	30.7
A-15	A	23	6.2	7.1	7.4	7.6	22	27.6	29.4
	B	22	5.9	8.3	9.2	9.7	20	36	37.9

Table C-4. Post-Treatment Corrosion Current as a Function of Time (continued)

		Corrosion Current, Icorr (mA/sq.ft)							
Specimen	Bar	Day 55	Day 62	Day 69	Day 76	Day 83	Day 90	Day 97	Day 104
B-1	A	9.7	10.1	10.5	13.2	12.6	12.9	12.9	13.3
	B	10.1	10.3	12.2	12.6	13	13.3	13.8	15
B-2	A	12.9	13.6	13	12	12	12.2	12.1	11.7
	B	16	16	13.8	21.4	19.5	18.6	19	20.4
B-3	A	4.2	4.2	3.6	3.3	3.5	3.8	3.9	3.9
	B	4.1	4.4	3.2	3.1	3.9	3.8	3.8	3.9
B-4	A	7	6.8	6.6	6.2	6.6	7.8	7.9	8.6
	B	7.6	7.5	8.1	10	12.2	13.7	13.5	16.1
B-5	A	8.5	8.8	7.2	8.2	8.2	8.6	8.8	9.6
	B	9.3	9.5	7.8	10.8	11.2	10	11.4	11.5
B-6	A	6.4	6.4	4.4	5.6	6.6	8.2	10	10.2
	B	6	6.3	3.1	4.7	6.2	7.8	7.7	8.5
B-7	A	4.8	4.8	3.1	2.5	4	4.4	4.3	4.4
	B	4.6	4.9	3.9	5.1	6	6.1	6.4	6.4
B-8	A	3.3	3.3	1.5	1.3	2	1.9	2	1.4
	B	5.2	5	2.6	3.4	3.7	4	3.9	3.8
B-9	A	2.7	2.6	1.3	1.7	2.5	2.6	2.9	3.7
	B	1.9	1.9	1.2	1.6	1.9	3	2.9	3.4
B-10	A	2.2	2.6	1.8	3.3	3.9	4.4	4.6	4.9
	B	2.6	2.8	2.5	4.3	4.7	5.8	5.6	5.9
B-11	A	3	3.3	2.2	2.9	3	4.2	4.8	6
	B	2.8	2.8	1.7	2.2	2.3	2.8	2.7	3.2
B-12	A	5.9	5.7	3.4	4	4.4	4.3	4.3	4.5
	B	5.7	5.9	5	6.6	5.9	5.8	6.1	5.9
B-13	A	1.5	1.6	1	1.3	1.3	1.3	1.2	1.2
	B	1.4	1.3	0.8	0.8	0.9	1	1	0.8
B-14	A	0.9	1	0.8	1	0.9	0.9	0.9	1.1
	B	1.2	1.2	1	1.7	1.6	1.4	1.6	1.9
B-15	A	0.5	0.5	0.4	0.4	0.6	0.6	0.7	1
	B	0.4	0.5	0.4	0.5	0.7	0.9	1	1.5
B-16	A	0.8	0.8	0.6	0.6	0.7	0.6	0.8	1
	B	0.7	0.7	1.7	0.7	0.6	0.7	0.7	0.7
A-13	A	32.1	24.5	25.2	26				
	B	28.7	29	27	28				
A-15	A	28.3	31.1	30.1					
	B	40.2	42.8	48.2					

Table C-5. Percent Change in Corrosion Current After Treatment

Positive (+) % = decrease in corrosion rate
Negative (-) % = increase in corrosion rate

Percent Change in Corrosion Current Magnitude

Specimen	Bar	Day 7	Day 11	Day 18	Day 27	Day 34	Day 41	Day 48	Day 55
B-1	A	5.7	2.3	-5.7	-18.4	-20.7	-13.8	-16.1	-11.5
	B	-4.9	14.6	9.8	9.8	2.4	-18.3	-24.2	-23.2
B-2	A	-3.3	36.3	30.8	19.8	31.9	16.5	0	-41.8
	B	-12.9	45.2	36.6	19.4	36.6	16.1	-29	-72
B-3	A	30.8	65	65	66.7	63.2	65.8	65.8	64.1
	B	33.9	70.6	69.7	67.9	63.3	61.5	62.4	62.4
B-4	A	18.7	34.7	22.7	16	8	9.3	9.3	6.7
	B	-6.8	4.1	8.1	10.8	-8.1	-5.4	-6.8	-2.7
B-5	A	13.8	40	32.3	18.5	1.5	-7.7	-10.8	-30.8
	B	17.4	29	20.3	1.4	23.2	4.3	-14.5	-34.8
B-6	A	-13.1	27.9	26.2	26.2	14.8	9.8	8.2	-4.9
	B	7.9	7.9	20.6	28.6	19	15.9	14.3	4.8
B-7	A	-14.5	37.1	33.9	29	32.3	27.4	29	22.6
	B	-21.5	43.1	41.5	36.9	29.2	30.8	29.2	29.2
B-8	A	27.1	67.8	44.1	3.4	35.6	40.7	39	44.1
	B	21.3	70.5	32.8	8.2	37.7	24.6	24.6	14.8
B-9	A	15	55	60	67.5	52.5	45	40	32.5
	B	21.1	55.3	63.2	63.2	65.8	40	57.9	50
B-10	A	-31.4	57.1	45.7	40	48.6	23.7	40	37.1
	B	-68.4	44.7	44.7	47.4	23.7	28.2	26.3	31.6
B-11	A	-7.7	53.8	43.6	38.5	41	41	33.3	23.1
	B	-5.1	46.2	43.6	35.9	51.3	-17.6	30.8	28.2
B-12	A	-2.9	61.8	38.2	0	11.8	-39.4	-41.2	-73.5
	B	-21.2	72.7	30.3	-3	-12.1	39.1	-30.3	-72.7
B-13	A	52.2	65.2	60.9	60.9	52.2	60	43.5	34.8
	B	48	64	64	64	56	56.3	52	44
B-14	A	37.5	56.3	56.3	62.5	68.8	28.6	56.3	43.8
	B	21.4	57.1	57	50	42.9	70.6	35.7	14.3
B-15	A	52.9	70.6	70.6	70.6	70.6	78.9	70.6	70.6
	B	57.9	73.7	73.7	73.7	78.9	46.2	73.7	78.9
B-16	A	-61.5	30.8	38.5	46.2	46.2	56.3	38.5	38.5
	B	-31.1	68.8	62.5	62.5	56.3	11.6	56.3	56.3
A-13	A	94.8	22.1	-15.3	-47.4	-49.8	-32.4	-16.5	-28.9
	B	99.1	27.4	-14.2	-51.6	-57.5	-20	-40.2	-31.1
A-15	A	73	69.1	67.8	67	4.3	-65.1	-27.8	-23
	B	72.9	61.9	57.8	55.5	8.3	-7.3	-73.9	-84.4

Table C-5. Percent Change in Corrosion Current After Treatment (continued)

Positive (+) % = decrease in corrosion rate
Negative (-) % = increase in corrosion rate

Percent Change in Corrosion Current Magnitude

Specimen	Bar	Day 62	Day 69	Day 76	Day 83	Day 90	Day 97	Day 104
B-1	A	-16.1	-20.7	-51.7	-44.8	-48.3	-48.3	-52.9
	B	-25.6	-48.8	-53.7	-58.5	-62.2	-68.3	-82.9
B-2	A	-49.5	-42.9	-31.9	-31.9	-34.1	-33	-28.6
	B	-72	-48.4	-130.1	-109.7	-100	-104.3	-119.4
B-3	A	64.1	69.2	71.8	70.1	67.5	66.7	66.7
	B	59.6	70.6	71.6	64.2	65.1	65.1	64.2
B-4	A	9.3	12	17.3	12	-4	-5.3	-14.7
	B	-1.4	-9.5	-35.1	-64.9	-85.1	-82.4	-117.6
B-5	A	-35.4	-10.8	-26.2	-26.2	-32.3	-35.4	-47.7
	B	-37.7	-13	-56.5	-62.3	-44.9	-65.2	-66.7
B-6	A	-4.9	27.9	8.2	-8.2	-34.4	-63.9	-67.2
	B	0	50.8	25.4	1.6	-23.8	-22.2	-34.9
B-7	A	22.6	50	59.7	35.5	29	30.6	29
	B	24.6	40	21.5	7.7	6.2	1.5	1.5
B-8	A	44.1	74.6	78	66.1	67.8	66.1	76.3
	B	18	57.4	44.3	39.3	34.4	36.1	37.7
B-9	A	35	67.5	57.5	37.5	35	27.5	7.5
	B	50	68.4	57.9	50	21.1	23.7	10.5
B-10	A	25.7	48.6	5.7	-11.4	-25.7	-31.4	-40
	B	26.3	34.2	-13.2	-23.7	-52.6	-47.4	-55.3
B-11	A	15.4	43.6	25.6	23.1	-7.7	-23.1	-53.8
	B	28.2	56.4	43.6	41	28.2	30.8	17.9
B-12	A	-67.6	0	-17.6	-29.4	-26.5	-26.5	-32.4
	B	-78.8	-51.5	-100	-78.8	-75.8	-84.8	-78.8
B-13	A	30.4	56.5	43.5	43.5	43.5	47.8	47.8
	B	48	68	68	64	60	60	68
B-14	A	37.5	50	37.5	43.8	43.8	43.8	31.3
	B	14.3	28.6	-21.4	-14.3	0	-14.3	-35.7
B-15	A	70.6	76.5	74.7	64.7	64.7	58.8	41.2
	B	73.7	78.9	75.3	63.2	52.6	47.4	21.1
B-16	A	38.5	53.8	53.8	46.2	53.8	38.5	23.1
	B	56.3	-6.2	56.3	62.5	56.3	56.3	56.3
A-13	A	1.6	-1.2	-0.04				
	B	-32.4	-23.3	-27.3				
A-15	A	-35.2	-30.9					
	B	-96.3	-119.1					

Table C-6. Average mortar cube strength for treated specimens

Treatment	Concentration (% s/s cement)	Compressive Strength (ksi)		
		Day 1	Day 3	Day 20
Control	-----	1.98	3.76	5.69
Cortec 1609	0.15 %	2.03	3.43	5.59
	0.30 %	1.89	3.14	5.11
	0.45 %	2.02	3.38	5.86
Hydroxyl-apatite	6.25 %	2.36	3.59	5.69
	12.50 %	2.02	3.27	5.33
	25.00 %	2.17	3.45	5.90
DCI	2.50 %	2.34	5.10	6.83
	5.00 %	2.69	5.20	7.67
	10.00 %	3.17	5.79	7.53
Sodium Borate	0.50 %	0.50	2.80	5.56
	1.00 %	0.07	0.47	5.03
	2.00 %	0.00	0.24	4.42
Zinc Borate	0.22 %	2.00	4.00	5.46
	0.43 %	0.09	1.28	4.32
	0.85 %	0.00	0.51	3.95
	1.70 %	0.00	0.00	3.25
	3.40 %	0.00	0.00	2.46

Table C-7. Average mortar cube resistivity for treated specimens

Treatment	Concentration (% s/s cement)	Resistivity (kohm-cm)			
		Day 1	Day 3	Day 10	Day 20
Control	-----	.40	.87	1.6	2.1
Cortec 1609	0.15 %	.37	.90	1.5	2.2
	0.30 %	.37	.85	1.6	2.0
	0.45 %	.47	.85	1.5	2.0
Hydroxyl-apatite	6.25 %	.49	.87	1.6	2.2
	12.50 %	.47	.84	1.4	2.3
	25.00 %	.52	.86	1.6	2.3
DCI	2.50 %	.62	1.0	1.9	2.4
	5.00 %	.63	1.2	1.8	2.3
	10.00 %	.62	1.3	2.2	2.5
Sodium Borate	0.50 %	.17	.84	1.4	2.0
	1.00 %	*	.45	.88	1.7
	2.00 %	*	.36	.69	1.5
Zinc Borate	0.22 %	.38	.89	1.7	2.1
	0.43 %	*	.61	1.1	1.9
	0.85 %	*	.51	.92	1.8
	1.70 %	*	*	*	.76
	3.40 %	*	*	*	.68

* = insufficient set strength to test resistivity

References

1. Seventh Annual Report to Congress-Highway Bridge Replacement and Rehabilitation Program, U.S. Department of Transportation, Federal Highway Administration, Office of Engineering, Bridge Division, 1986, 00. 59.

2. "Corrosion of Metals in Concrete," Report by ACI Committee 222, Report No. ACI 222B-89, American Concrete Institute, Detroit, MI, 1990, pp. 18-19.

3. Wallbank, E. J. The Performance of Concrete Bridges: A Survey of 200 Highway Bridges, Her Majesty's Stationary Office, London, April 1989.

4. D. E. Tonini and S. W. Dean, Eds. Chloride Corrosion of Steel in Concrete, STP 629, ASTM, 1977.

5. D. G. Manning and J. Ryell. Durable Bridge Decks. Ontario Ministry of Transportation and Communications, April 1976.

6. P. H. Perkins. Repair, Protection, and Waterproofing of Concrete Structures. Elsevier, Applied Science Publishers, New York, 1986.

7. ACI Committee 515 Report "A Guide to the Use of Waterproofing, Dampproofing, Protective and Decorative Barrier Systems for Concrete. American Concrete Institute, 1R-79, Revised 1985, Detroit.

8. N. E. Hammer. Inhibitors for Use on Reinforcing Steel in Concrete, Corrosion Inhibitors. Ed. C. C. Nathan, 1973, pps. 259-260.

9. N. E. Hammer. Inhibitors in Organic Coatings, Corrosion Inhibitors. Ed. C. C. Nathan. 1973, pp. 190-195.

10. E. McCafferty. Mechanisms of Corrosion Control by Inhibitors, Corrosion Control by Coatings. Science Press, Princeton, 1979, pp. 279-318.

11. N. E. Hammer. Inhibitors for use on Reinforcing Steel in Concrete, Corrosion Inhibitors. Ed. C. C. Nathan. 1973, pp. 190-195.

12. N. S. Berke. The Effects of Calcium Nitrite and Mix Design on the Corrosion Resistance of Steel in Concrete. Paper #132 presented at the Annual Meeting of the National Association of Corrosion Engineers, San Francisco, 1987.

13. Y. P. Virmani. Time-to-Corrosion of Reinforcing Steel in Concrete Slabs. Volume VI: Calcium Nitrite

Admixture. Publication FWHA-RD-88-165, Federal Highway Administration, McLean, Virginia, 1988.

14. Rosenberg, A. et al, "Mechanisms of Corrosion of Steel in Concrete," Materials Science of Concrete, pp. 285-309.

15. Mehta, P.K., Concrete: Structure, Properties, and Materials, Prentice-Hall, Englewood Cliffs, NJ, 1986, pp. 152-158

16. Cook, H.K. and McCoy, W.J., "Influence of Chloride in Reinforced Concrete," Chloride Corrosion of Steel in Concrete, ASTM STP 629, ASTM, Philadelphia, PA, 1977, pp. 20-29.

17. Shiessel, P. and Bakker, R., "Measures of Protection," Corrosion of Steel in Concrete, Chapman and Hill, New York, 1988, pp. 71-78.

18. Cady, P.D. and Weyers, R.E., "Chloride Penetration and Deterioration of Concrete Bridge Decks," Cement, Concrete, and Aggregates, CCAGDP, Vol. 5, No. 2, Winter 1983, pp. 81-82.

19. Verbeck, G.J., "Mechanisms of Corrosion of Steel in Concrete," Corrosion of Metals in Concrete, SP 49-3, ACI, 1975, pp. 21-38.

20. Locke, C.E., "Corrosion of Steel in Portland Cement Concrete: Fundamental Studies," Corrosion Effects of Stray Currents and the Techniques for Evaluating Corrosion of Rebars in Concrete, ASTM STP 906, ASTM, Philadelphia, PA, 1985, pp. 5-13.

21. Shalon, R. and Raphael, M., "Influence of Seawater on Corrosion of Reinforcement," ACI Journal, Proceedings Vol. 55, No. 8, Feb 1959, pp. 1251-1268.

22. Griffin, D.F., "Corrosion Inhibitors for Reinforced Concrete," Corrosion of Metals in Concrete, SP 49-8, ACI, Detroit, MI, pp. 95-101.

23. Boyd, W.K. and Tripler, A.B., "Corrosion of Reinforcing Steel Bars in Concrete," Materials Protection, Vol. 7, No. 10, 1968, pp. 40-47.

24. Rosenberg, A.M. et al, "A Corrosion Inhibitor Formulated with Calcium Nitrite for Use in Reinforced Concrete," Chloride Corrosion of Steel in Concrete, ASTM STP 629, ASTM, Philadelphia, PA, 1977, pp. 89-99.

25. Craig, R.J. and Wood, L.E., "Effectiveness of Corrosion Inhibitors and the Influence on the Physical Properties of Portland Cement Mortars," Highway Research Record, No. 328, Highway Research Board, 1970, pp. 77-88.

26. A. Moragues, A. Macias, and C. Andrade. Equilibria of the Chemical Composition of the Concrete Pore Solution. Cement and Concrete Research, Vol. 17, 1986, 00. 173-182.

27. K. Siegbahn, C. N. Nordling, A. Fahlman, R. Nordberg, K. Hamrin, J. Hedman, G. Johansson, T. Bergmark, S. E. Karlsson, L. Lindgren, and B. Lindberg. Electron Spectroscopy for Chemical Analysis (ESCA): Atomic, Molecular, and Solid State Structure Studies by Means of Electron Spectroscopy. Almqvist and Wiksells, Uppsala, 1967.

28. (a) J. G. Dillard and I. M. Spinu. An Investigation of the Effect of Plasma Treatment on the Surface Properties and Adhesion in Sheet Molded Composite (SMC). J. Adhesion, Vol. 31, 1990, pp. 137-159.

(b) J. M. Epp, J. G. Dillard, A. Siochi, R. Zallen, S. Sen, and L. C. Burton. Effects of Ion Bombardment on the Chemical Reactivity of GaAs (100): Variation of Bombarding Ion Mass. Chem. Materials, Vol. 2, 1990, pp. 173-180.

29. D. Briggs and M. P. Seah. Practical Surface Analysis by Auger and X-ray Photoelectron Spectroscopy. Eds., John Wiley and Sons, New York, 1983.

30. "Standard Test Method for Half-Cell Potentials of Uncoated Reinforcing Steel in Concrete," C-876-87, Annual Book of ASTM Standards, Vol. 04.02, ASTM, Philadelphia, PA, pp. 563-570, 1992.

31. Standard Practice for Examination and Evaluation of Pitting Corrosion. ASTM Standard G46-76 (Reapproved 1986), American Society of Testing Materials, Philadelphia, PA, 1986.

32. McCutcheon's Functional Materials: Corrosion Inhibitors. The Manufacturing Confectioner Publishing Company, Glen Rock, New Jersey, 1989.

33. J. T. Lundquist, A. M. Rosenberg, and J. M. Gaidis. Calcium Nitrite as an Inhibitor of Rebar Corrosion in Chloride Containing Concrete. Materials Performance, Vol. 18, 1979, pp. 36-48.

34. A. M. Rosenberg and J. M. Gaidis. The Mechanism of Nitrite Inhibition of Chloride Attack on Reinforcing Steel in Alkaline Aqueous Environment. Materials Performance, Vol. 18, 1979, pp. 45-48.

35. E. W. Washburn. The Dynamics of Capillary Flow. Phys. Rev. Vol. 177, 1921, pp. 273.

36. C. D. Wagner, L. H. Gale, and R. H. Raymond. Two Dimensional Chemical State Plots: A Standardized Data Set for Use in Identifying Chemical States By X-ray Photoelectron Spectroscopy. Anal. Chem., Vol. 51, 1979, pp. 466-482.

37. Berry, L.G. et al, Mineralogy, 2nd ed., W.H. Freeman and Company, San Francisco, CA, 1983, pp. 372-376.

38. P.D. Cady, "Corrosion of Reinforcing Steel in Concrete - A General Overview of the Problem," Chloride Corrosion of Steel in Concrete, ASTM 629, ASTM, Philadelphia, PA, 1977, pp. 7-8.

39. 3LP Corrosion Rate Meter: Test Procedures, Data Analysis, and General Information, K. C. Clear, Inc., Boston, VA, July 1990, Appendix, p. 9.

40. Ott, L., An Introduction to Statistical Methods and Data Analysis, 3rd ed., PWS-Kent Publishing, Boston, MA, 1988, pp. 149-151.

41. Dodson, V.H., Concrete Admixtures, Van Nostrand Reinhold, New York, 1990, pp. 103-127.

42. Chander, S. and Fuerstenau, D.W., "Solubility and Interfacial Properties of Hydroxyapatite: A Review," Adsorption on and Surface Chemistry of Hydroxyapatite, Plenum Press, New York, 1984, pp. 29-50.